

THE UNIVERSITY OF CALGARY

Recovery of Heavy Oil by Steam-Assisted Gravity Drainage
- A Three-Dimensional Approach

by

Tee Sing Ong

A THESIS

SUBMITTED TO THE FACULTY OF GRADUATE STUDIES
IN PARTIAL FULFILLMENT OF THE REQUIREMENTS FOR THE
DEGREE OF
MASTER OF SCIENCE
DEPARTMENT OF CHEMICAL AND PETROLEUM ENGINEERING

CALGARY, ALBERTA

AUGUST, 1988

© Tee Sing Ong 1988

Permission has been granted to the National Library of Canada to microfilm this thesis and to lend or sell copies of the film.

The author (copyright owner) has reserved other publication rights, and neither the thesis nor extensive extracts from it may be printed or otherwise reproduced without his/her written permission.

L'autorisation a été accordée à la Bibliothèque nationale du Canada de microfilmer cette thèse et de prêter ou de vendre des exemplaires du film.

L'auteur (titulaire du droit d'auteur) se réserve les autres droits de publication; ni la thèse ni de longs extraits de celle-ci ne doivent être imprimés ou autrement reproduits sans son autorisation écrite.

ISBN 0-315-46641-3

THE UNIVERSITY OF CALGARY

FACULTY OF GRADUATE STUDIES

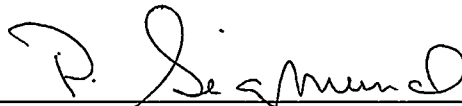
The undersigned certify that they have read, and recommend to the Faculty of Graduate Studies for acceptance, a thesis entitled,

"RECOVERY OF HEAVY OIL BY STEAM-ASSISTED GRAVITY
DRAINAGE -- A THREE DIMENSIONAL APPROACH"

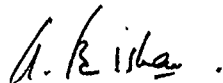
submitted by Tee Sing Ong in partial fulfillment of the requirements for the degree of Master of Science.



Dr. R.M. Butler, Committee Chairman
Department of Chemical & Petroleum Engineering



Dr. P. Sigmund
Department of Chemical & Petroleum Engineering



Dr. A. Badakhshan
Department of Chemical & Petroleum Engineering



Dr. I. Wierzb
Department of Mechanical Engineering

29. 08. 88.

Date

ABSTRACT

"Communication" between the steam injector and the producer is essential in the steam-assisted gravity drainage (SAGD) process. In this research programme, a vertical steam injector and a horizontal production well were studied. A three-dimensional, scaled physical model was developed. The experiments used a homogeneous reservoir (2 mm glass beads) and Cold Lake bitumen (100 percent saturation).

Heating the horizontal production well was expected to increase oil production rate and recovery factor. Three types of heating were investigated: indirect heating, letting steam out of the well freely, and introducing steam at the end of the well. Indirect heating was effective in keeping the well hot and increased oil production rate and recovery factor were observed. Letting steam out of the production well also increased the production rate and recovery factor but excessive steam was used. Introducing steam at the end of the well was effective but tended to impede drainage of produced fluids.

A single vertical steam injector located above a horizontal production well resulted in an oil production rate which was only 30 to 40 percent of that which would be expected from the Tandrain theory for the efficient distribution of steam along the length of the well. In the experiments, the steam chamber grew slowly along the length of the well and this limited the rate. Using two injectors increased the performance to approximately 55 to 65 percent of the theoretical.

When using two injectors, it was found that drainage of the produced fluids in the production well could be impeded due to

excessive wellbore flow restriction. The size of the horizontal well was questioned and a new sizing criterion was developed. It was found that the scaling factor for the horizontal well should not be the linear ratio of the respective heights of the reservoirs but should be equal to the one-fourth power of this ratio.

A theory was formulated to describe the drainage of produced fluids in the SAGD process. A computer programme was written based on the theory and the effects of fluid viscosity, well size and well length were investigated under laboratory and field conditions. The studies showed that the 3/8" well used in the experiments was too small for effective drainage of the produced fluids. Using a 1" well was calculated to be sufficient. An experiment using a 1" production well verified this. The computer programme also showed that the use of a 7" production well in the field would eliminate, almost entirely, the wellbore restriction found with the 3/8" well used in the laboratory model.

ACKNOWLEDGEMENTS

It is an honour and a pleasure to acknowledge the encouragement and knowledgeable advice of my supervisor, Dr. R.M. Butler for the period of this research programme.

I would also like to express my sincere gratitude to:

The Department of Chemical and Petroleum Engineering and AOSTRA for the financial support,

The Alberta Oil Sands Technology and Research Authority (AOSTRA) for supporting the project under contracts 432 and 432A,

To Mr. Ron Turner, Mr. W. Wong and Mr. G. Quon for their technical support and enthusiastic views,

To Dr. K.H. Chung for his technical advice and for familiarizing me with the laboratory work,

To Mr. S. Sugianto for providing his friendship and encouragement,

To Mr. G.H. Yang for his friendship and his assistance in the laboratory,

To Mr. C. Urness for his timely assistance in some tedious laboratory work,

To Mr. A. Kohl and Mr. D. Fantini for constructing the apparatus,

To Mr. M. Grigg for the design and construction of the load cell amplifier,

To Mrs. P. Stuart-Bakes for her encouragement and friendship,

To Mr. D. Castellino for technical assistance and his assistance in compiling the thesis,

To fellow graduate students who made this period of study pleasant, inspiring and stimulating.

I dedicate this thesis to my son, Christopher, and my wife, Poh King, for her support, encouragement and patience without which this work would not be possible.

TABLE OF CONTENTS

	Page
ABSTRACT	iii
ACKNOWLEDGEMENTS	v
TABLE OF CONTENTS	vii
LIST OF TABLES	ix
LIST OF FIGURES	x
NOMENCLATURE	xiii
1 INTRODUCTION	1
2 LITERATURE REVIEW	6
3 THEORY	11
3.1 The original theory and the TANDRAIN assumption	10
4 EXPERIMENTAL	22
4.1 Design of the apparatus	22
4.1.1 The three-dimensional reservoir model	22
4.1.2 The data acquisition system	30
4.1.3 The thermocouples	31
4.1.4 The load cell and load cell amplifier	38
4.1.5 The electric motor and the control system	42
4.2 Preparation procedure of the experiments	44
4.3 Steam	47
4.4 Sample analysis	47
4.5 The steam injector	51
4.6 The horizontal producer	51
4.7 Experiments	55
4.7.1 Repeatability of results	55
4.7.2 The effect of heating the horizontal well during production	55
4.7.3 The effect of eliminating the use of the cold end of the horizontal well	56
4.7.4 Comparison of production performance between vertical and horizontal well steam injection	56
4.7.5 Performance using two injectors	60
5 RESULTS AND DISCUSSION	61
5.1 Repeatability of results	61

5.2	The effect of heating the horizontal well during production	61
5.3	The effect of eliminating the use of the cold end of the horizontal well	85
5.4	Comparison of production performance between vertical and horizontal well steam injection	88
5.5	Performance of using two injectors	91
6	FURTHER DISCUSSION	105
6.1	Sizing the horizontal well	105
6.2	Pressure drop along the horizontal production well	110
6.3	Results of computer simulation	116
6.3.1	Laboratory conditions	116
6.3.2	Field conditions	130
7	CONCLUSIONS AND RECOMMENDATIONS	138
	REFERENCES	142
	APPENDIX	
	A Computer programme for the data acquisition system	144
	B Computer programme for simulation of the steady state flow along the horizontal well	148

LIST OF TABLES

4.1	Load cell amplifier parts list	40
4.2	Properties of Cold Lake bitumen	45
4.3	Physical parameters of 3-D reservoir model and the Cold Lake fields	46
4.4	Results of control experiments in sample analysis	50
4.5	Summary of experimental conditions	57

LIST OF FIGURES

1.1	Steam-assisited gravity drainage concept	3
2.1	Continuous steam flooding process	7
3.1.1	A small vertical section of interface	12
3.1.2	Interface curve for infinite reservoir - original theory	20
3.1.3	Interface curve for infinite reservoir - TANDRAIN assumption	20
4.1.1	Schematic diagram of 3-D apparatus	23
4.1.2	Photograph of the partially assembled apparatus	24
4.1.3	Construction materials and dimensions of the scaled reservoir model	25
4.1.4	Bolts and O-ring location and external dimensions of side A	26
4.1.5	Bolts and O-ring location and external dimensions of side B	27
4.1.6	Location of thermowells and thermocouple identification numbers	28
4.1.7	Assembly of the thermowell	29
4.1.8	Construction of the thermocouple	32
4.1.9	Thermocouple linearity response	34
4.1.10	Thermocouple temperature variation	35
4.1.11	Thermocouple time constant measurement experimental setup	36
4.1.12	Thermocouple response curve	37
4.1.13	Circuit diagram of the load cell amplifier	39
4.1.14	Load cell calibration curve	41
4.1.15	Apparatus control system	43
4.4.1	Decanting diluted bitumen	49
4.5.1	Schematic diagram of steam injector during startup and operation	52
4.6.1	Schematic diagram of horizontal well during startup and operation for the case of unheated and indirectly heated well	53
4.6.2	Schematic diagram of horizontal well during startup and operation for the case of introducing steam into the well	54
4.7.1	Well configuration for Runs #1, #2 and #3	58
4.7.2	Well configuration for Runs #4, #5 and #6	58
4.7.3	Well configuration for Run #7	59
4.7.4	Well configuration for Runs #8, #9, #10, #11 and #12	59
5.1.1	Comparison of cumulative oil production for Run #1 and #3	62
5.2.1	Effect of indirectly heating the production well on percent recovery	63
5.2.2	Effect of indirectly heating the production well on oil production rate	65
5.2.3	Effect of hot wellbore on penetration depth	66
5.2.4a	Movement of steam/oil interface in Run #2 20 to 80 minutes	68

5.2.4b	Movement of steam/oil interface in Run#2, 100 to 160 minutes	69
5.2.4c	Movement of steam/oil interface in Run#2, 180 to 240 minutes	70
5.2.5a	3-dimensional steam chamber growth in Run #2, 20 to 80 minutes	71
5.2.5b	3-dimensional steam chamber growth in Run #2, 100 to 160 minutes	72
5.2.5c	3-dimensional steam chamber growth in Run #2, 180 to 240 minutes	73
5.2.6	Comparison of cumulative oil production for Runs #4, #5 and #6	74
5.2.7a	Movement of steam/oil interface in Run #4, 20 to 80 minutes	76
5.2.7b	Movement of steam/oil interface in Run #4, 100 to 160 minutes	77
5.2.7c	Movement of steam/oil interface in Run #4, 180 to 240 minutes	78
5.2.8a	Movement of steam/oil interface in Run #6, 20 to 80 minutes	79
5.2.8b	Movement of steam/oil interface in Run #6, 100 to 160 minutes	80
5.2.8c	Movement of steam/oil interface in Run #6, 180 to 240 minutes	81
5.2.9	Comparison of cumulative water production for Runs #4, #5 and #6	82
5.2.10	Measured weight loss and oil production in Run #4	83
5.3.1	Effect of eliminating the use of the cold end of horizontal well	86
5.4.1	Comparison of predicted result with experimental result for run #8	89
5.4.2	Comparison of predicted result with experimental result for run #4.	90
5.5.1a	Movement of steam/oil interface in Run #8, 20 to 80 minutes	92
5.5.1b	Movement of steam/oil interface in Run #8, 100 to 160 minutes	93
5.5.1c	Movement of steam/oil interface in Run #8, 180 to 240 minutes	94
5.5.2	Comparison of cumulative oil production for Run #4 and Run #8	95
5.5.3a	Movement of steam/oil interface in Run #9, 20 to 80 minutes	97
5.5.3b	Movement of steam/oil interface in Run #9, 100 to 160 minutes	98
5.5.3c	Movement of steam/oil interface in Run #9, 180 to 240 minutes	99
5.5.4a	Movement of steam/oil interface in Run #11, 20 to 80 minutes	101
5.5.4b	Movement of steam/oil interface in Run #11, 100 to 160 minutes	102
5.5.4c	Movement of steam/oil interface in Run #11, 180 to 240 minutes	103

6.2.1	Mechanisms of drainage of oil in the SAGD process	112
6.2.2	Steady state Darcy flow between injector and producer	113
6.3.1	The effect of mixing viscosity on gravity head using a 3/8" production well in the model	117
6.3.2	The effect of mixing viscosity on oil flow rate along a 3/8" production well in the model	118
6.3.3	The effect of mixing viscosity on production well pressure using a 3/8" production well in the model	119
6.3.4	The effect of well size on gravity head in the model	121
6.3.5	The effect of well size on oil flow rate along the production well in the model	122
6.3.6	The effect of wellbore size on production well pressure in the model	123
6.3.7	The effect of mixing viscosity on gravity head using a 1" production well in the model	124
6.3.8	The effect of mixing viscosity on oil flow rate along a 1" production well in the model	125
6.3.9a	Movement of steam/oil interface in Run #12, 20 to 80 minutes	127
6.3.9b	Movement of steam/oil interface in Run #12, 100 to 160 minutes	128
6.3.10	Comparison of cumulative oil production for Run #4 and Run #12	129
6.3.11	The effect of well length on gravity head using a 7" production well in the field	131
6.3.12	The effect of well length on oil flow rate along a 7" production well in the field	132
6.3.13	The effect of well length on production well pressure using a 7" production well in the field	133
6.3.14	The effect of well size on gravity head in the field	135
6.3.15	The effect of well size on oil flow rate along the production well in the field	136

NOMENCLATURE

B_3	dimensionless scaling number defined by equation (6.1.1)
C	a constant defined by equation (6.2.9)
g	gravitational constant, m/s^2
H	reservoir height, m
K	oil effective permeability, m^2
L	Horizontal well length, m
m	dimensionless parameter defined by equation (3.1.10)
P	pressure, Pa
q	drainage rate, m^3/s
Q^*	dimensionless production rate defined by equation (3.1.25)
r	radius, m
R	radius, m
ΔS_o	difference between initial oil saturation and residual oil saturation
t	time, s
T	temperature, $^{\circ}C$
T'	dimensionless time defined by equation (3.1.22)
T^*	dimensionless time defined by equation (3.1.26)
U	velocity of interface, m/s
V	volume, m^3
w	horizontal distance to the no-flow boundary of the steam chamber
x	horizontal distance away from the horizontal well, m
X	x/H
y	the vertical distance away from the bottom of the well, m
Y	y/H

α	thermal diffusivity of reservoir materials, m^2/s
θ	angle of inclination of interface as defined in Figure 3.1.1
μ	dynamic viscosity of oil, Pa.s
ν	kinematic viscosity of oil (m^2/s)
ξ	perpendicular distance from the interface, m
\emptyset	porosity
ρ	density, kg/m^3
κ	ratio of inner tubing radius to horizontal well radius

Subscripts

field	refers to field conditions
g	gas phase
i	injection well
model	refers to model conditions
o	oil phase
p	production well
r	refers to reservoir condition
s	refers to steam temperature eg. ν_s is oil viscosity at steam temperature
sc	steam chamber
wi	wellbore injection
wp	wellbore production

CHAPTER 1

INTRODUCTION

Canada has approximately one-sixth of all discovered petroleum deposits in the world (Butler, 1985c). Approximately 95 percent of this petroleum consists of bitumen and is not recoverable by conventional means. Most of this bitumen is buried too deeply for open pit mining and therefore some kind of in-situ recovery process with an acceptable rate of production is necessary. A number of in-situ recovery processes has been developed to assist the production of this type of heavy oil.

Most of these techniques reduce the viscosity of heavy oil in their respective ways and thus enhance the production rate. A special technique is the continuous steam flooding process known as steam-assisted gravity drainage (SAGD); this is the main concern of this research programme. Butler and co-workers (1981a, 1981b, 1985a, 1985b, 1986) have successfully developed a theory which predicts the rate of production of heavy oil using the concept of SAGD. Results of experiments performed with scaled models support the theory very well.

The SAGD process uses gravity as the chief driving force for oil displacement. In one form of the process steam is introduced into a horizontal injection well near the bottom of the reservoir and as it rises a steam chamber is formed with steam condensate and heated oil falling to the bottom and being removed continuously. In the theory the steam chamber is maintained at a constant pressure and condensation only occurs at the interface. As the liquids are removed more steam

can be introduced and thus a steady growth of the steam chamber results. In the theory flow toward the horizontal production well is assumed to be two dimensional and "end effects" of the steam chamber are neglected. The mechanism is illustrated in Figure 1.1 which is adopted from Butler's work.

"Communication" between the steam injector and the producer is essential in the process described. Communication is needed to allow the condensate from the injected steam to be removed so as to permit the further injection of steam. Without this ability, the process is ineffective. One approach to achieve the desired communication in bitumen-containing sand is to have the pair of horizontal wells placed close together. The two wells are heated initially and mobility of the intervening bitumen is obtained by conductive heating. This is the approach used at AOSTRA's Underground Test Facility (UTF).

There are a number of disadvantages associated with this well configuration. One disadvantage is that the steam chamber must grow upward. Rising steam chambers pose some problems. Chung and Butler (1987) reported experimental results which indicated substantial increase in emulsification of water into the produced oil when the chamber is rising. The reason was thought to be due to the interfering flow of steam and heated oil during this stage. The viscosity of the produced fluid increased substantially resulting in drainage being impeded. Another disadvantage is that the well location is critical. The wellbores must be approximately two metres apart and the injector must be above the producer. Also once the project becomes mature it would be desirable to inject steam at a high elevation. These

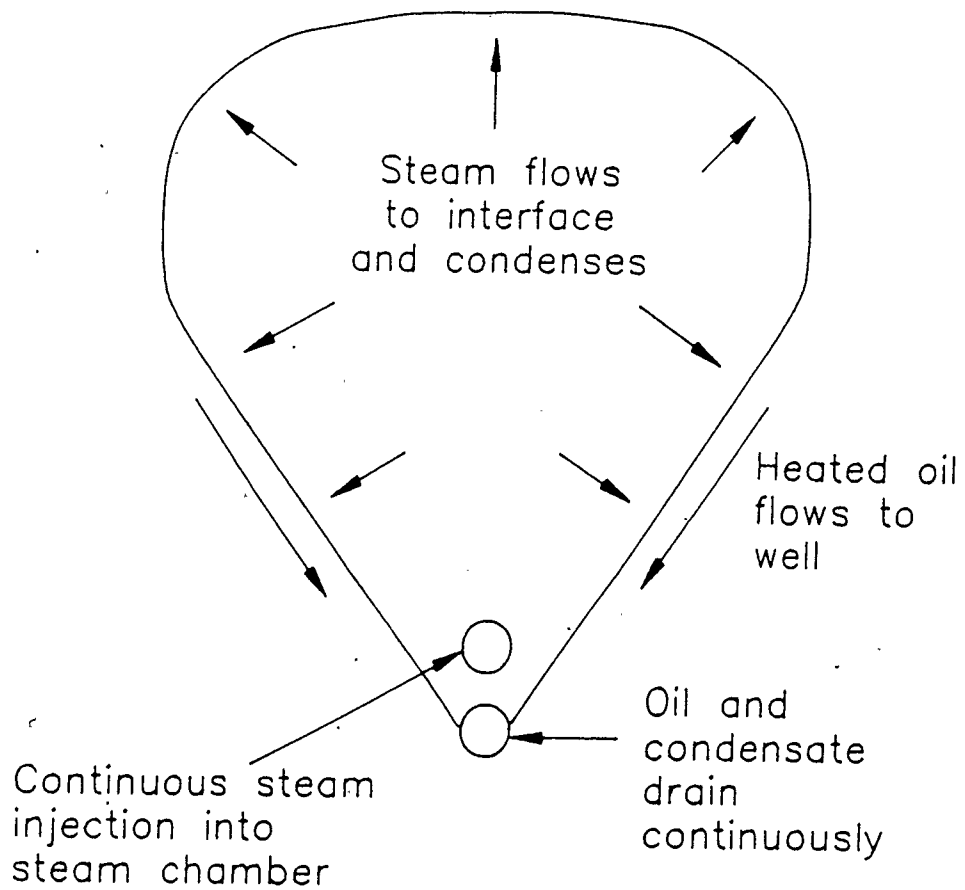


Figure 1.1 Steam-assisted gravity drainage concept

limitations can be overcome when the process is applied to reservoirs having less viscous oil such as the Lloydminster type oils. In this case the injection can be located high and communication can be obtained by simple pressure displacement.

Another approach to initiate communication between the injector and the producer is to use steam injection from the top of a heated vertical well instead of injection from a horizontal well. There are a number of advantages associated with this well configuration. One important advantage is the immediate vertical extension of the steam chamber. This eliminates the interfering flow of rising steam with produced oil as in the previous approach. Water in oil emulsification is minimized and thus effective viscosity is not increased. In addition, well location is not as critical as in the previous approach. The injector can be terminated slightly above the horizontal well or it can pass nearby terminating somewhere below it. One other important advantage of using the vertical injection well over the horizontal well would be its cost advantage if it performs nearly as well as the latter in recovering the oil.

Although vertical injection well geometry is cost effective and is advantageous in the immediate establishment of the steam chamber over the entire thickness of the reservoir, there is concern over its effectiveness on the growth of the steam chamber along the horizontal production well. This process might be too slow for it to be economically viable. The challenge is to develop a process in which vertical steam injection would perform as well as the horizontal steam injection in terms of recovery rate and energy efficiency. A possible

and exciting application of top vertical steam injection with horizontal production wells in the SAGD process is in the use of existing cyclic steam wells with newly drilled horizontal wells at the bottom of the reservoir. In principle, the cyclic steaming process should be designed with the intention of continuing recovery with the SAGD process at a later stage. In addition to the 15 percent recovery by cyclic steaming the SAGD process may be able to remove as much as 50 percent or more of the oil in place.

The primary objective of this research programme was to study these advantages and concerns of the vertical well geometry with horizontal well production and to undertake the challenge mentioned earlier using experiments. A three-dimensional, scaled physical model was developed. The experiments were performed using a homogeneous reservoir with 2 mm glass beads as the porous medium. The reservoir was saturated (100 percent) with Cold Lake bitumen for all the experiments.

CHAPTER 2

LITERATURE REVIEW

Steam injection for the recovery of heavy oil has been used as early as 1931. However, most large scale steam drives started in the early 1950's in Venezuela.

The cyclic steam stimulation process was discovered by accident in October 1959 in Venezuela. A steam drive pilot test in the tar sands of Mene Grande field (Prats, 1982) near Lake Maracaibo was suspended. The pressure in the injectors was relieved and suprisingly a considerable amount of oil was produced at a rate of about 100 to 200 BPD with only a small amount of steam. Since then, there has been rapid growth in the use of cyclic steam stimulation, also known as "steam soak" or "huff and puff", particularly in California.

Cyclic steam stimulation is an economic process because the payoff period is short, the capital cost incurred is relatively low and the risk involved is minimum (Farouq Ali, 1974). Its major drawback is that only about 15 to 20 percent of the original oil in-place can be recovered economically. Most often but not yet in Alberta bitumen sands, more oil is produced with continuous steam flooding after initial production and communication with cyclic steam stimulation. Continuous steam flooding is now the main recovery process in California and recovery can exceed 50 percent.

Figure 2.1 shows the mechanism involved in the continuous steam flooding process. Due to gravity segregation, steam tends to override the reservoir and leave the heated oil and condensate below. It can be

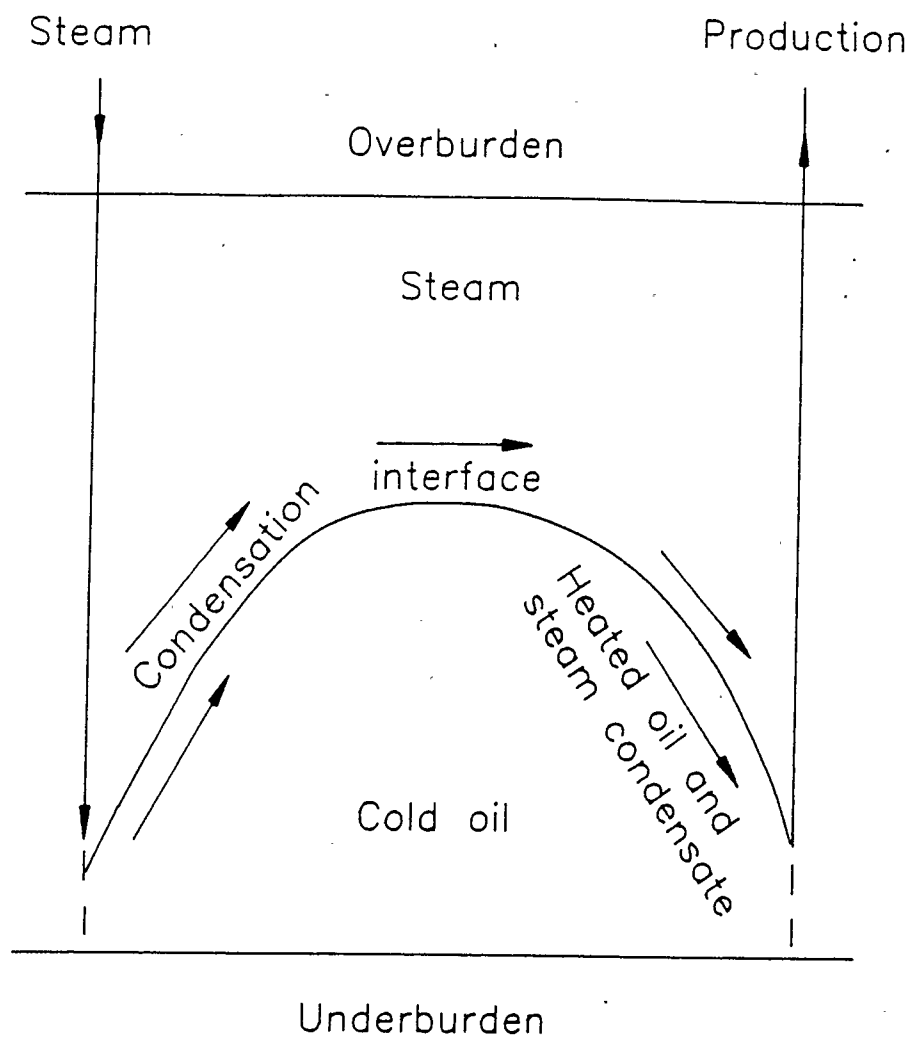


Figure 2.1 Continuous steam flooding process

observed that gravity has a negative effect on the movement of oil and condensate to the producer near the injector. However, gravity has a positive effect near the producer. The concept of SAGD utilizes this positive effect of gravity to provide a systematic drainage of the heated oil and condensate. It has the potential of high ultimate recovery and energy efficiency.

Butler et al (1981a) introduced the concept of SAGD and developed a theory which predicts the production rate for the process. The theory was developed for a reservoir of infinite extent and a finite height. The continuous steam flooding process is considered as "drive" in which steam (or condensate) pushes the oil toward the production well. The process tends to leave considerable oil behind below the steam chamber. Once steam has reached the production well there is little pressure gradient to push this bypassed oil. It has been found that downward steam flooding in steeply dipping reservoirs is more effective because gravity helps to move the oil. The SAGD technique makes effective use of gravity to move the oil to the production well even in reservoirs with no dip; this increases recovery and energy efficiency.

Later the same year, Butler and Stephens (1981b) extended the original theory of SAGD to handle confined well arrangements. The TANDRAIN theory was formulated and the production rate of oil predicted by the original theory was reduced by 13 percent. Experimental results in good agreement with the theory were presented. Following these papers, Butler (1985a, 1985b, 1986a) published several more papers which further improved the original theory and described a theory of

rising steam chamber in the SAGD process.

Griffin and Trofimenkoff (1984) presented an extended version of Butler's work in an attempt to formulate a simple equation for the oil production rate for the case of using a vertical steam injection well with a horizontal production well. The result was unsatisfactory because the production from the "ends" of the steam chamber was not included. However, by incorporating the end effects into the extended theory, good agreement was obtained with experimental results.

Joshi (1986) reported experimental results using SAGD with vertical and horizontal steam injection. He found that vertical steam injection with horizontal well production in reservoirs with shale barriers gives faster oil recovery than those obtained using horizontal steam injection with horizontal well production. He also indicated that vertical fractures, perpendicular to the horizontal injection plane, improve recovery rate. His results showed that there might be potential in the use of a vertical injection well with a horizontal production well in the SAGD process.

Chung and Butler (1987) reported experimental work with both vertical and horizontal injection wells in the SAGD process. They found more water-in-oil emulsification resulted from horizontal pair production than from using a preheated vertical injection well, perforated at the top of the reservoir, with horizontal production well. This is because of the immediate extension of the steam chamber over the entire height of the reservoir which excluded the need for the steam chamber to rise from the bottom. When the steam chamber rises the flow of oil and steam are intermingled resulting in the formation

of emulsion. They also found that recovery rate was faster for the vertical injection well arrangement.

CHAPTER 3

THEORY

This chapter describes the development of the original theory and the subsequent TANDRAIN theory (Butler et al, 1981a, 1981b) in the SAGD process.

3.1 The original theory and the TANDRAIN assumption

Imagine a pair of very long horizontal wells parallel to each other at the bottom of a reservoir placed about 2 metres apart, one well over the other. Steam is injected into the reservoir through the upper well. The lower horizontal well acts as the producer. The theory was first developed for sideways steam propagation. The theory applies for the case whereby there is a vertical fracture along the horizontal wells so that there is initially a heated vertical plane through the two wells.

Figure 3.1.1 shows a vertical section of a small part of the drainage interface. The initial reservoir temperature is T_r and the steam temperature is T_s . The interface at which steam is condensing is inclined at an angle θ to the horizontal. Heat is transferred by conduction to the reservoir from the interface. Successive layers of material are cooler as one proceeds further from the interface. If it is assumed that oil drains parallel to the interface (this assumption is valid for homogeneous tar sands formations) then, Darcy's law can be written for one of these layers with unit thickness as in equation (3.1.1).

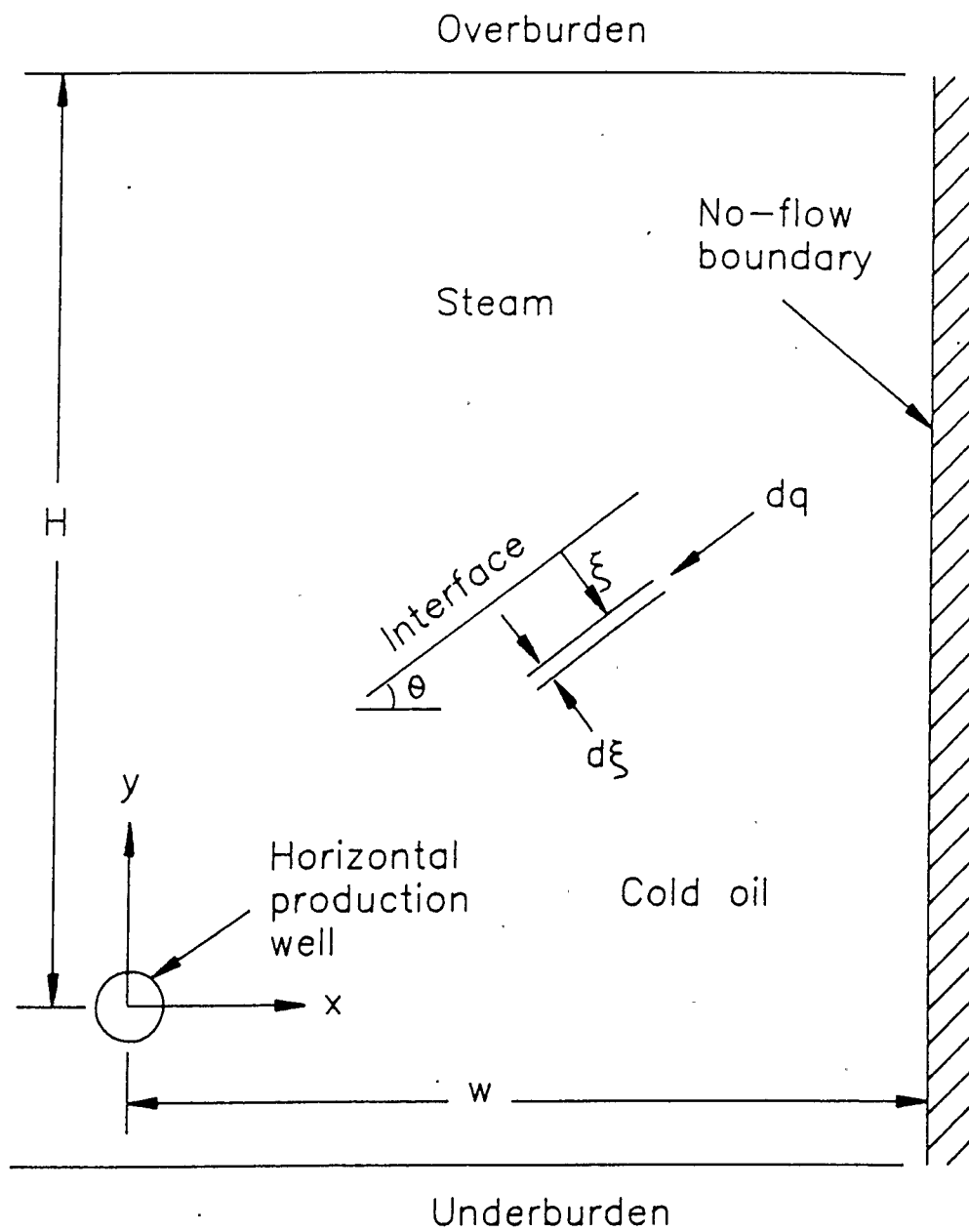


Figure 3.1.1 A small vertical section of interface

$$dq = \frac{Kg(\rho_o - \rho_g)\sin\theta}{\mu} d\xi \quad (3.1.1)$$

The potential gradient $(\rho_o - \rho_g)\sin\theta$ can be approximated by $\rho_o\sin\theta$ since ρ_g is negligible. If we replace μ/ρ_o with ν , the kinematic viscosity, then the rate of drainage of oil within the element $d\xi$ can be written as,

$$dq = \frac{Kg\sin\theta}{\nu} d\xi \quad (3.1.2)$$

If it is assumed that the interface moves at a constant velocity U normal to the interface, and that heat transfer is only by conduction, then the temperature ahead of the interface is given by equation (3.1.3).

$$\frac{T - T_r}{T_s - T_r} = e^{-U\xi/\alpha} \quad (3.1.3)$$

The increased flow of the bitumen due to heating can be written as in equation (3.1.4).

$$dq - dq_r = Kg\sin\theta \left(\frac{1}{\nu} - \frac{1}{\nu_r} \right) d\xi \quad (3.1.4)$$

Note that dq_r represents the rate of drainage if there is no

heating and ν_r is the kinematic viscosity of the oil at T_r , the initial reservoir temperature. Redefining dq as $(dq - dq_r)$ results in equation (3.1.5).

$$dq = Kg \sin \theta \left(\frac{1}{\nu} - \frac{1}{\nu_r} \right) d\xi \quad (3.1.5)$$

This manipulation is needed because the total flow would be infinite using equation (3.1.2) since ν_r must be finite.

Equation (3.1.5) can be integrated to yield equation (3.1.6).

$$q = Kg \sin \theta \int_0^{\infty} \left(\frac{1}{\nu} - \frac{1}{\nu_r} \right) d\xi \quad (3.1.6)$$

The total rate of drainage through a section normal to the interface, q , is given by equation (3.1.6). In order to evaluate the integral the viscosity of the oil as a function of distance from the interface must be known.

Since equation (3.1.3) represents the temperature as a function of distance it is now only necessary to know viscosity as a function of temperature in order to evaluate the integral. An arbitrary function which corresponds reasonably well with actual oil performance given by equation (3.1.7) was used originally.

$$\frac{\nu_s}{\nu} = \left(\frac{T - T_r}{T_s - T_r} \right)^m \quad (3.1.7)$$

Substituting equation (3.1.3) into equation (3.1.7) yields equation (3.1.8).

$$\frac{1}{\nu} = \frac{1}{\nu_s} e^{-U\xi m/\alpha} \quad (3.1.8)$$

Using equation (3.1.8) the integral can be evaluated as:

$$\int_0^{\infty} \left(\frac{1}{\nu} - \frac{1}{\nu_r} \right) d\xi = \frac{\alpha}{U m \nu_s} \quad (3.1.9)$$

The use of these equations has been expanded to oils for which the viscosity-temperature relationship does not fit equation (3.1.7) by redefining the parameter m (Butler, 1985b) as,

$$m = \left[\nu_s \int_{T_r}^{T_s} \left(\frac{1}{\nu} - \frac{1}{\nu_r} \right) \frac{dT}{T - T_r} \right]^{-1} \quad (3.1.10)$$

Corresponding values of m can be calculated for specific types of crude and input parameters since the integral of equation (3.1.10) can easily be evaluated numerically if we know the function of ν with respect to temperature. This approach also makes it possible to allow for the effect of T_r .

The integrated rate of drainage for a section across the interface is obtained by substituting equation (3.1.9) into (3.1.6) and the

result is given by equation (3.1.11).

$$q = \frac{Kg\alpha \sin\theta}{m\nu_s U} \quad (3.1.11)$$

Performing a material balance about a thin vertical element yields another relationship between the flow of oil q and the front velocity. The result is shown in equation (3.1.12).

$$\left(\frac{\partial q}{\partial x}\right)_t = \phi \Delta S_o \left(\frac{\partial y}{\partial t}\right)_x \quad (3.1.12)$$

The velocity U is related to $(\partial y/\partial t)_x$ and θ by equation (3.1.13).

$$U = - \cos\theta \left(\frac{\partial y}{\partial t}\right)_x \quad (3.1.13)$$

Substituting equations (3.1.12) and (3.1.13) into equation (3.1.11) and setting $\sin\theta/\cos\theta = (\partial y/\partial x)$ results in equation (3.1.14).

$$q = - \frac{Kg\alpha \phi \Delta S_o}{m\nu_s} \left(\frac{\partial y}{\partial x}\right)_t \quad (3.1.14)$$

Equation (3.1.14) can be integrated by separating the variables as shown in equation (3.1.15) and the result is given by equation (3.1.16).

$$\int_0^q q \, dq = \int_0^{H-y} \frac{\phi \Delta S_o K g \alpha}{m \nu_s} d(H-y) \quad (3.1.15)$$

$$q = \sqrt{\frac{2 \phi \Delta S_o K g \alpha (H-y)}{m \nu_s}} \quad (3.1.16)$$

The rate of drainage q given by equation (3.1.16) is a function of drainage height. It does not depend on the shape of the interface or on its horizontal extension.

The position of the interface can be found using equation (3.1.17).

$$\left(\frac{\partial x}{\partial t} \right)_y = - \left(\frac{\partial y}{\partial t} \right)_x / \left(\frac{\partial y}{\partial x} \right)_t \quad (3.1.17)$$

Substituting the value of $(\partial y / \partial t)_x$ obtained from equation (3.1.12) and the value of q obtained from equation (3.1.16) into equation (3.1.17) yields equation (3.1.18).

$$\left(\frac{\partial x}{\partial t}\right)_y = \sqrt{\frac{Kg\alpha}{2\phi\Delta S_o \nu_s (H-y)}} \quad (3.1.18)$$

Since the horizontal velocity is only dependent on vertical height and independent of time, integrating equation (3.1.18) yields equation (3.1.19) which gives the position of the interface and time t .

$$x = t \sqrt{\frac{Kg\alpha}{2\phi\Delta S_o \nu_s (H-y)}} \quad (3.1.19)$$

Rearranging equation (3.1.19) gives y as a function of x and t as in equation (3.1.20).

$$y = H - \frac{Kg\alpha}{2\phi\Delta S_o \nu_s} \left(\frac{t}{x}\right)^2 \quad (3.1.20)$$

Equation (3.1.20) can be written in dimensionless form as in equation (3.1.21).

$$Y = 1 - \frac{1}{2} \left(\frac{T}{X}\right)^2 \quad (3.1.21)$$

where $X = (x/H)$
 $Y = (y/H)$

$$T' = \frac{t}{H} \sqrt{\frac{Kg\alpha}{\phi \Delta S_o m \nu_s H}} \quad (3.1.22)$$

A set of curves calculated from equations (3.1.21) and (3.1.22) is shown on Figure 3.1.2. It can be observed that the interface at the bottom moves away horizontally from the production well. This characteristic was not observed in laboratory experiments. The bottom interface did not move away from the production well but remained at the well because there is no means of draining the produced fluids anywhere else except at the well. The TANDRAIN theory was formulated to approximate this behaviour. The lower part of the interface was approximated by drawing a tangent originating from the production well to each of these curves as shown in Figure 3.1.3.

The TANDRAIN assumption reduces the production rate predicted by equation (3.1.16) by 13 percent ($y = 0$ for drainage over the entire height of the formation) and is given by equation (3.1.23).

$$q = \sqrt{\frac{1.5Kg\alpha\phi\Delta S_o H}{m\nu_s}} \quad (3.1.23)$$

For a confined well configuration Butler et al (1981b) revised the theory to provide a relationship which allows the effect of depletion on the drainage rate. It was found that the drainage rate could be represented by equation (3.1.24).

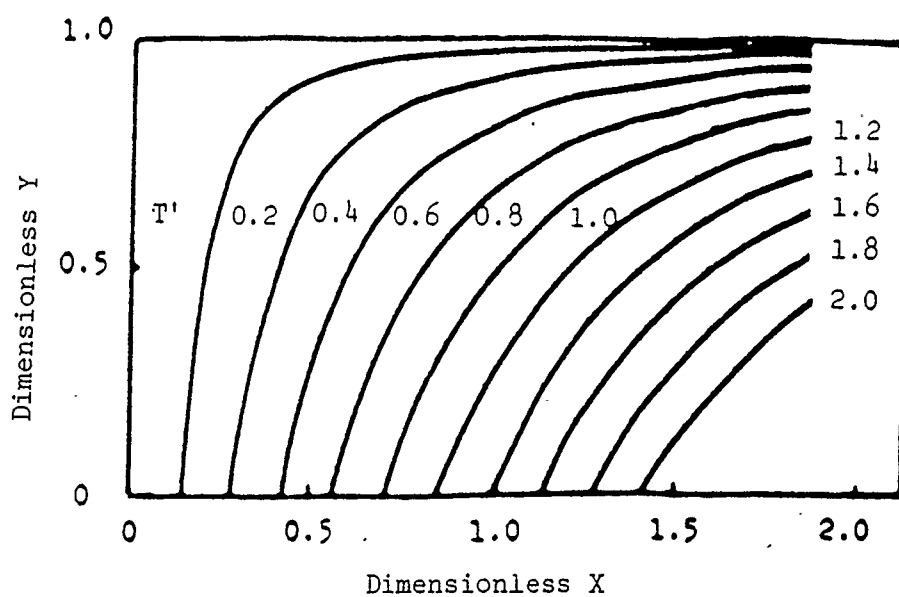


Figure 3.1.2 Interface curves for infinite reservoir
- original theory

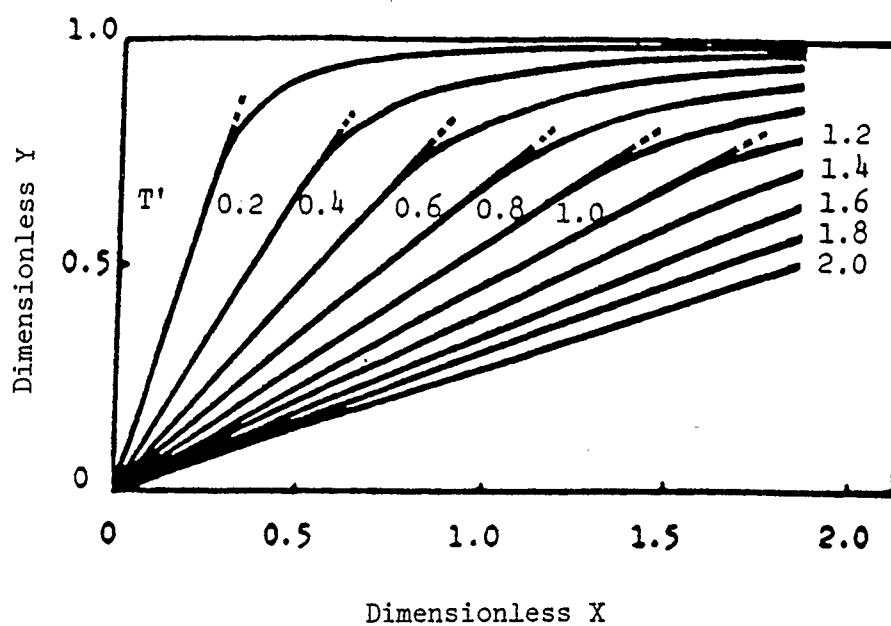


Figure 3.1.3 Interface curves for infinite reservoir
- TANDRAIN assumption

$$Q^* = \sqrt{3/2} - T^* \sqrt{3/2} \quad (3.1.24)$$

Q^* and T^* were defined as,

$$Q^* = q \sqrt{m\nu_s / Kg\alpha H \phi \Delta S_o} \quad (3.1.25)$$

$$T^* = t/w \sqrt{Kg\alpha / \phi \Delta S_o m\nu_s H} \quad (3.1.26)$$

and w is the horizontal distance from the production well to the vertical no-flow boundary.

CHAPTER 4

EXPERIMENTAL

4.1 Design of the apparatus

A scaled laboratory model was designed with the capability of monitoring the growth of the steam chamber in the SAGD process with top vertical steam injection and horizontal well production in three dimensions. The schematic diagram of the apparatus is shown in Figure

4.1.1

The reservoir model had internal dimensions of 9"x9"x18". It contained forty five glass thermowells (5 mm O.D. glass tubes). Type T thermocouples which were made from 36 SWG wire with exposed ends slid along these tubes to monitor the temperature profile of the reservoir periodically during operation. The thermocouples were held by an L-shaped metal plate which was moved by an AC electric motor through a lead screw. A personal computer was used to control the electric motor which moved the thermocouples. Data were acquired through a TAURUS ONE computer and stored on a floppy disk in the personal computer; they were also printed by the printer. A photograph of the partially assembled apparatus is shown in Figure 4.1.2.

4.1.1 The three-dimensional reservoir model

The reservoir was constructed of reinforced phenolic 1" thick plates on all sides except for one side which was made of clear plexiglass as shown in Figure 4.1.3. There are two reasons for this clear plexiglass side. The first reason is to aide the experimenter to

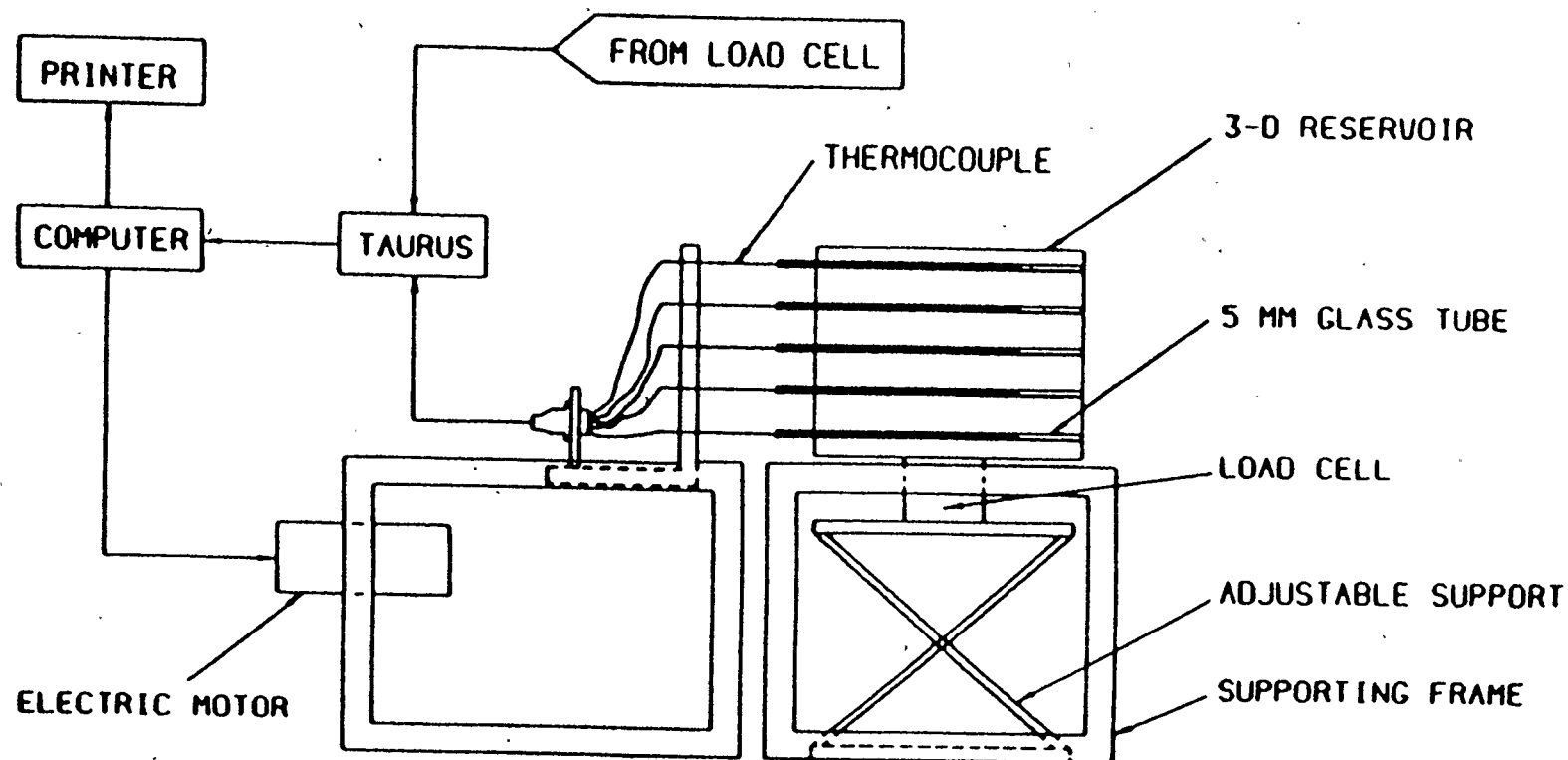


Figure 4.1.1 Schematic diagram of 3-D apparatus

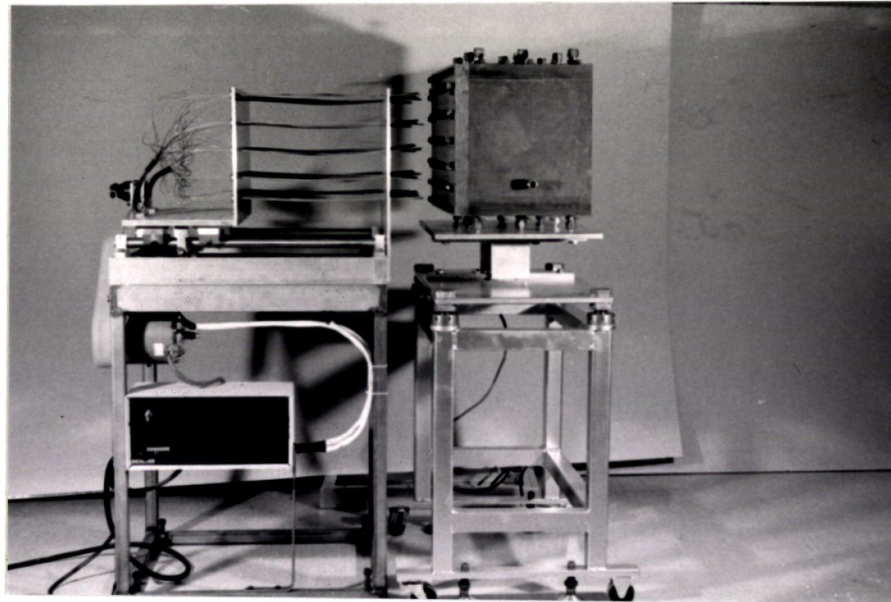


Figure 4.1.2 Photograph of the partially assembled apparatus

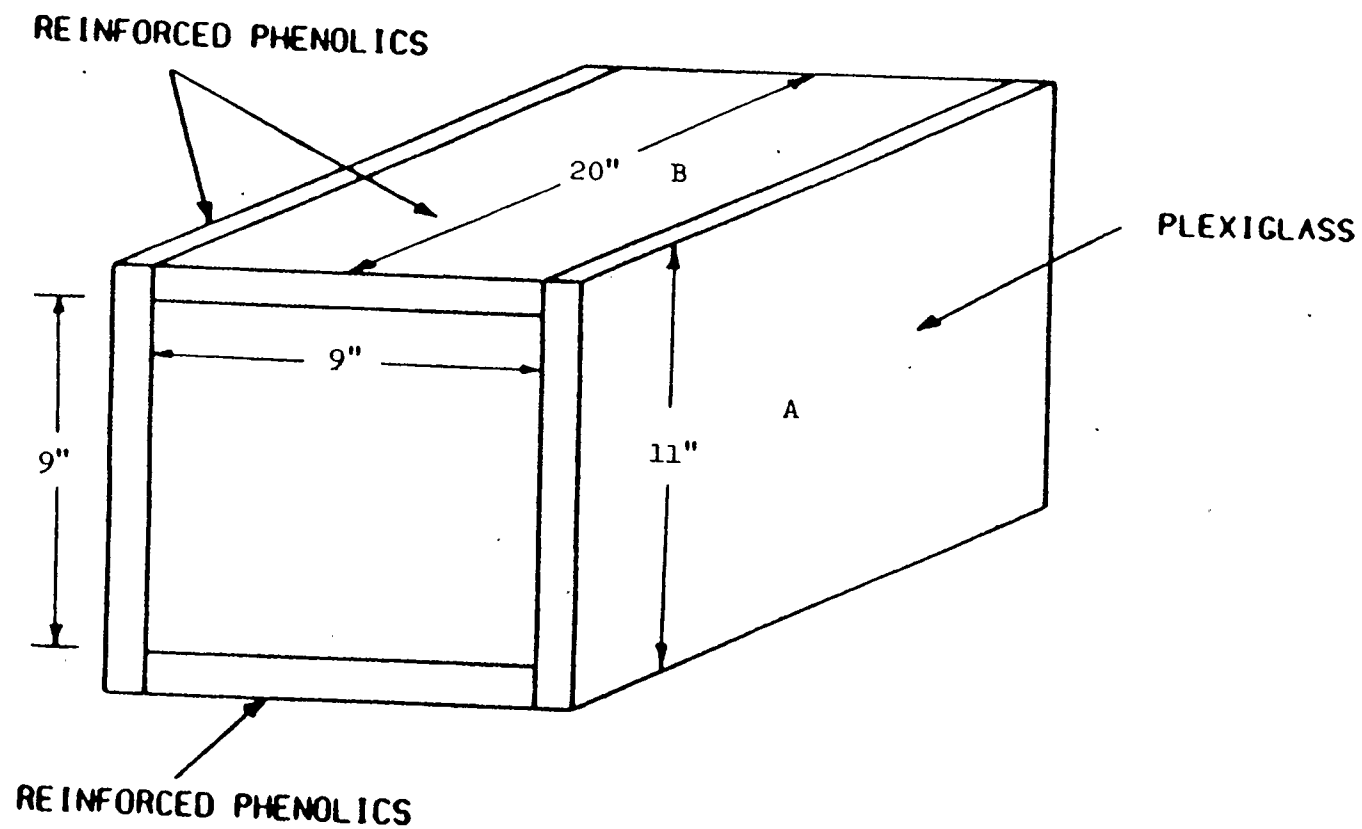


Figure 4.1.3 Construction materials and dimensions of the scaled reservoir model

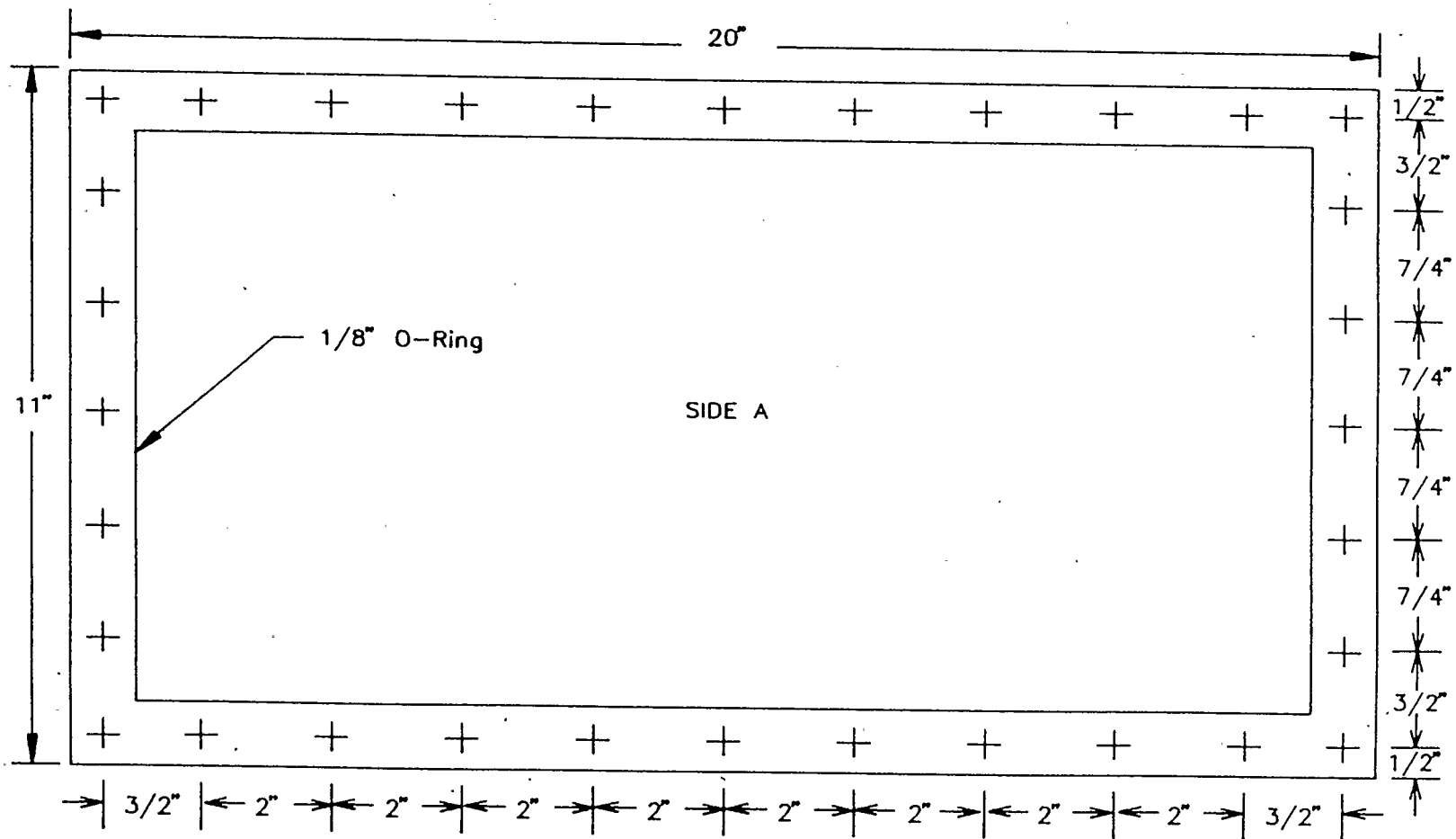


Figure 4.1.4 Bolts and O-Ring location and external dimensions of side A

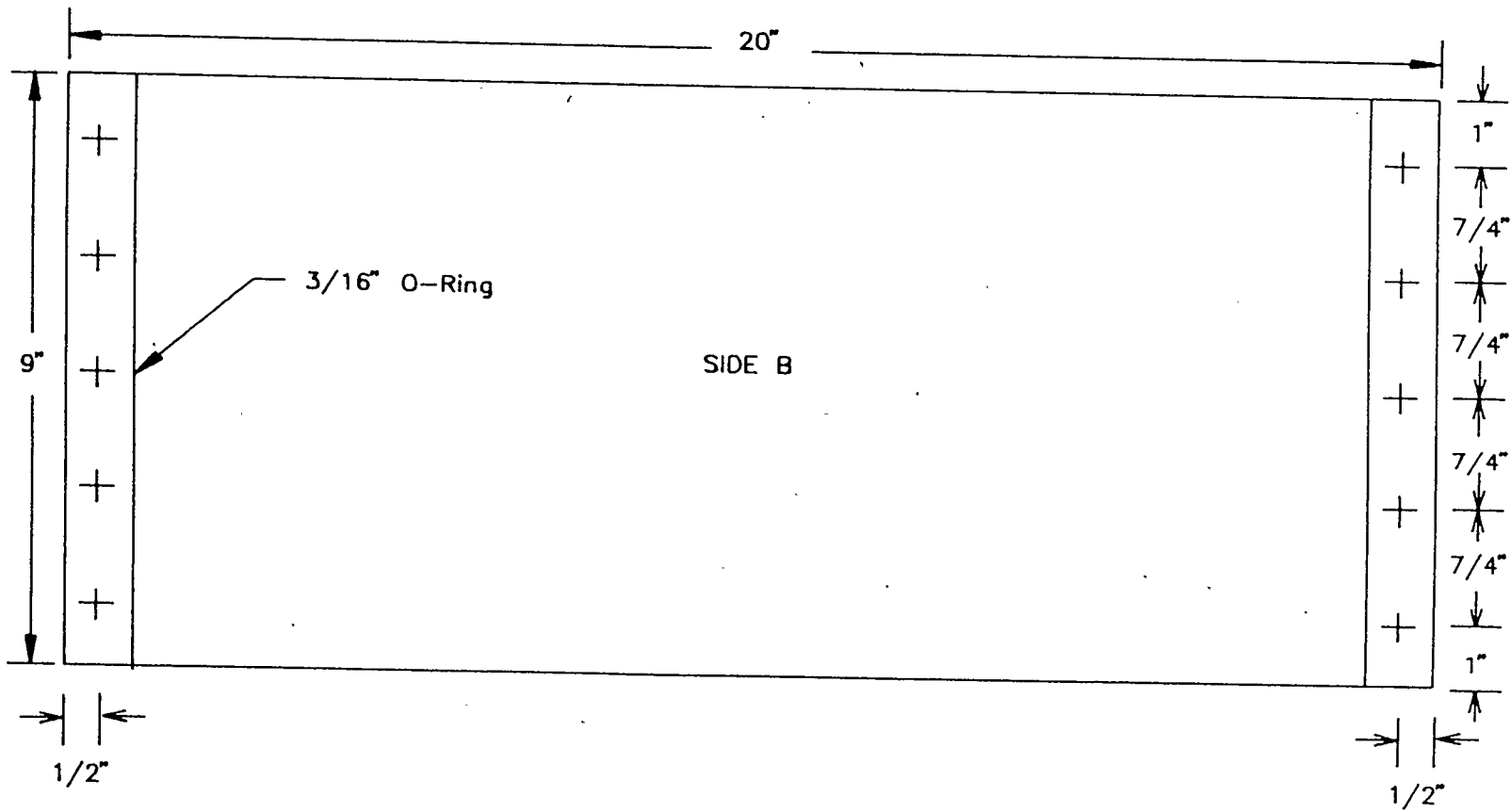


Figure 4.1.5 Bolts and O-ring location and external dimensions of side B

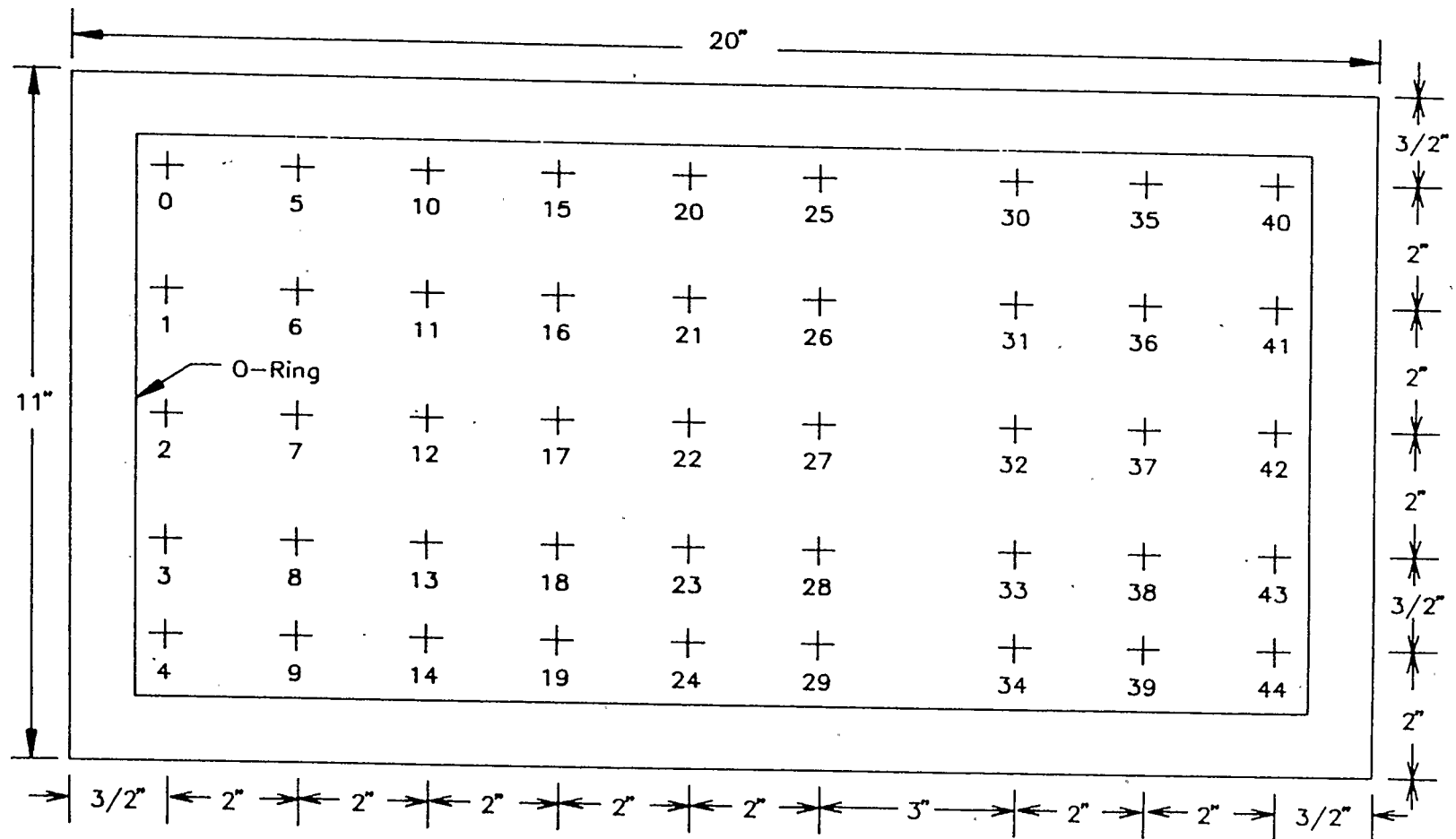


Figure 4.1.6 Location of thermowells and thermocouple identification number

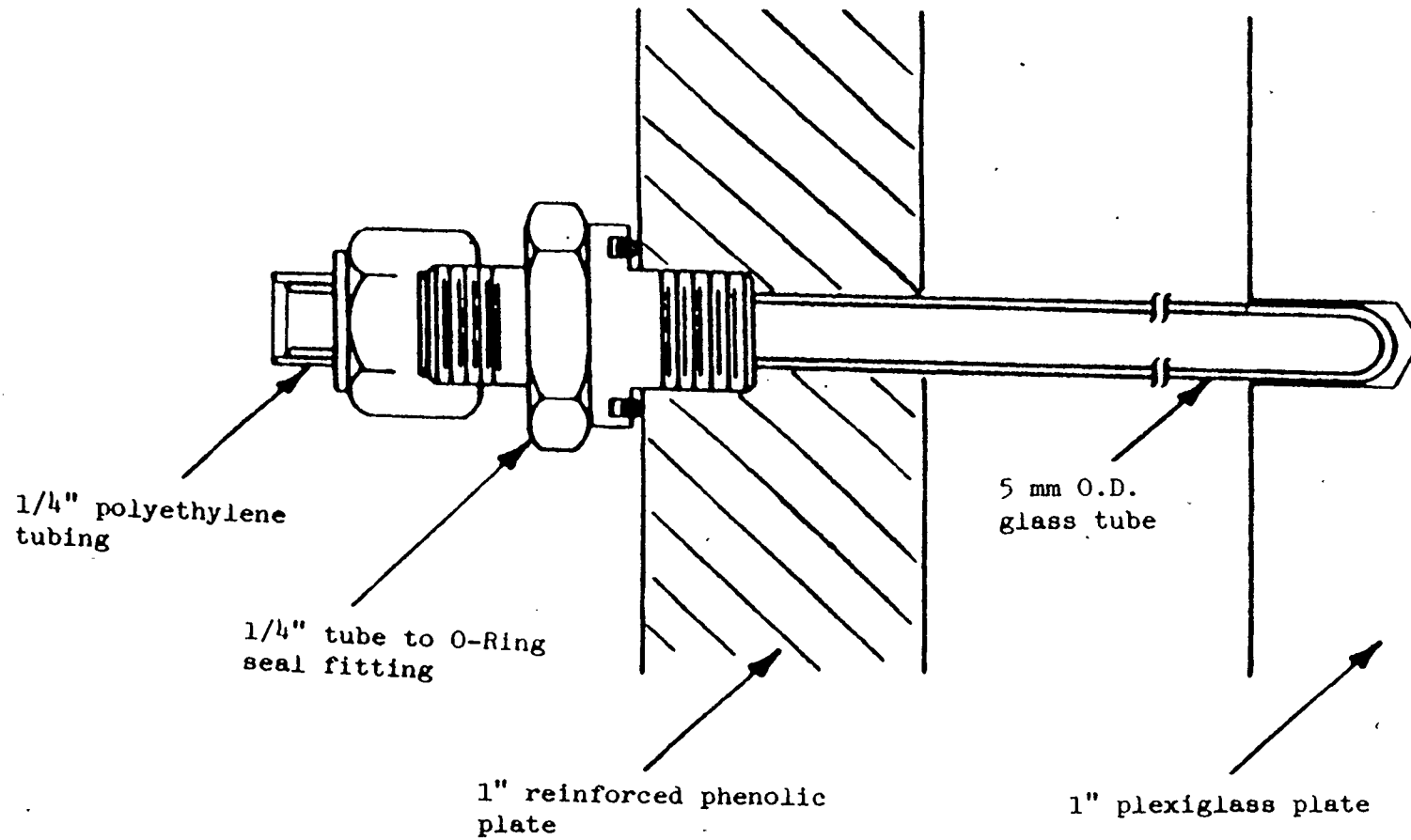


Figure 4.1.7 Assembly of the thermowell

monitor the progress when saturating the reservoir with heavy oil. The second reason is to allow photographs to be taken during the experiment so that the growth of the steam chamber for that plane of the reservoir can be verified with the data obtained from the thermocouples.

The details of the construction are shown in Figure 4.1.3 to 4.1.5. 5/16"x3/2" steel bolts and 5/16"x.469" helicoils were used to fasten the sides together. In order to prevent any leakage viton O-ring was used as shown in the figures.

Forty five glass thermowell tubes were contained in the reservoir. Figure 4.1.6 shows the location of the thermowells and the thermocouple identification numbers. The thermowell tubes were constructed of standard size 5 mm glass tubes sealed at one end and fire-polished on the other. The details of the assembly of the thermowells are shown in Figure 4.1.7. 1/4" O-ring seal type Swagelok fittings were used to hold the thermowells in place. 1/4" O.D. polyethylene sleeves were mounted over the 5 mm glass tubes on the fire-polished end so that 1/4" Swagelok fittings could be used. These sleeves also served to prevent the glass tubes from breaking when the reservoir was vibrated for compaction of the porous medium used.

4.1.2 The data acquisition system

A Taurus One computer was used for data acquisition. It consisted of a T-200 mother board with a Z80A microprocessor and two T-3700 daughter boards. One of the daughter boards was capable of measuring 64 channels of thermocouples connected single-endedly. The thermocouples were connected to this daughter board. The other

daughter board was capable of handling 32 channels of differential analog inputs. The load cell was connected to one these channels in this daughter board. The hardware allowed direct input of type J, K or T types thermocouples. The normal analog input range was between ± 10 mV DC to ± 10 V DC depending on the gains specified in the protocols used. The analog/digital converters used in the daughter boards had a 12 bit resolution.

The Taurus One was controlled by a personal computer (HP Vectra) through an RS 232C serial communication port. The communication baud rate was set at 9600.

The computer programme written for the data acquisition system used for the experiments is shown in Appendix A.

4.1.3 The thermocouples

36-gauge T-type thermocouple wires were used for the construction of these thermocouples. The exposed ends were first twisted together and then soldered. 1/8" O.D. Polypenco (nylon) tubing was used as the shell for housing the thermocouple wire. Polypenco tubing comes in rolls; it can be straightened effectively by tempering it at 50 °C. The thermocouple wire and the polypenco tubing were held together by shrinkable tubings. The soldered tip of the thermocouple was held in place by applying a small amount of epoxy glue. The details of the construction is shown in Figure 4.1.8.

In order to check the reliability of the thermocouples, four thermocouples were randomly selected for calibration to check the linearity of their response using the data acquisition system. They

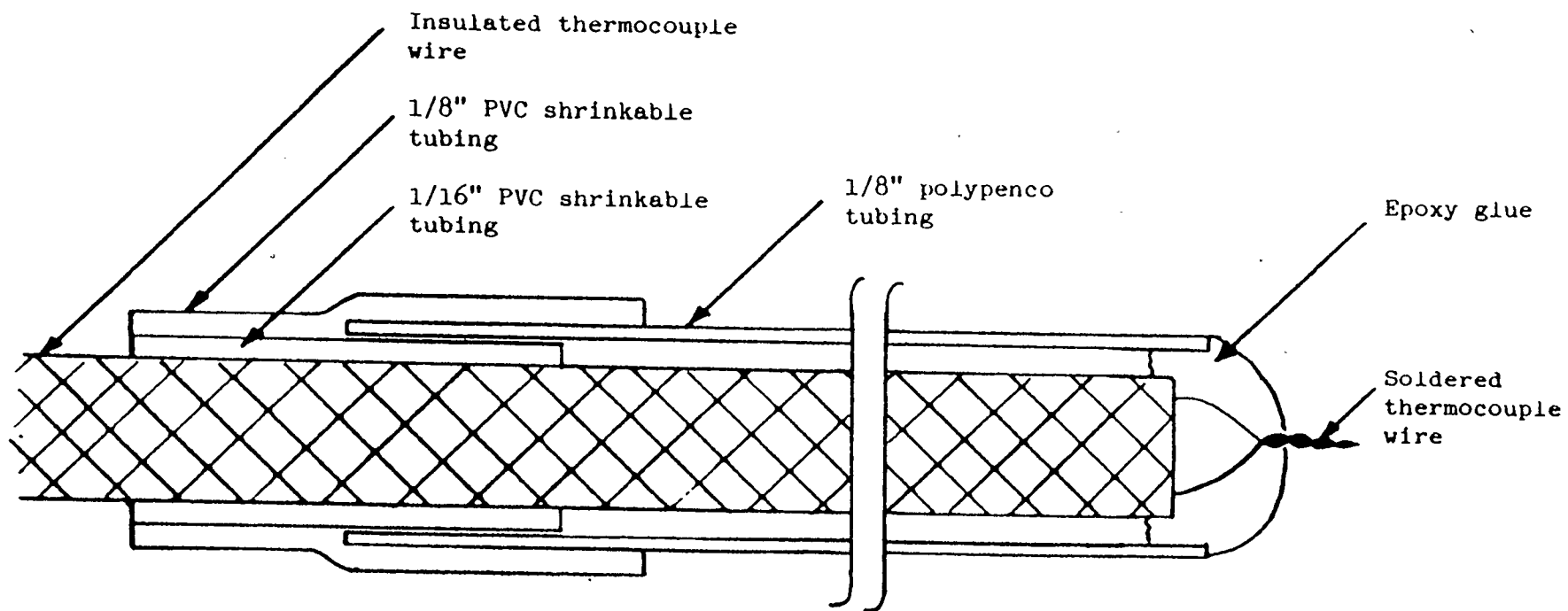


Figure 4.1.8 Construction of the thermocouple

were placed in thermowells and dipped into a beaker of distilled water. The beaker was stirred by a magnetic stirrer and heated to various temperatures. The temperatures were recorded by three other devices. Two of these devices were glass thermometers made by Fischer Scientific model 14-985E and 15-043B. The third device was a Fluke multimeter model 8024B with a K-type thermocouple. The results of the experiment is summarized in Figure 4.1.9. Of the three devices used to verify the thermocouple readings Fischer model 15-043B thermometer was considered to be the most accurate. It has an accuracy of 0.05°C . It can be observed that the response of the thermocouples constructed using the data acquisition system was linear. The accuracy of the thermocouples was then checked. Since we were most interested in monitoring the growth of the steam chamber, the temperature of boiling pure water was used as the standard. The same experimental set-up was used but all the thermocouples were used. A typical response by the system is shown in Figure 4.1.10. The maximum error was found to be 3°C .

The time constant of the thermocouples for the system was investigated in order to determine the approximate stabilization time needed. The experimental set-up is shown in Figure 4.1.11. The thermocouple was first placed into the thermowell at point B away from the beaker. The thermocouple was then quickly slid into the beaker which contained hot water at point A until it read the temperature as indicated by the thermometer T1. The response obtained gave the heating process. The thermocouple was then quickly slid out of the beaker back to point B and the temperature was recorded until the reading reached the value indicated by thermometer T2. The response

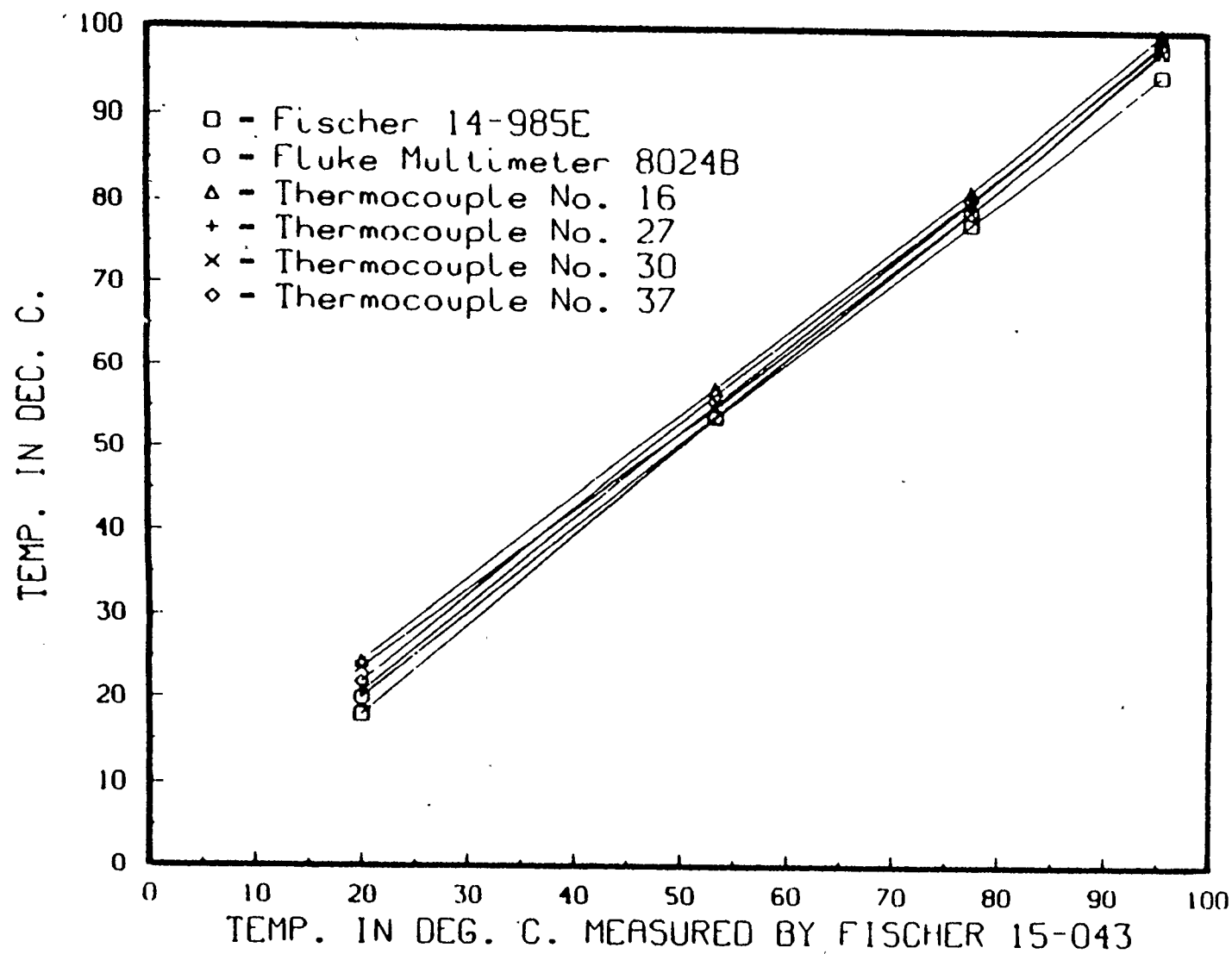


Figure 4.1.9 Thermocouple linearity response

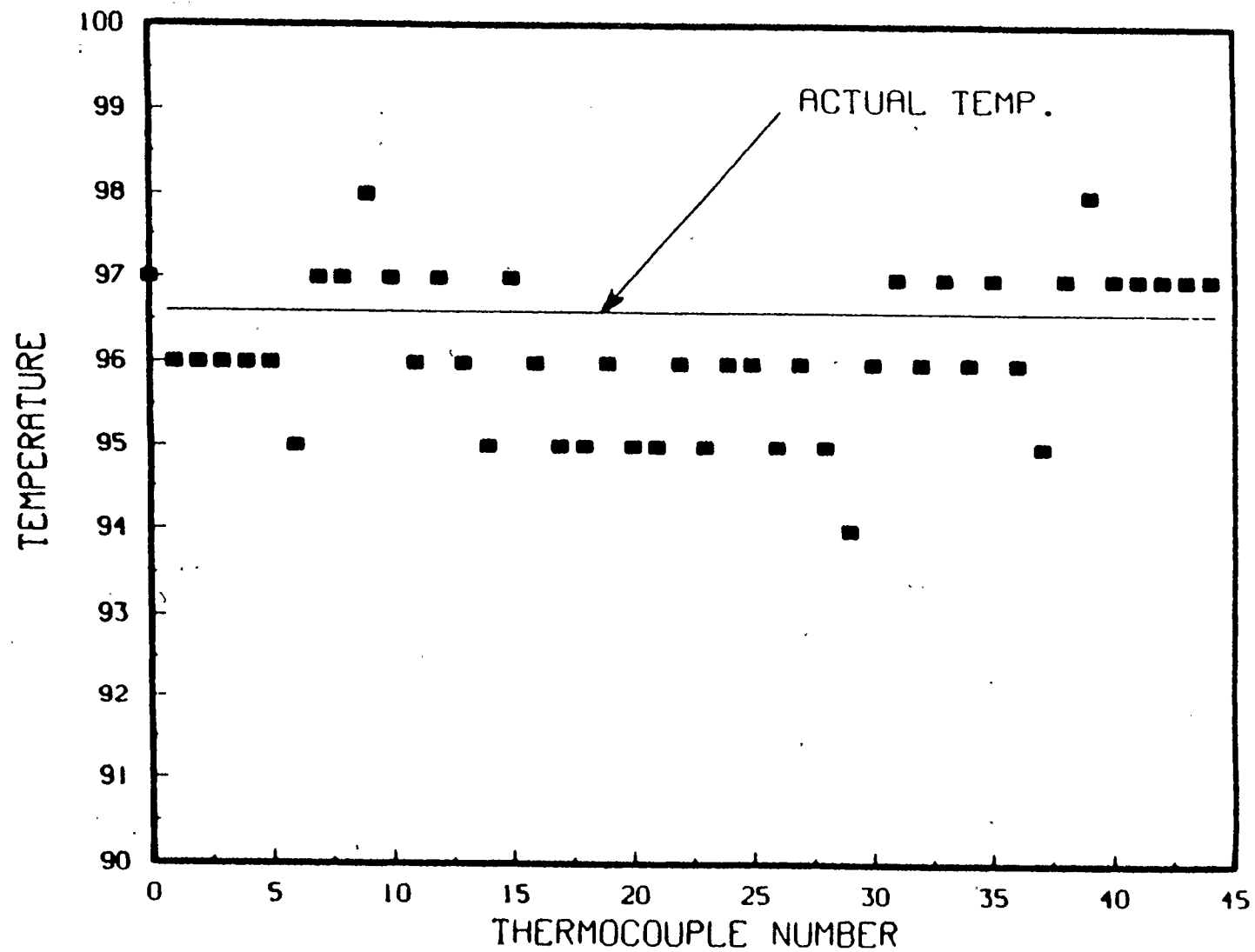


Figure 4.1.10 Thermocouple temperature variation

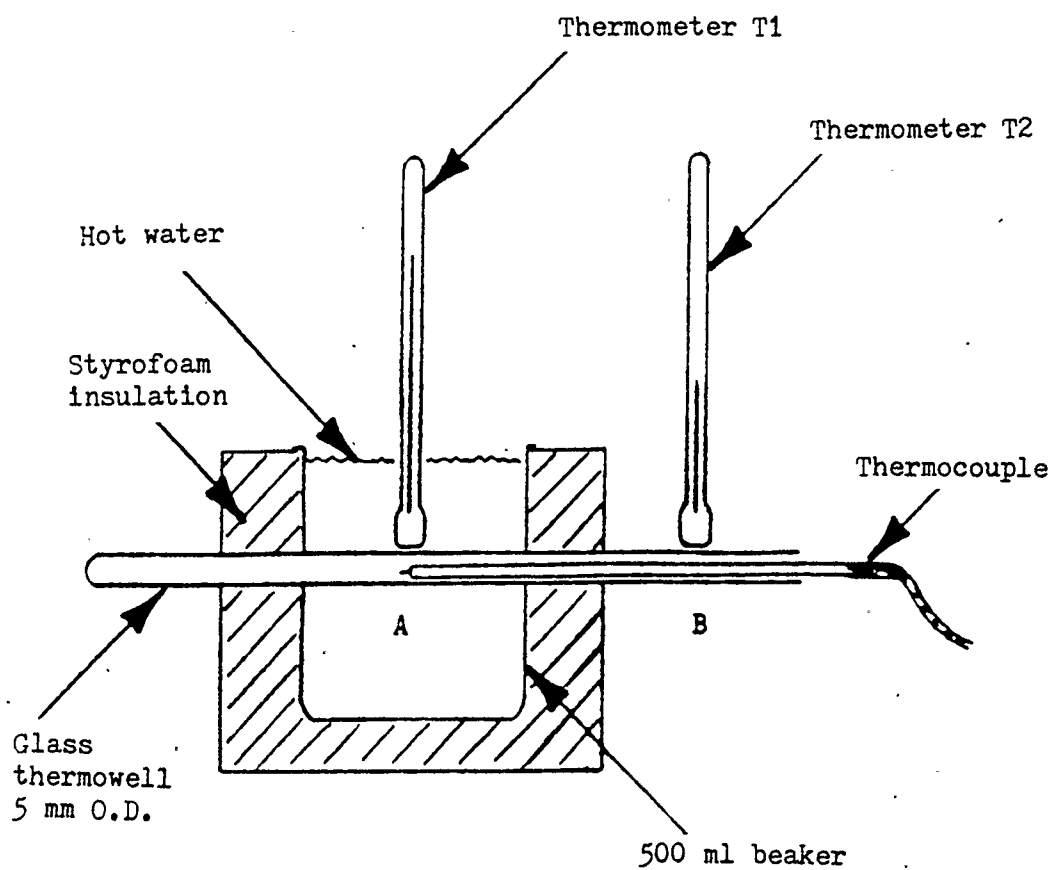


Figure 4.1.11 Thermocouple time constant measurement experimental setup

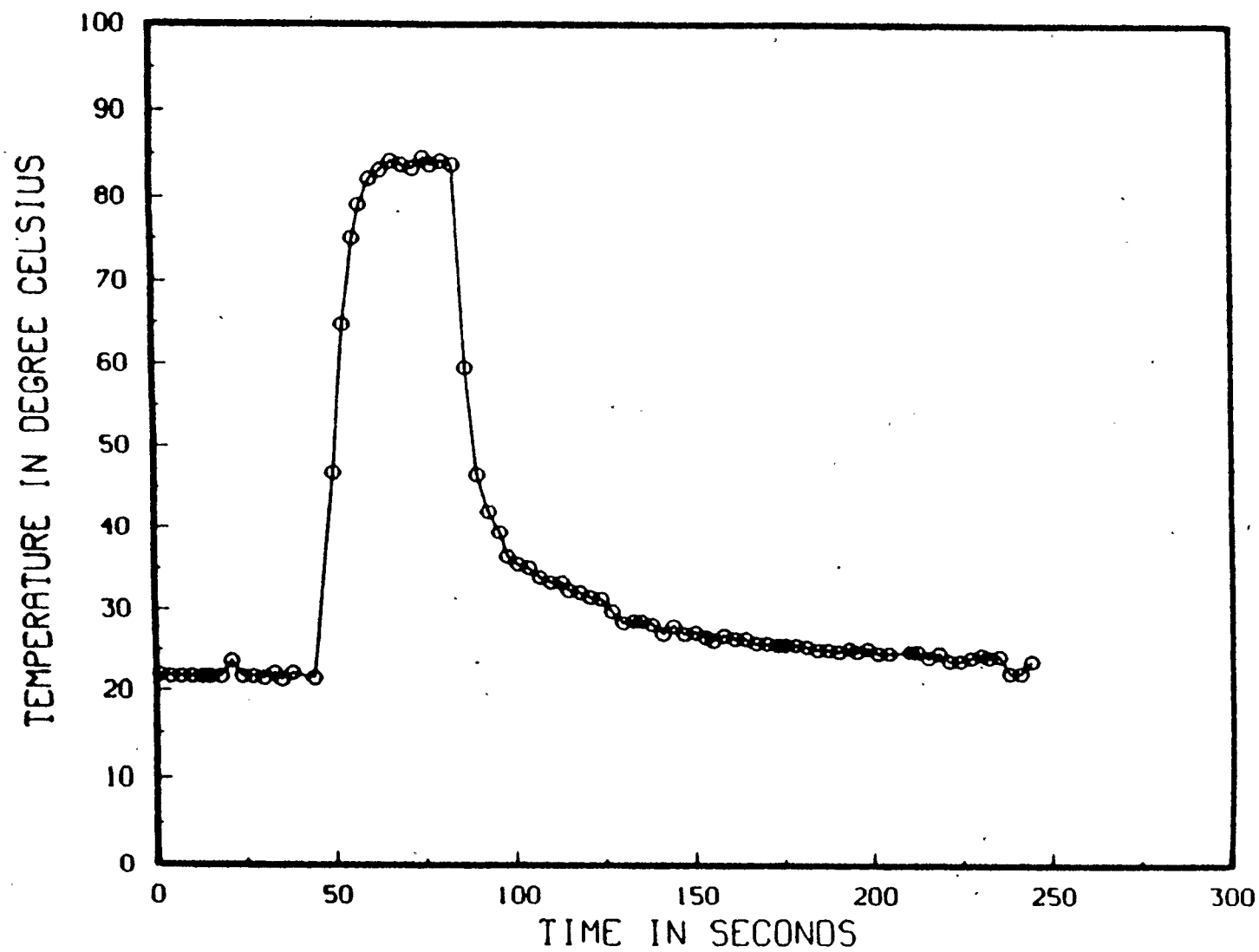


Figure 4.1.12 Thermocouple response curve

obtained gave the cooling process. The response curve obtained for the heating and cooling processes is shown on Figure 4.1.12. The critical time constant for the cooling process was estimated to be 13 seconds and an arbitrary stabilization time of 2 minutes was chosen for the thermocouples.

4.1.4 The load cell and load cell amplifier

A high capacity platform load cell (model 6762, Transducers Inc., California) was used to monitor the change in weight of the reservoir model during the experiments. It is a single point load cell designed for floor scales or process weighing. It allows for high impact loading and can be safely used right up to its full capacity of 400 pounds. The load cell by itself did not give the desired analog output since it was designed for the full range. In order to utilize the maximum resolution of the Taurus One it was necessary to tare the dead weight of the reservoir (approximately 200 pounds) and sense only the change in weight during the experiment (the maximum amount of oil the reservoir can hold was about 18 pounds). The load cell amplifier was designed and built by the Department's technician, Mr. Mike Grigg, for this purpose. The circuit diagram of the load cell amplifier is shown in Figure 4.1.13. The load cell amplifier parts list is shown in Table 4.1.

The load cell was then calibrated. The load cell was loaded with the three-dimensional model which was first filled with glass beads and left for at least 20 minutes. This was very important because of the creep effect of the load cell (maximum of 0.03 percent of load in 20

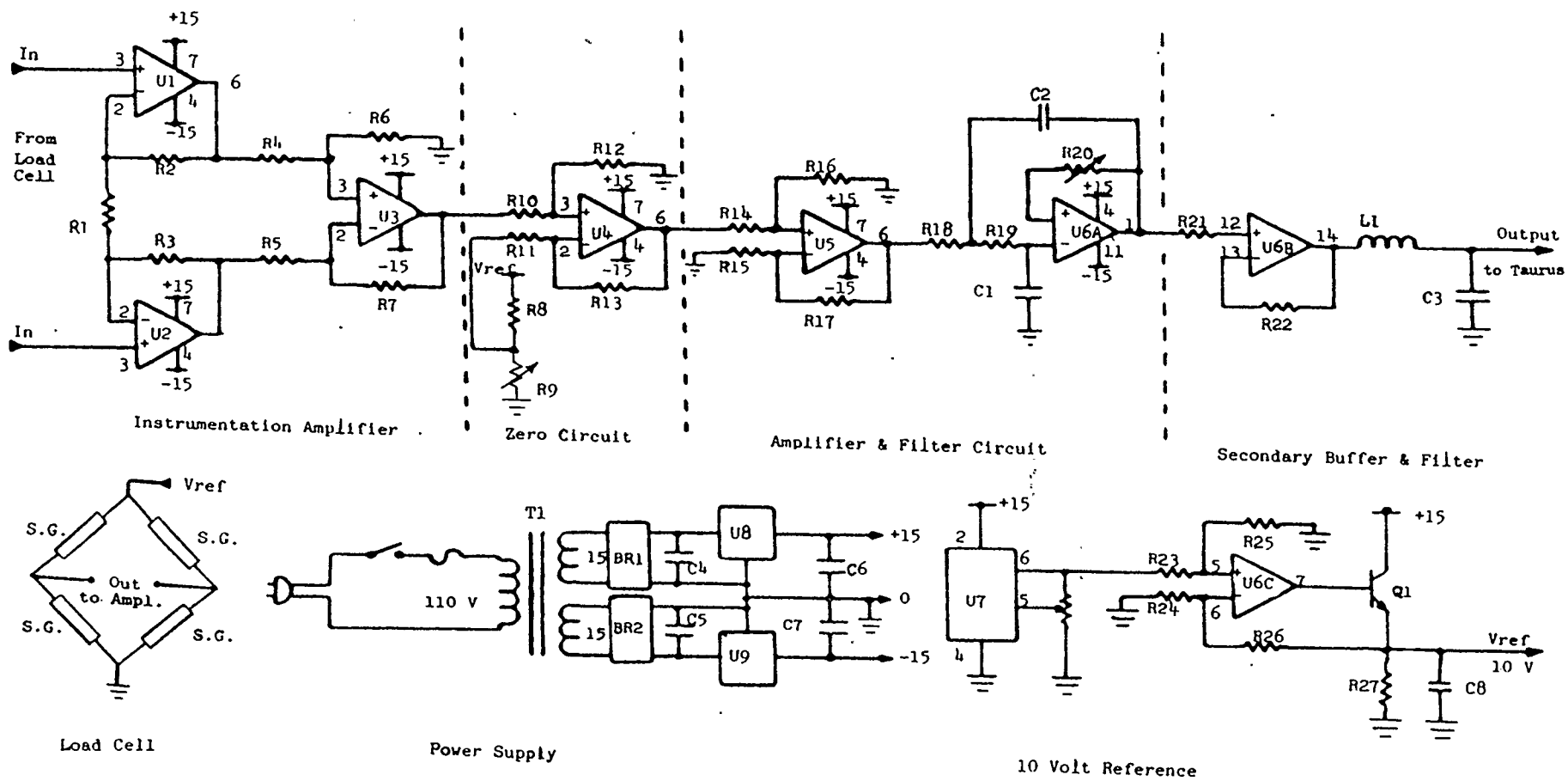


Figure 4.1.13 Circuit diagram of the load cell amplifier (Grigg, 1987)

Table 4.1 Load cell amplifier parts list (Grigg, 1987)

Capacitors:

C1,3,6,7	1 μ F
C2	2 μ F
C4,5	1000 μ F electrolytic
C8	10 μ F solid tantalum

Resistors:

R1	400 ohm 1% 1/4 watt metal film
R2,3	20k " " " " " "
R4-7,10-13,23-27	10k " " " " " "
R8	1050 " " " " " "
R9,20	200 ohm 10 turn potentiometer
R14,15	1k ohm 1% 1/4 watt metal film
R16,17	200k " " " " " "
R18,19	100k " " " " " "
R21,22	10k ohm 10% 1/4 watt

Semiconductors:

BR1,2	STS-56324-2 bridge rectifier
L1	1 μ H coil
T1	Hammond transformer 116G25 (modified)
Q1	2N3904 transistor
U1-5	OP-07 operational amplifier
U6	LM324 quad operational amplifier
U7	REF-01 precision 10 volt reference
U8	7815 positive 15 volt regulator
U9	7915 negative 15 volt regulator

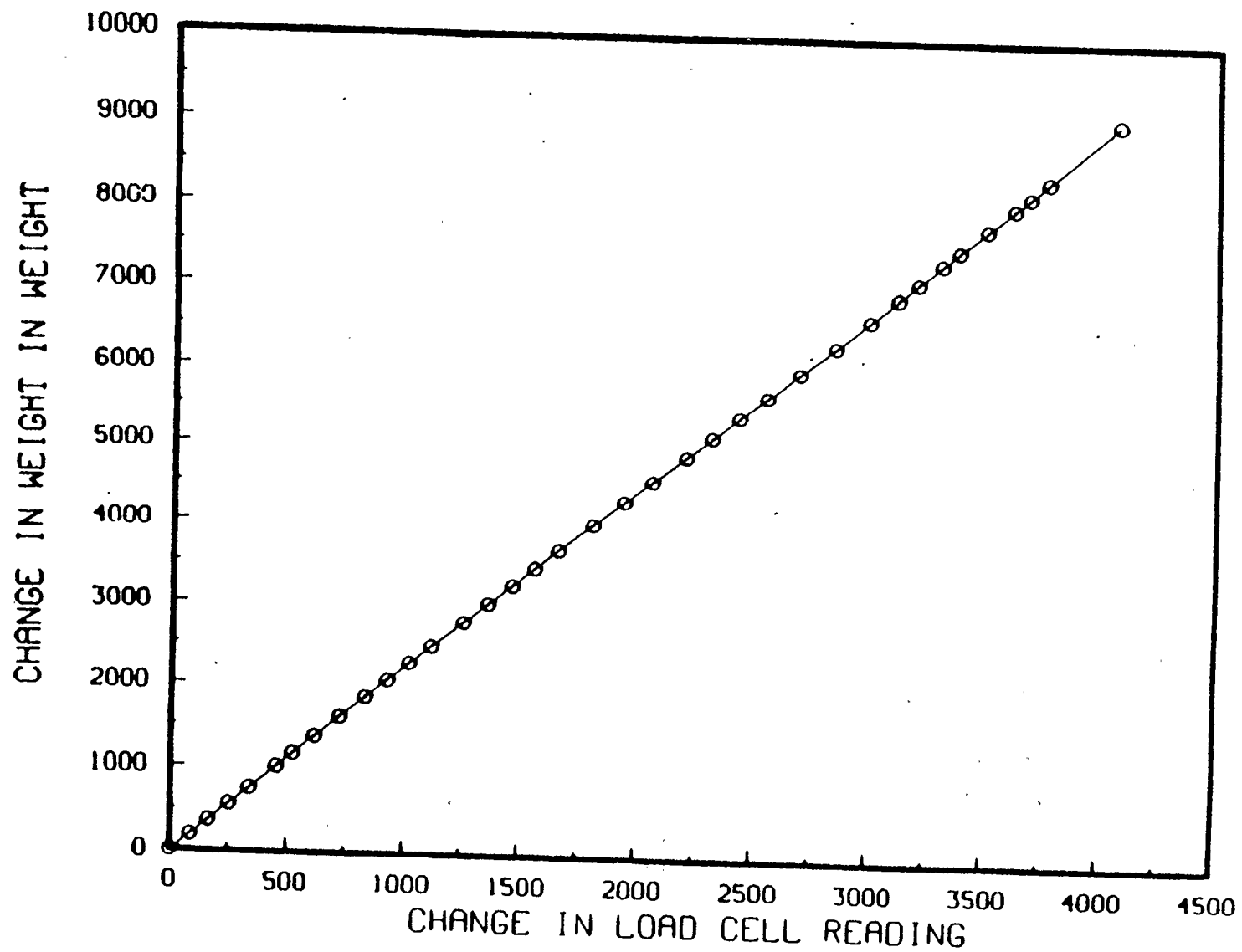


Figure 4.1.14 Load cell calibration curve

minutes). A pail of approximately 20 pounds of water was then placed over the reservoir and small amounts of water (weighed by a balance) were removed periodically and the response of the load cell was recorded. The calibration curve obtained is shown in Figure 4.1.14. The response was linear and the proportionality constant obtained was 2.232 grams/count. Since the response could be measured to a single count, the load cell could measure a change of weight within ± 3 grams. This calibration was used for all the experiments. The load cell was periodically checked for its reliability to ensure that the calibration was valid. It was found that there was no need for recalibration at any time.

4.1.5 The electric motor and the control system

An AC synchronous motor (model SS150BE, Superior Electric, Connecticut, USA) was used to drive the L-shaped plate carrying the thermocouples. It operated at 72 rpm at 60 hertz. The motor was chosen because of its rapid starting, stopping and reversing characteristics. It was capable of stopping within 5 degree of a turn. It could also start and reach its full synchronous speed within 5 to 25 milliseconds.

The control system designed for the motor consists of a personal computer, 2 relays and 4 microswitches. Figure 4.1.15 shows the circuit diagram of the control system. When power is turned on by the toggle switch, reverse motion occurs. The motor, M, drives the L-shaped plate in the reverse direction until microswitch A is triggered. As soon as this happens, relay coil CR1 is energized and

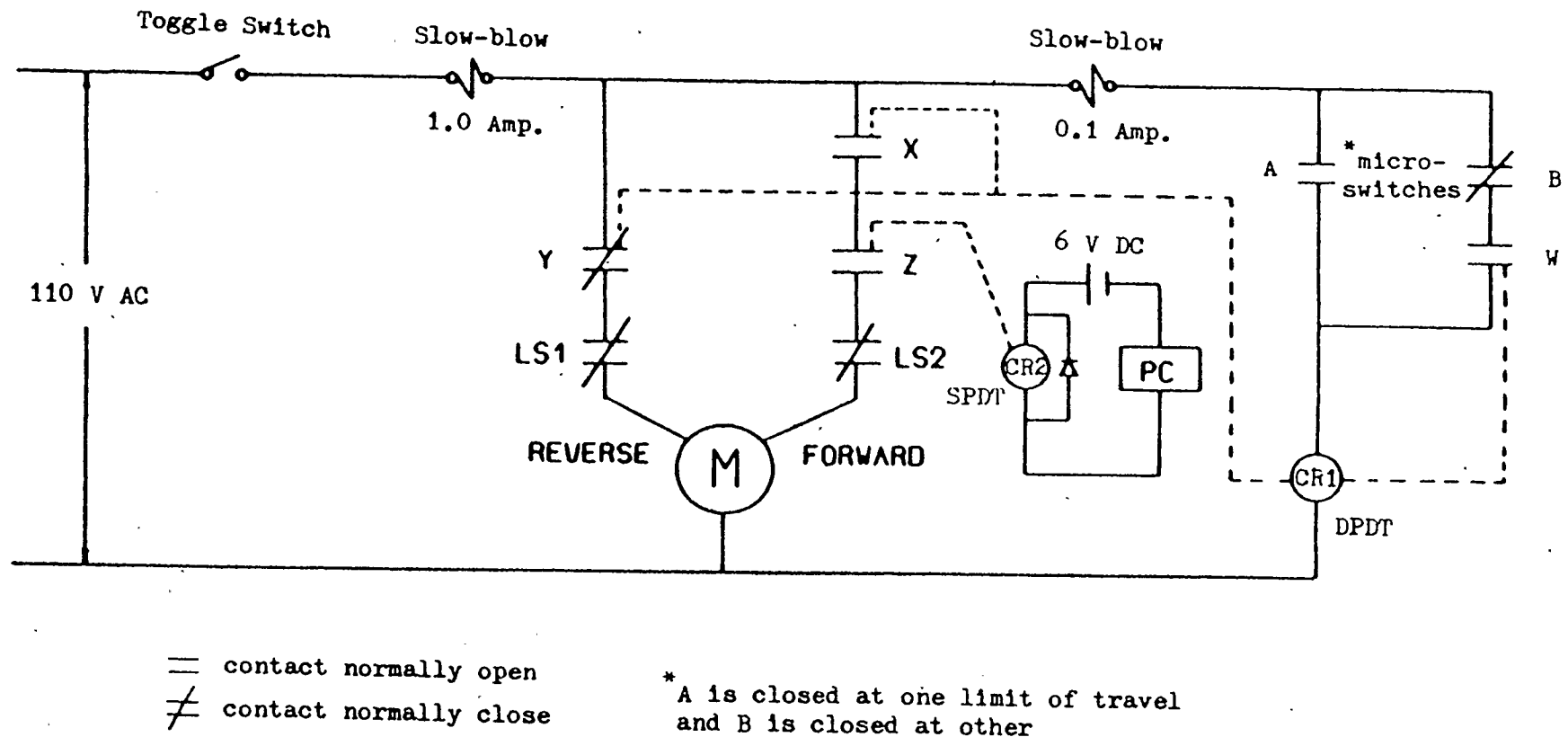


Figure 4.1.15 Apparatus control system

results in contact Y being opened and contacts W and X being closed. CR1 is now latched and continuously energized and reverse motion stops. Forward motion is now possible if contact Z is closed. Contact Z closes only if CR2 is energized. CR2 is powered by a 6 VDC supply which is turned on and off by the second serial communication port of the personal computer, PC, as desired. The second serial communication port in the personal computer effectively controls the forward motion by acting as a switch. Forward motion occurs until microswitch B is triggered which de-energizes CR1. Reverse motion now occurs and the operation cycle ends. Limit switches LS1 and LS2 were placed at each end of the direction of motion for safety. LS1 limits the reverse motion and LS2 limits forward motion of the L-shaped plate.

4.2 Preparation procedure of the experiments

In preparing for an experimental run, the model was pressure-tested and then bolted to a stool which was vibrated by a pneumatic vibrator. It was partially filled with water and 2 mm glass beads, which had been washed with detergent earlier, through fitting openings on the top. This provided uniform random packing which can be easily replicated. Water was drained through bottom fitting openings after the beads were in place and the reservoir was dried for 24 hours at 75 °C. with air passing through. The model was pressure-tested again for leakage prior to saturation with bitumen.

Homogenized Cold Lake bitumen (Batch 82-23) obtained from Alberta Research Council was used for saturating the model. The specifications of the bitumen are given in Table 4.2. The reservoir was flooded

Table 4.2 Properties of Cold Lake bitumen, Batch 82-23
(Alberta Research Council)

Well Location: 4-65-3-W4M (Cold Lake - Clearwater formation)

Production Method: Steam stimulation

Production Date: August 1982

API: 10.1

Specific gravity: 0.999 at 15 °C

Viscosity:

<u>Temperature (°C)</u>	<u>Viscosity (cp)</u>
15	110,000
25	32,800
60	1,130
100	170

Ramsbottom carbon residue: 11.5 Wt%

Acid number: 0.94 mg KOH/gm bitumen

Contents:

	<u>Wt. %</u>
C	83.35
H	10.7
N	0.94
S	4.26
O	0.89
Vn	166 ppm
Ni	66 ppm
C ₅ asphaltenes	15.7
Naphtha	3.3 (b.p. < 195 °C)
Light gas oil	15.5 (195 °C ≤ b.p. < 343 °C)
Heavy gas oil	29.6 (343 °C ≤ b.p. < 524 °C)
Water	1.5
Ash	0.06

Table 4.3 Physical parameters of 3-D reservoir model and the Cold Lake fields (some data were obtained from Chung, 1988)

	<u>Model</u>	<u>Field</u>
K, m^2	9.44×10^{-10}	2.64×10^{-13}
$g, m/s^2$	9.81	9.81
$\alpha, m^2/s$	5.87×10^{-7}	6.48×10^{-7}
$\phi \Delta S_o$	0.37	0.20
m	3.6	3.4
H, m	0.184	21.5
w, m	0.114	14.9
$T_s, ^\circ C$	109	200
$T_r, ^\circ C$	20	15
$\nu_s, m^2/s$	1.04×10^{-4}	6.02×10^{-6}

$$B_3 = \sqrt{\frac{KgH}{\phi \Delta S_o \alpha m \nu_s}} \quad \begin{array}{cc} 4.57 & 4.57 \end{array}$$

$$T' = \frac{t}{H} \sqrt{\frac{Kg\alpha}{\phi \Delta S_o m \nu_s H}} \quad \begin{array}{cc} 7.92 \times 10^{-5} t & 6.41 \times 10^{-9} t \end{array}$$

$$\frac{t_{\text{field}}}{t_{\text{model}}} = 12360 \quad \text{i.e.} \quad 1 \text{ hr}_{\text{model}} = 1.41 \text{ years}_{\text{field}}$$

upwards from the bottom at 75 °C. in the oven and cooled for 48 hours at room temperature (20 °C.) before operation. A 100 percent saturation of oil was achieved.

After each experiment, the model was cleaned by circulating varsol continuously for 24 hours. After this, a dishwashing solution (Joy 2 detergent) was circulated for another 12 hours and the model was flushed with tap water for 4 hours. It was dried and was then ready for saturation if the same well configuration was to be used. If a different configuration was required the glass beads were removed and the model was vibrated as described earlier after the desired well configuration was in place.

The physical parameters of the reservoir model and the Cold Lake fields are shown in Table 4.3.

4.3 Steam

The steam supplied by the University's physical plant was used in all the experiments. To ensure that only dry steam was used, the steam line was insulated and heated to 5 °C. above the saturated steam temperature.

The steam pressure used for all the experiments was regulated at approximately 139 kpa absolute (7.5 psig).

4.4 Sample analysis

Samples collected from the experiments at five minutes intervals in preweighed 500 ml sample bottles were analyzed for the amount of oil and steam condensate produced. The samples were cooled to 5 °C in a

refrigerator and weighed. Most of the free water in the samples was easily removed from the bottles by carefully tilting the bottles and pouring away only the water. This was simple because, due to the low temperature, the bitumen was too viscous to flow. The samples were weighed again to determine the amount of water removed. Toluene containing 2.5 percent of a demulsifier, "Breaxit 8204", was added to the samples (approximated twice the volume of the sample) and the samples were allowed to soak for 48 hours at room temperature. The toluene (specific gravity = 0.867 at 20 °C) increased the density difference between the two phases (water and diluted bitumen) and also reduce the viscosity of the bitumen. Following this, the remaining water in each sample settled to the bottom of the sample bottles. Most of the diluted bitumen was then removed carefully by a peristaltic pump. A light source was placed against the sample bottle so that the water level could be observed to be undisturbed during the decanting process as shown in Figure 4.4.1. The samples were then transferred into 100 ml centrifuge tubes with an additional small amount of toluene used to rinse the bottles. The centrifuge method, (ASTM D4007-81) was used to determine the amount of water in these tubes. The tubes were centrifuged for 20 minutes at 2450 rpm in an IEC model K machine.

A simple mass balance was performed from the information obtained using the above procedure and the amount of oil and steam condensate produced at each time interval were calculated.

The analytical technique was tested for its reliability using several control experiments. Five samples of Cold Lake bitumen were used. The samples were first heated to 100 °C. and specific amount of

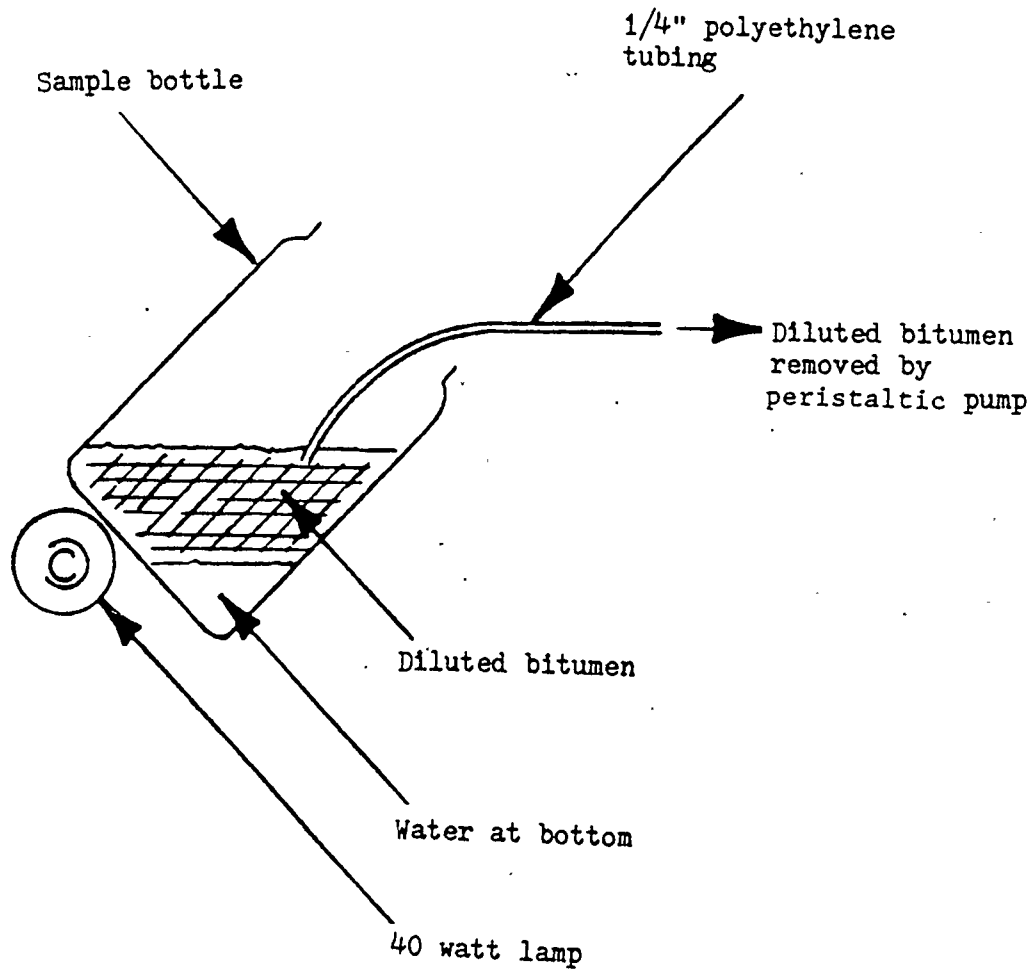


Figure 4.4.1 Decanting diluted bitumen

Table 4.4 Results of control experiments in sample analysis

Sample #	Oil Content (grams)		Water Content (grams)	
	Actual	From Analysis	Actual	From Analysis
1	58.27	58.6	10.67	10.4
2	42.58	42.5	18.67	18.9
3	37.53	37.8	44.70	44.1
4	75.83	76.8	67.30	66.9
5	78.82	78.9	22.50	22.5

distilled water was added into each sample with the bottles being slightly agitated. The samples were then stored in the refrigerator and analyzed as described earlier. Results obtained are shown in Table 4.4.

The above procedure was again tested for its reliability by collecting the removed fluid from the outlet of the peristaltic pump and centrifuging it for water content. Four samples were collected from a sample bottle and centrifuged as mentioned earlier. No water was found from these samples.

4.5 The steam injector

Steam was injected into the model through vertical steam injectors perforated at the top of the reservoir. Figure 4.5.1 shows the schematic diagrams of the steam injector during start up and operation respectively. The perforations were made up of four 2.5 mm diameter holes which were covered by 200 mesh wire gauze to prevent the glass beads from plugging the holes.

4.6 The horizontal producer

Produced fluids from the reservoir were recovered by the perforated horizontal well. The perforation were made up of 1.75 mm diameter holes spaced approximately at 3 mm apart (centre to centre). The schematic diagrams of the horizontal producer during startup and during production are shown in Figure 4.6.1 and 4.6.2 for the cases studied.

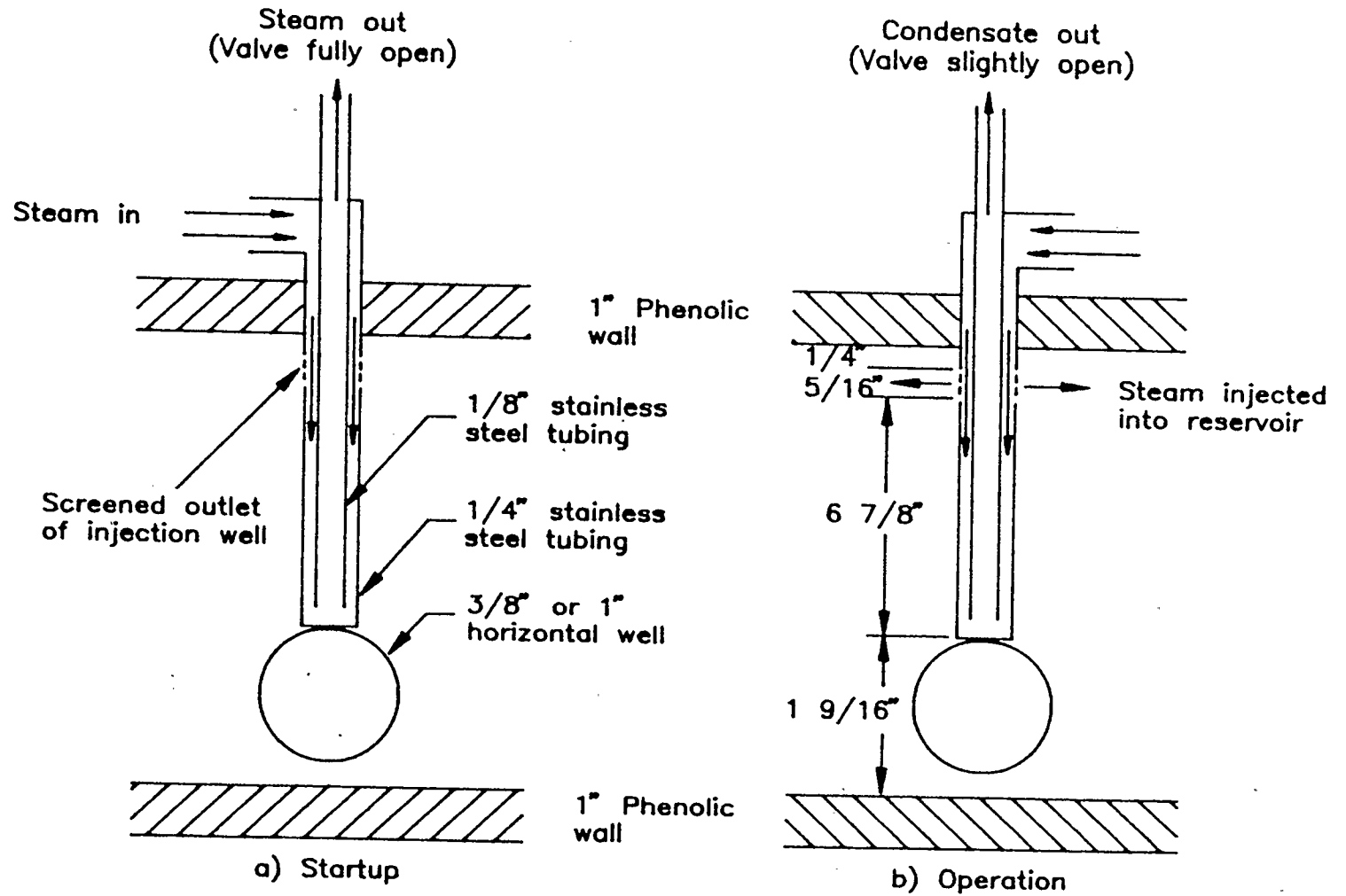


Figure 4.5.1 Schematic diagram of steam injector during startup and operation

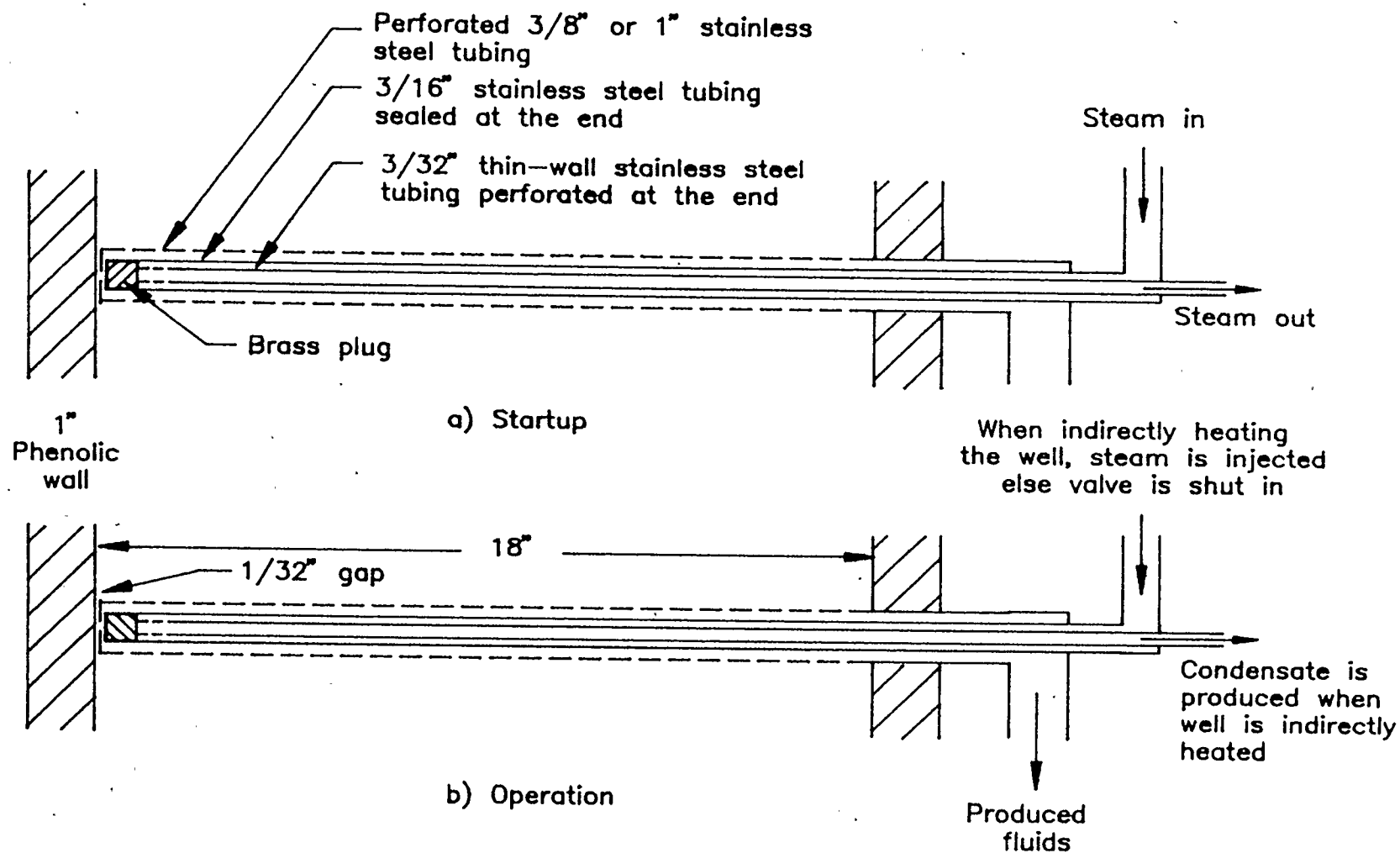


Figure 4.6.1 Schematic diagram of horizontal well during startup and operation for the case of unheated and indirectly heated well

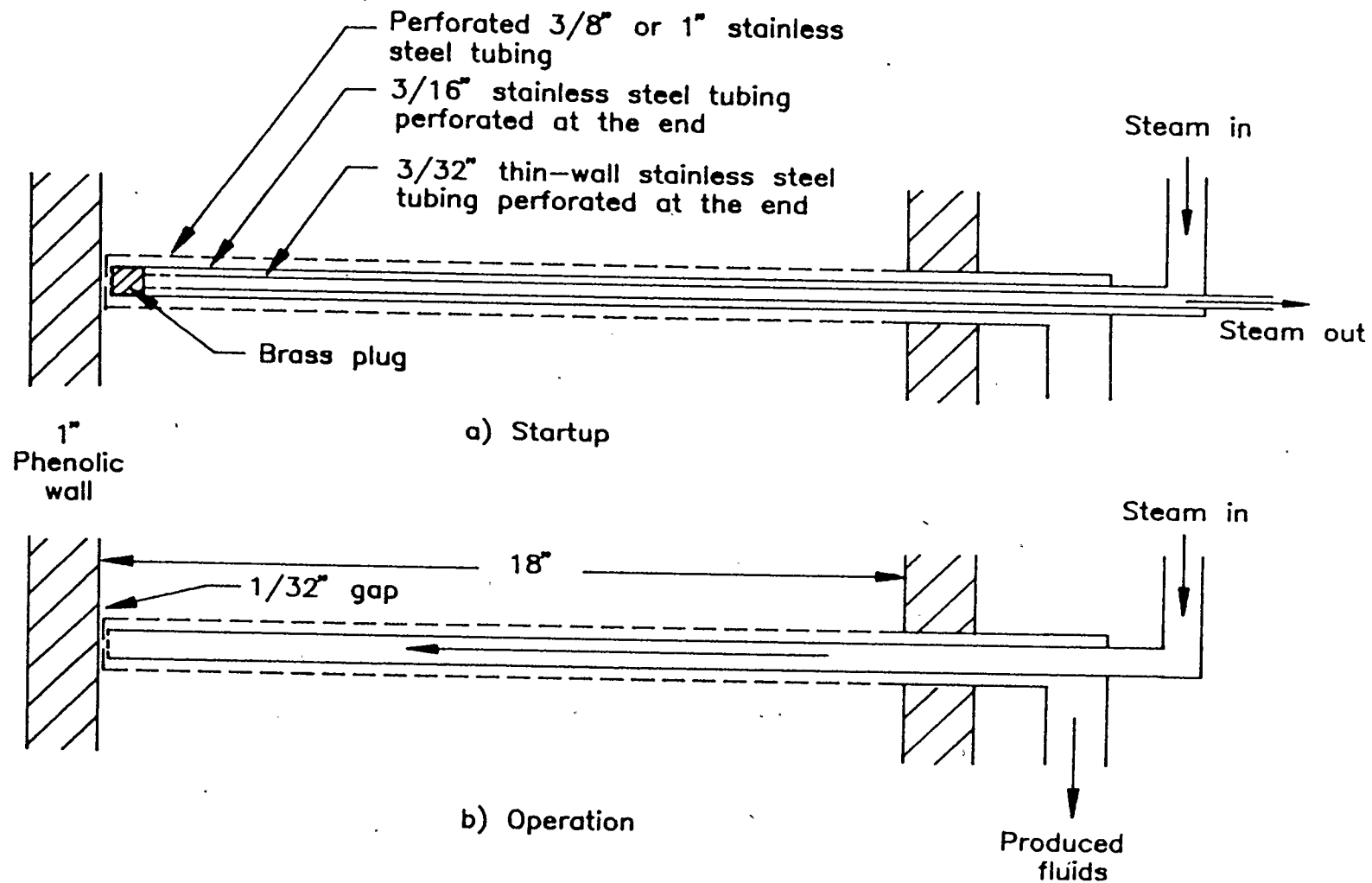


Figure 4.6.2 Schematic diagram of horizontal well during startup and operation for the case of introducing steam into the well

4.7 Experiments

A total of 12 experiments was conducted to study the performance of top vertical steam injection with horizontal well production. Table 4.5 summarizes the various types of experiments performed. Please refer to Figure 4.7.1 to 4.7.4 for further clarification. The purposes of these experiments are summarized below.

4.7.1 Repeatability of results

Two repeat experiments (Run #1 and #3) were performed with the same operating conditions. The steam injector was placed at the middle of the reservoir as shown in Figure 4.7.1. The horizontal well was operated with just the minimal amount of steam being produced. It is termed "unheated".

4.7.2 The effect of heating the horizontal well during production

Run #2 was performed with the configuration as shown in Figure 4.7.1. The horizontal well was heated continuously by introducing steam into the inner tubing. It is termed "indirectly" heated. The results can be compared with those of Run #1 or #3 to see the effect of indirect heating. The well temperature was kept at approximately 100 °C (measured steam condensate temperature was 100 °C) throughout the experiment.

The effect of heating was expected to affect the "hot" end more than the "cold" end of the horizontal well. The hot end is defined as the portion of the horizontal well from the position of the vertical well toward the production outlet. The other portion of the horizontal

well is defined as the cold end. Run #4 to #6 were performed to observe the effect of heating only the hot end. The well configuration is shown in Figure 4.7.2. Run #4 was performed with the horizontal well being unheated. Run #5 was performed with the well being indirectly heated. The process of heating can also be achieved by letting steam flow out of the horizontal well freely. This was done in Run #6.

4.7.3 The effect of eliminating the use of the cold end of the horizontal well

Run #7 was performed to observe this effect. The horizontal well only extended to the middle of the reservoir model with the steam injector placed over the end of the well. The well configuration is shown in Figure 4.7.3. The experiment was performed with the horizontal well being unheated. The results can be compared with those of Run #1 to observe the above effect.

4.7.4 Comparison of production performance between vertical and horizontal well steam injection

The results of Run #4 (vertical well steam injection) was used to compare production performance with the theoretical prediction using the TANDRAIN equation (horizontal well steam injection described by equation (3.1.24)) for a confined well. Butler et al (1981b) reported good match between predicted production performance using this equation and experimental results. The objective of this effort was to evaluate the overall performance of the vertical steam injector/horizontal well scheme. A similar comparison is also made for Run #12 in which two

Table 4.5 Summary of experimental conditions

Run #	No. of vertical injectors	Location of vertical injectors	Conditions of 3/8" horizontal well
1	1	middle	unheated
2	1	middle	indirectly heated
3	1	middle	repeat of run # 1
4	1	end	unheated
5	1	end	indirectly heated
6	1	end	steam let out
7	1	middle	unheated (half-length)
8	2	front, end (Both well at same pressure - 7.5 psig)	unheated
9	2	front @ 7 psig end @ 8 psig	unheated
10	2	front @ 7 psig end @ 8 psig	steam let out
11	2	front @ 7 psig end @ 8 psig	steam introduced @ end of horizontal well
12	2	same as Run #8	unheated 1" well

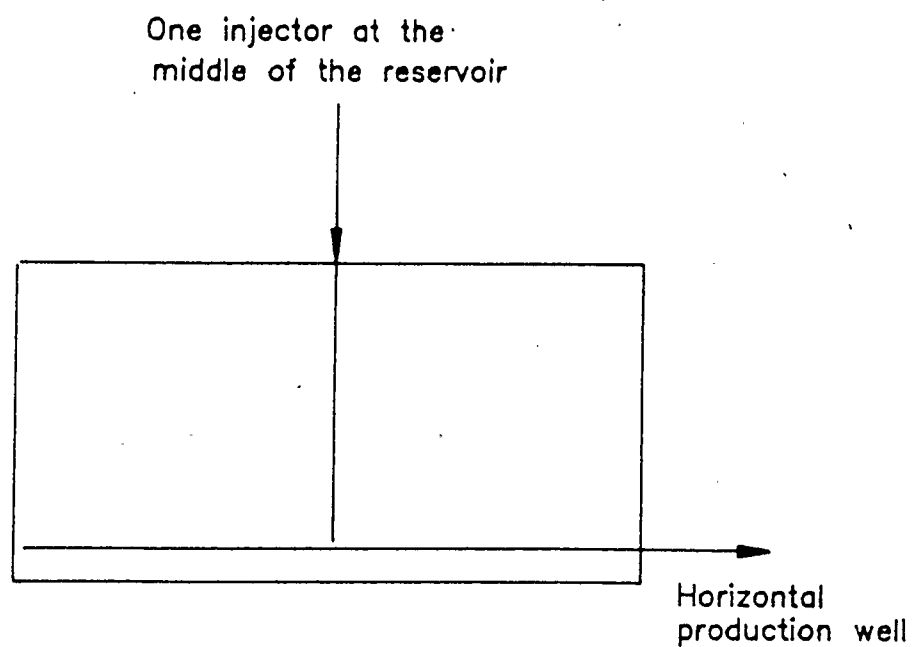


Figure 4.7.1 Well configuration for Runs #1, #2 and #3

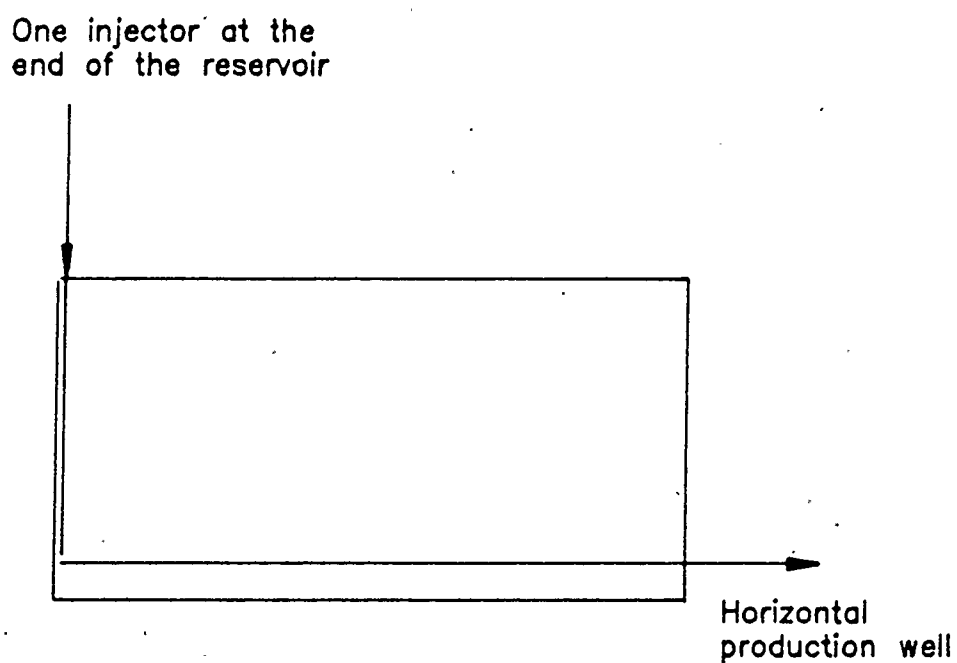


Figure 4.7.2 Well configuration for Runs #4, #5 and #6

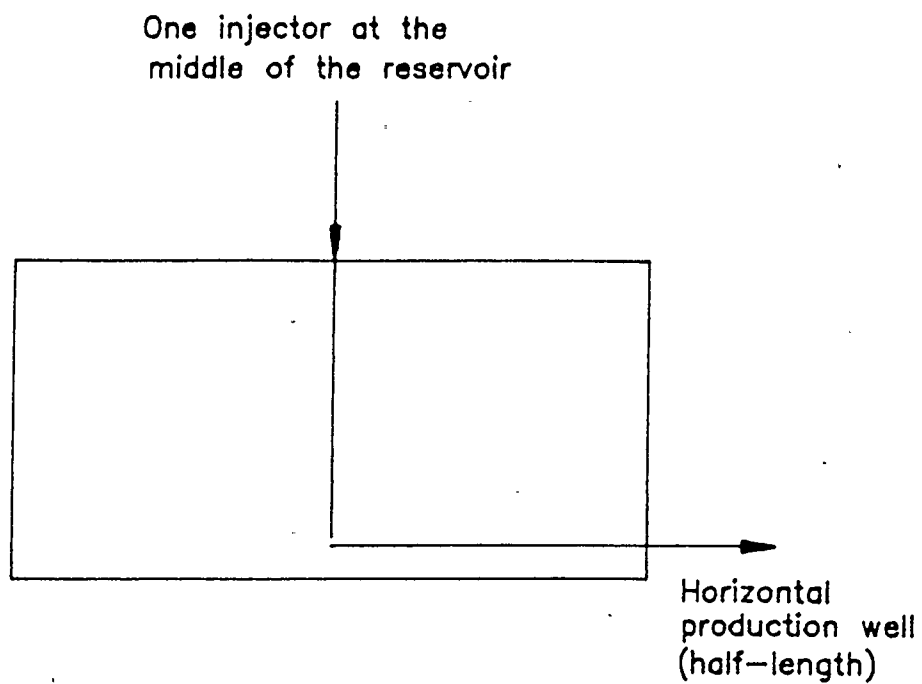


Figure 4.7.3 Well configuration for Run #7

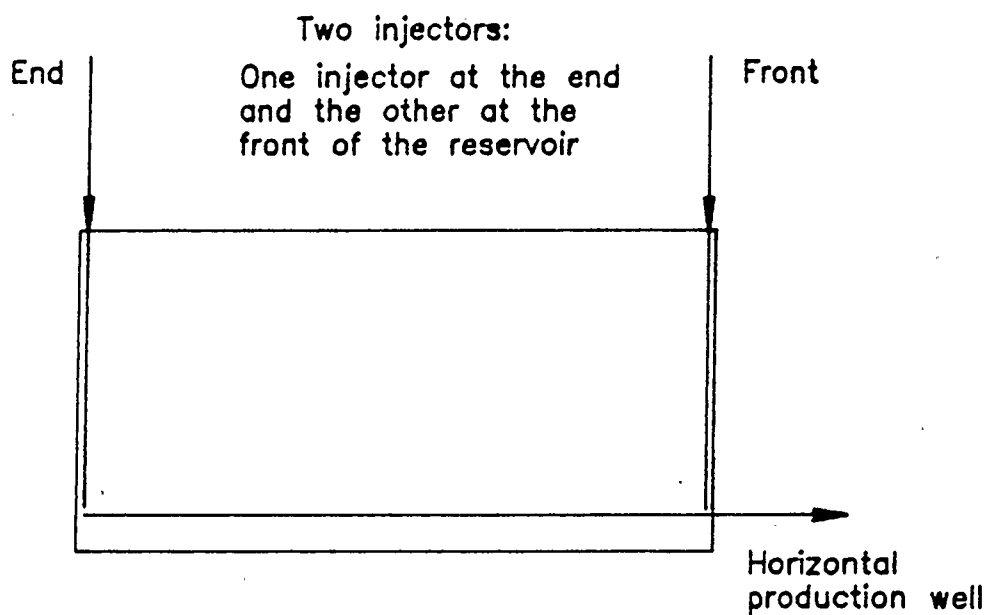


Figure 4.7.4 Well configuration for Runs #8, #9, #10, #11 and #12

injectors were placed along the production well at each end of the reservoir model (Figure 4.7.4).

4.7.5 Performance using two injectors

To study the performance with two vertical wells along the horizontal well, Runs #9 to #12 were performed. One injector was placed at the end while the other was placed at the front of the reservoir model. The spacing between the wells was 17.5 inches. The well configuration is shown in Figure 4.7.4. The purpose of these experiments was to determine the effect of increasing the number of injectors on the cumulative oil production.

As a result of these experiments, it was found that the end of the horizontal well could not be drained effectively because of excessive flow resistance along the well. This problem is discussed later. Run #12 was performed using a larger horizontal well (1" O.D.) instead of the regular 3/8" well used for all the other experiments for the purpose of studying this concern.

CHAPTER 5

RESULTS AND DISCUSSION

This chapter presents the results of twelve experiments performed with Cold Lake bitumen. The results of experiment Run #12 is also discussed in Chapter 6. A summary of the operating conditions was presented earlier in Chapter 4 on page 57. The results and discussion are divided into five sections as outlined in the previous chapter.

5.1 Repeatability of results

Two indential runs were performed using the 3-D apparatus. Run #1 and #3 were performed for the purpose of obtaining reproducible results. The oil production curves shown in Figure 5.1.1 show that results obtained from the experiments were almost identical. Experiments can thus be repeated and results are reproducible.

5.2 The effect of heating the horizontal well during production

The effect of heating the horizontal well during production was first studied by performing Run #2. The horizontal well was heated indirectly by means of a central 3/32" diameter steam-filled tube (please refer to Figure 4.6.1). The vertical steam injector was placed at the middle of the reservoir model. The results of Run #2 and #3 are compared in Figure 5.2.1.

Figure 5.2.1 shows the increase in percent recovery due to the effect of indirect heating. The overall recovery was increased by approximately 6 percent after 5 hours of experimental time.

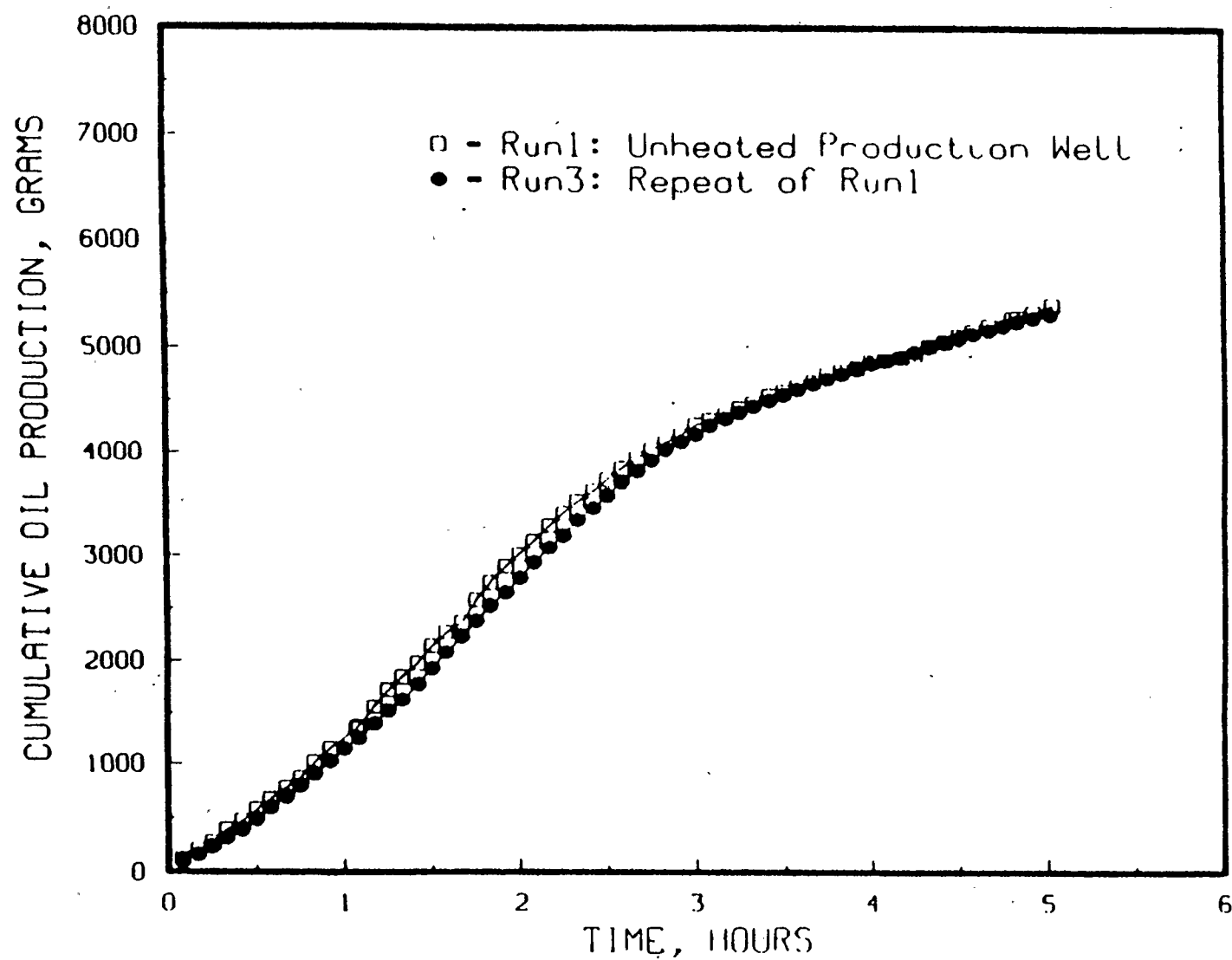


Figure 5.1.1 Comparison of cumulative oil production for Runs #1 and #3

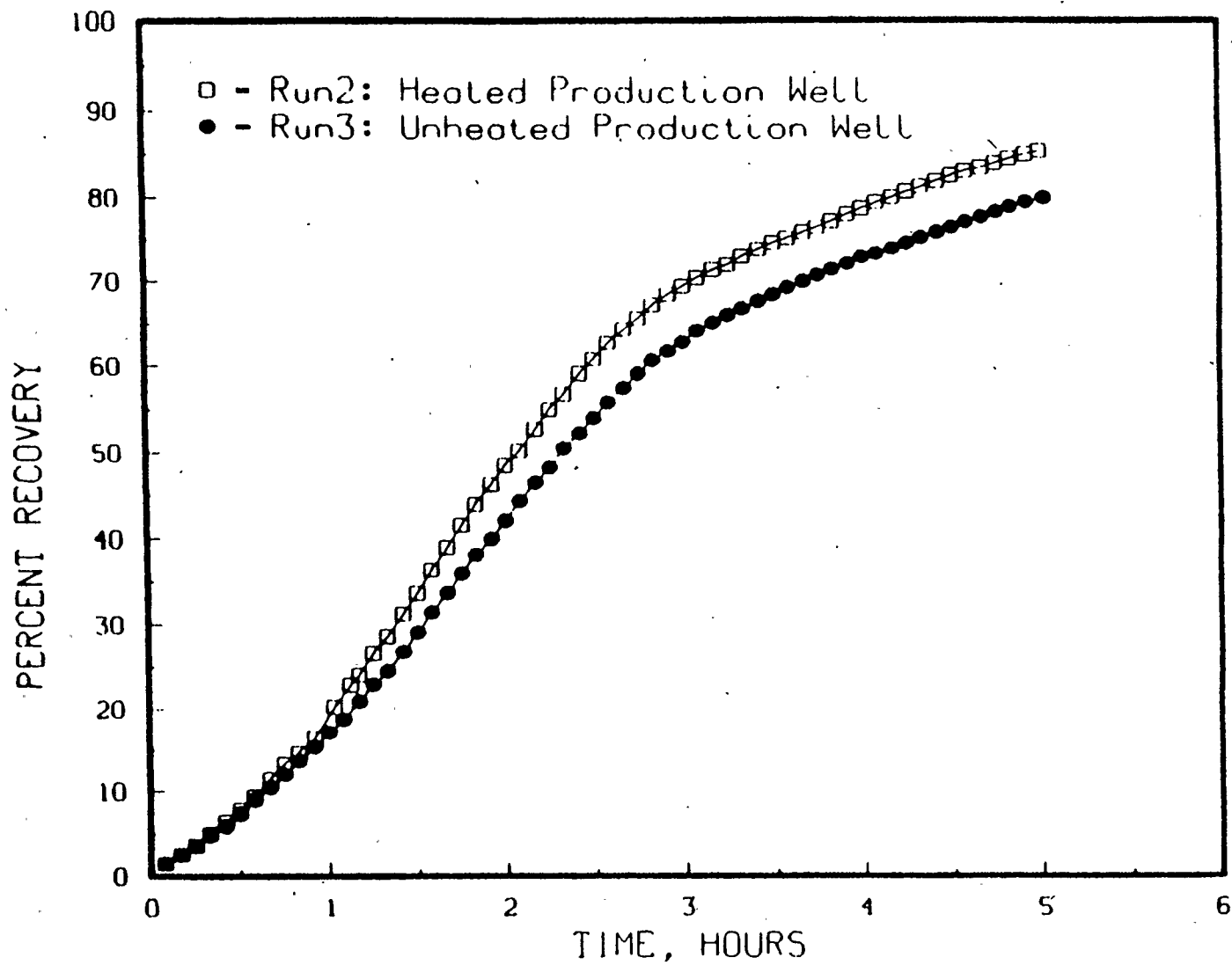


Figure 5.2.1 Effect of indirectly heating the production well on percent recovery

During the first hour of the experiments, that is during the period of recovering the first 20 percent of the bitumen, the effect of heating the horizontal well was not noticeable. Figure 5.2.2 which compares the oil production rates shows the effect in greater details. After the period of 20 percent recovery, the production rate was observed to have increased by approximately 15 percent. This increment was being continuously sustained till the end of the experiment at 5 hours.

The above observations can be explained as follows. Heat was transferred radially around the horizontal well by conduction through the indirect heating. Since conduction is a relatively slow process, the heat front moved slowly. The change of viscosity around the wellbore was dramatic but the penetration depth was insignificant. Figure 5.2.3 illustrates the process. As the experiment progressed and the heat front propagated further, the effect of heating the well became more significant. Referring to the figure, the steam chamber at the hot end of the horizontal well propagates faster than the steam chamber at the cold end. The hot end of the well was heated in two ways in Run #2. The first was by the indirect heating. The second was by the steam escaping from the steam chamber. During the experiment the production valve was controlled such that a minimal amount of steam escaped. Nevertheless, the effect of this small amount of steam escaping was tremendous since the heat transfer from the steam to the fluids within the well was by convection instead of conduction as in the cold end of the well. Effectively, the radius of hot zone was the full radius of the $3/8$ " pipe instead of the $3/16$ " inner tubing.

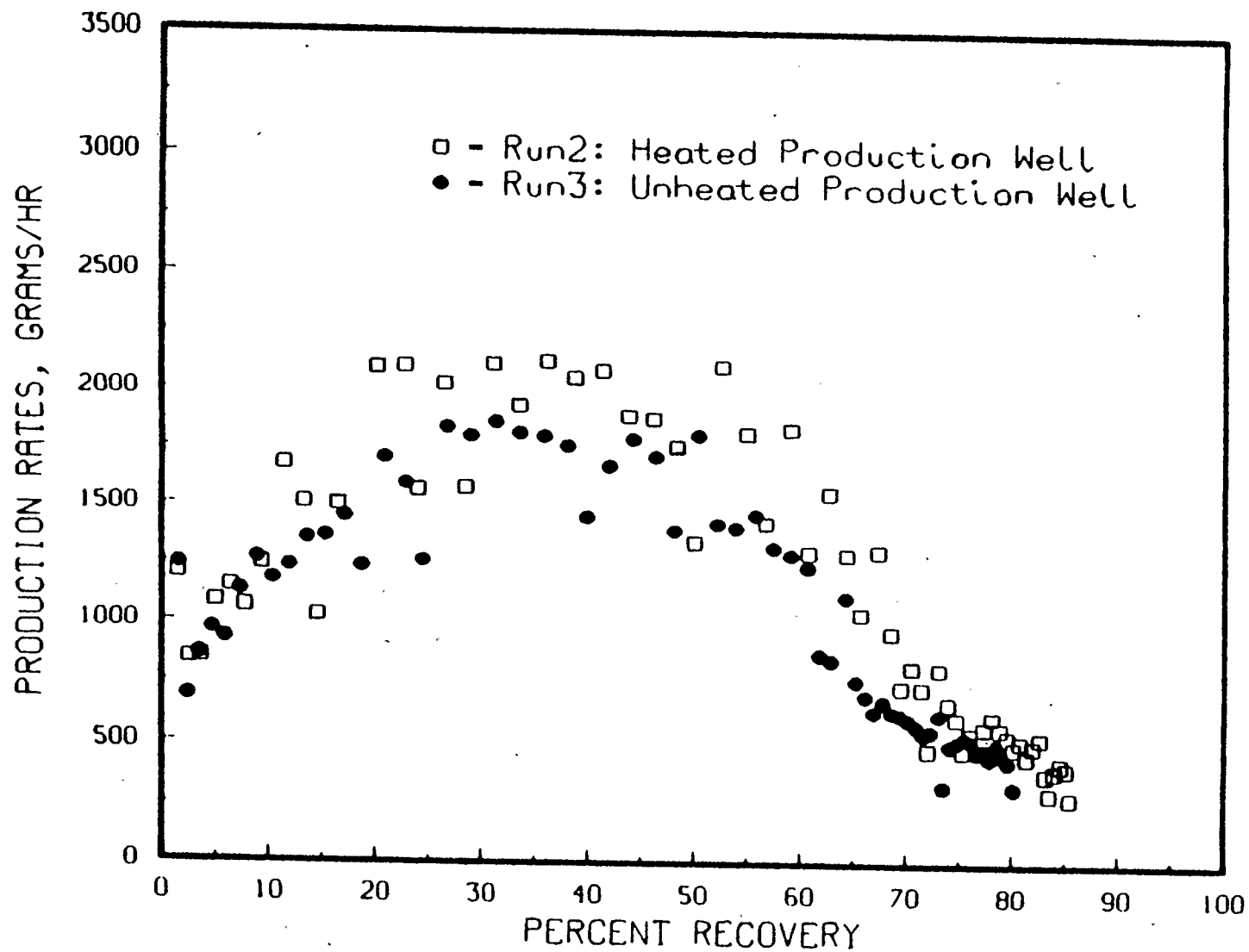


Figure 5.2.2 Effect of indirectly heating the production well on oil production rate

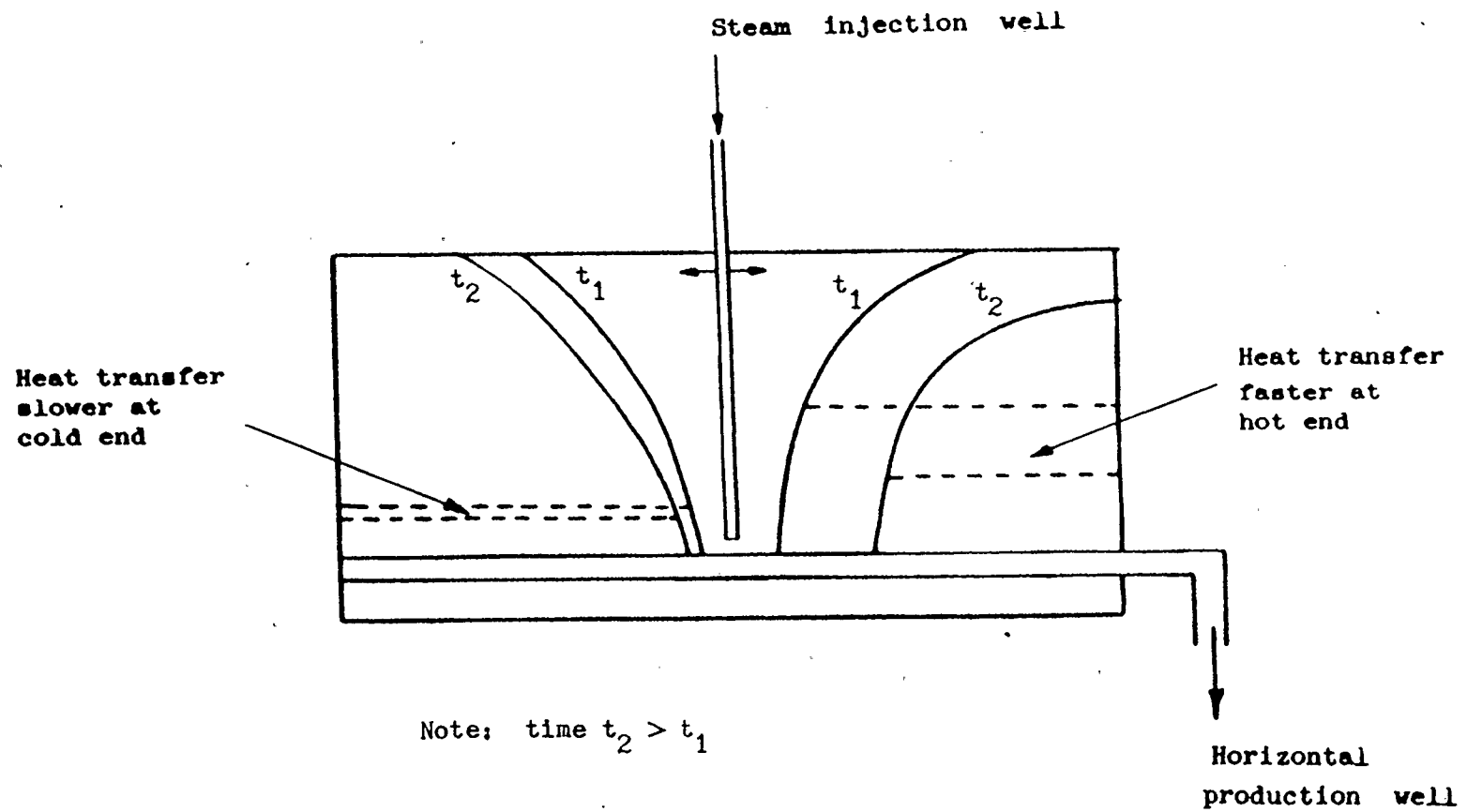


Figure 5.2.3 Propagation of heat front from horizontal well

Essentially, the indirect heating along the hot end of the well was not effective because the convective heat transfer due to the steam in the annulus of the pipe was dominant. In contrast, at the cold end of the well, the heating was only due to the indirect heating. So, the radius of the heated well was effectively that of the 3/16" inner tubing. Hence, the radial heat transfer at this end of the well was much slower. Consequently, the propagation of the steam chamber along this end of the well was slower than the hot end. This effect was also reported by Griffin and Trofimenkoff (1984). They attributed this phenomenon to a lower m factor due to higher temperature at the hot end of the production well. However, it was later discovered in the course of this thesis work that the phenomenon described would not have any significant impact if the production well used in the experiments were large enough to handle the flow of the produced fluids. Flow restriction along the pipe was the main reason that the propagation of the steam chamber along the cold end was inhibited. This was not reported by Griffin and Trofimenkoff.

Figure 5.2.4a to 5.2.4c shows the movement of the steam interface along the horizontal well during the experiment. The temperature profile taken during the experiment along the central plane were plotted using SURFACE II (Sampson, 1978) contouring software. The approximate steam/oil interface was located at the 100°C isotherms (Chung, 1988). The movement of the interface in the figures supports the explanation given above. Successive planes across the reservoir model of these interfaces were digitized and the data obtained were used to plot the steam chamber in three dimensions using DISSPLA/9.0

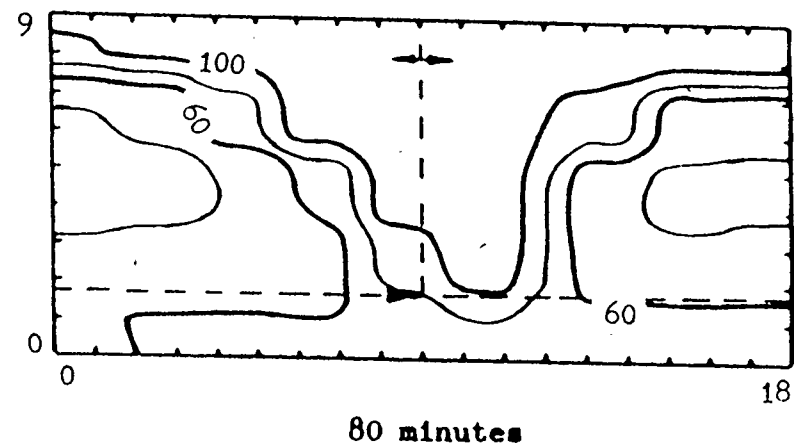
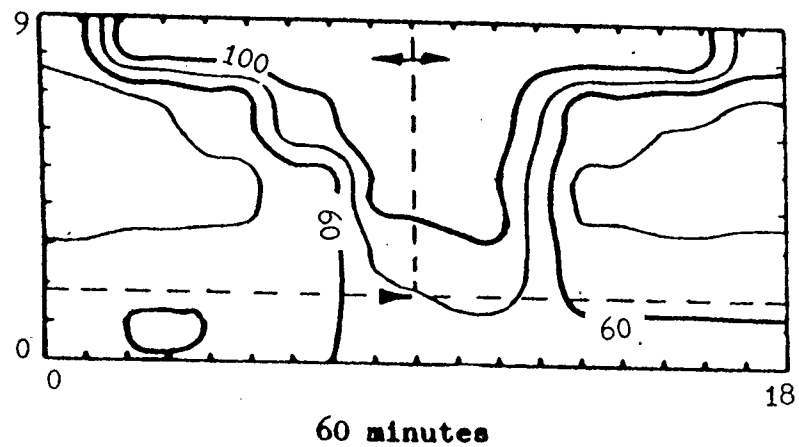
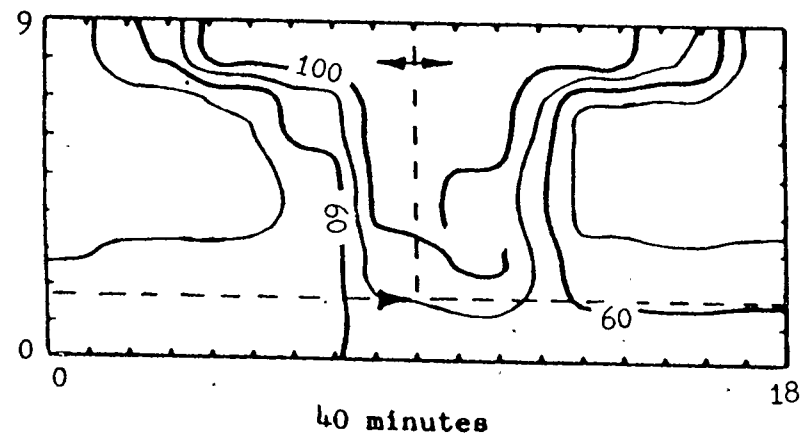
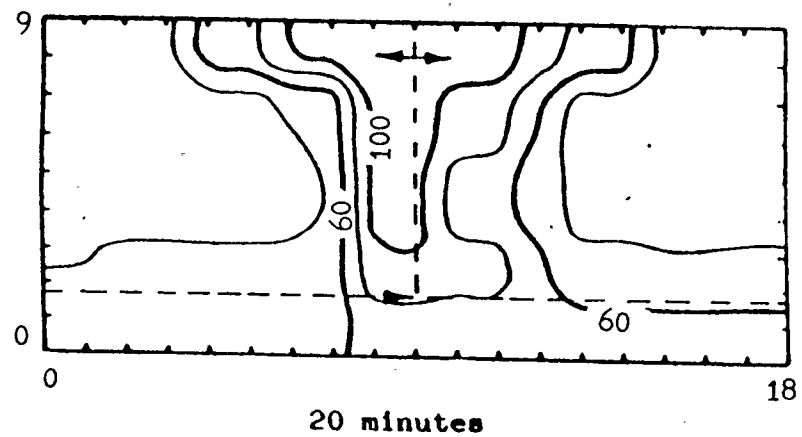


Figure 5.2.4a Movement of steam/oil interface in Run #2, 20 to 80 minutes

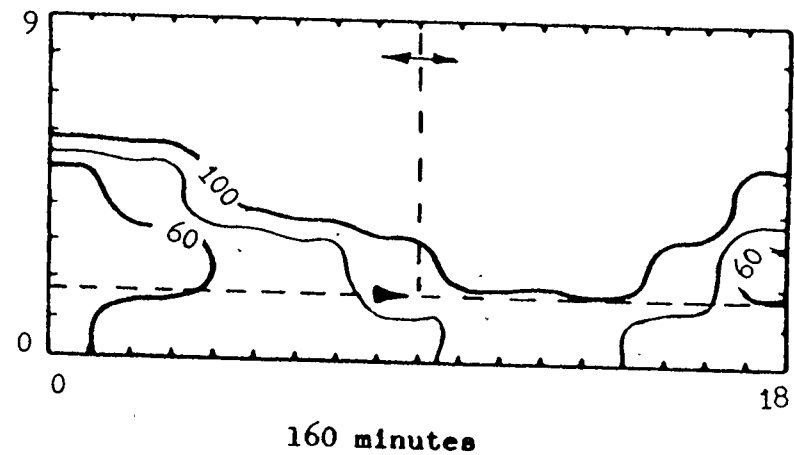
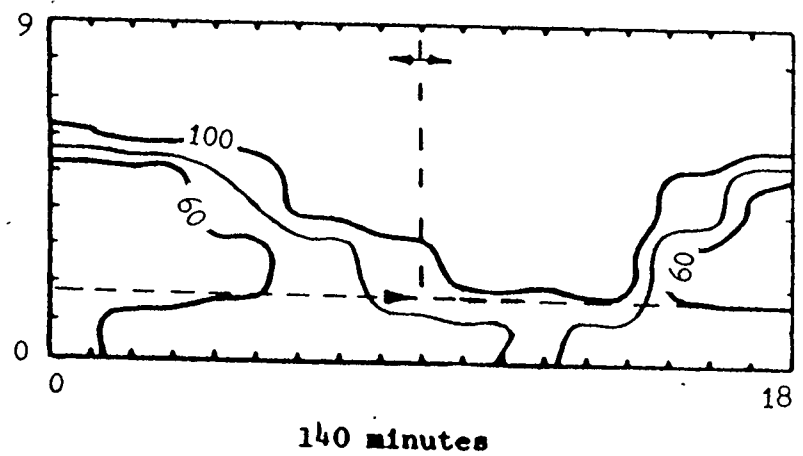
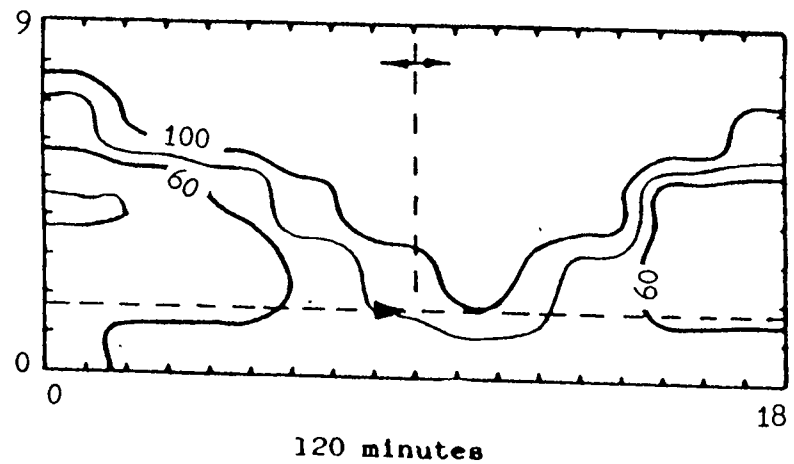
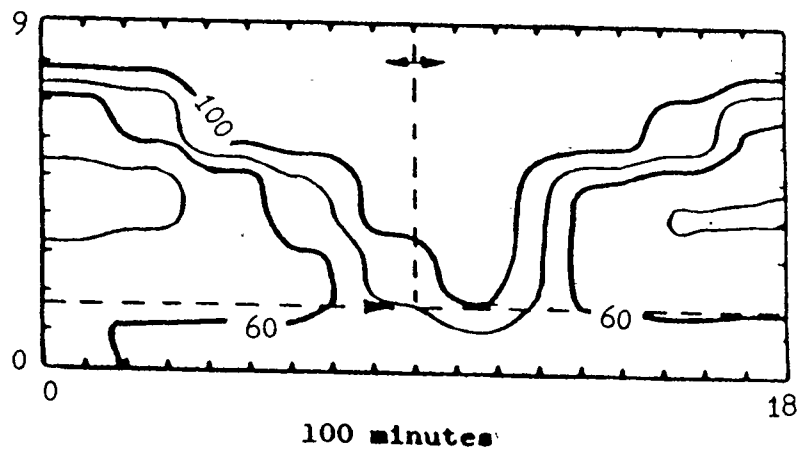


Figure 5.2.4b Movement of steam/oil interface in Run #2, 100 to 160 minutes

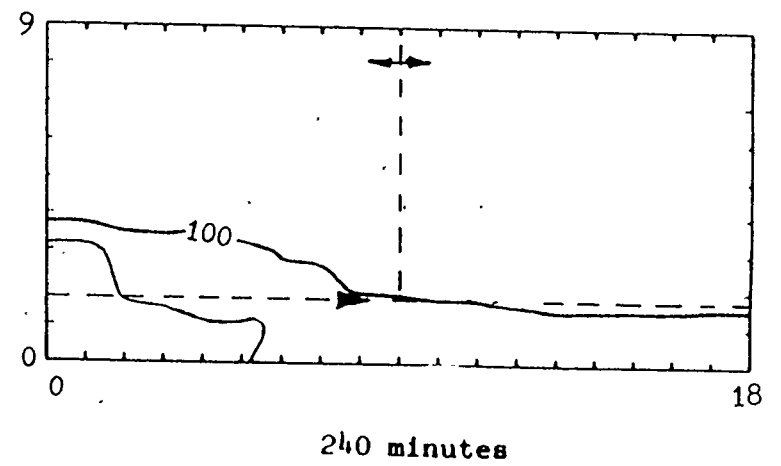
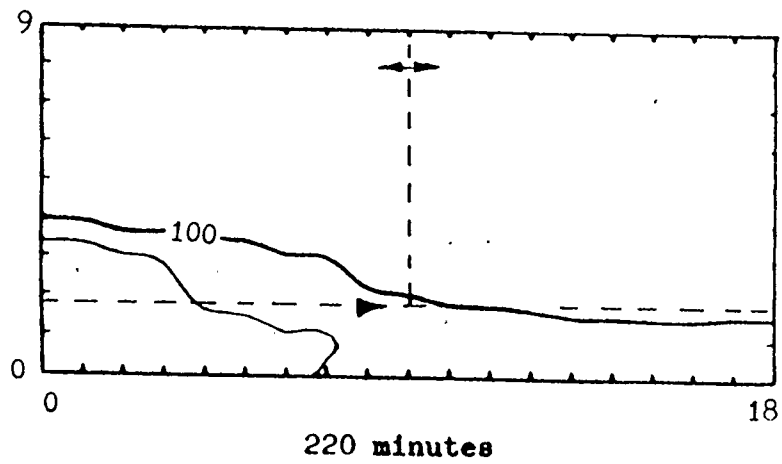
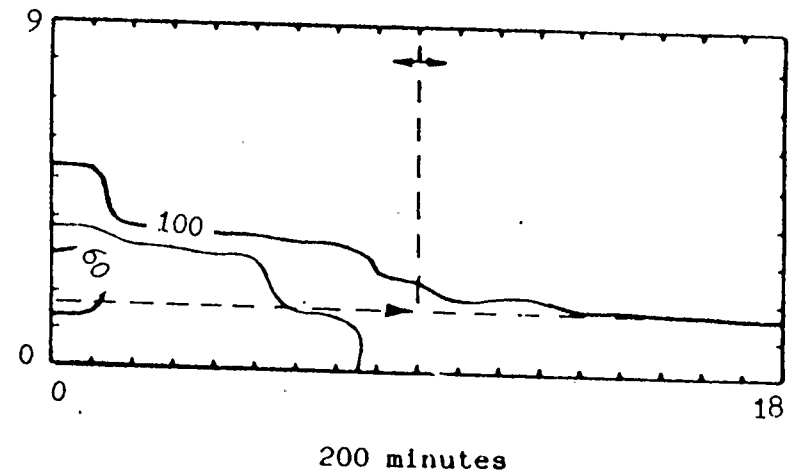
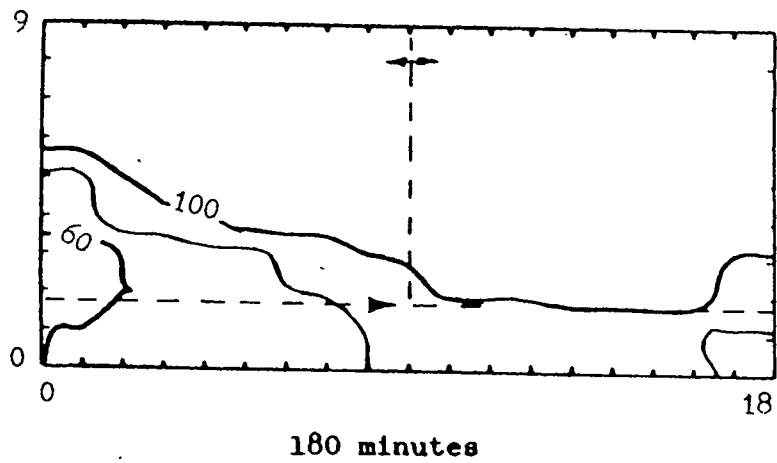
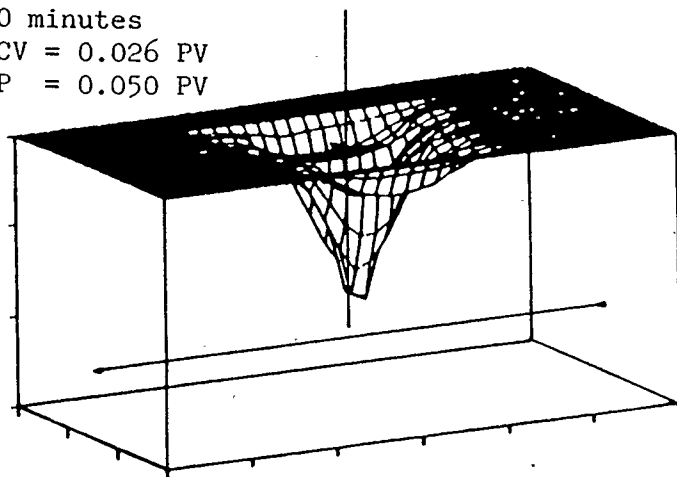
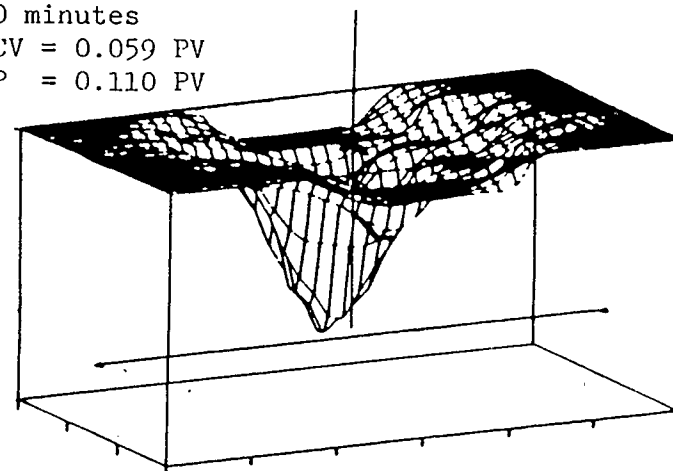


Figure 5.2.4c Movement of steam/oil interface in Run #2, 180 to 240 minutes

20 minutes
SCV = 0.026 PV
OP = 0.050 PV

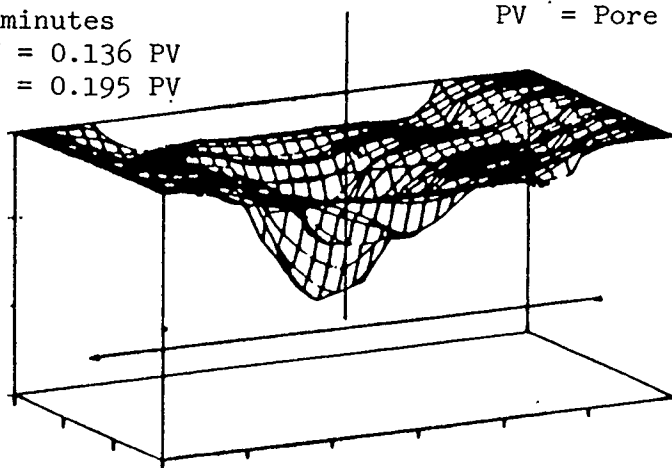


40 minutes
SCV = 0.059 PV
OP = 0.110 PV



Note:
SCV = Steam Chamber Volume
OP = Oil Produced
PV = Pore Volume

60 minutes
SCV = 0.136 PV
OP = 0.195 PV



80 minutes
SCV = 0.195 PV
OP = 0.291 PV

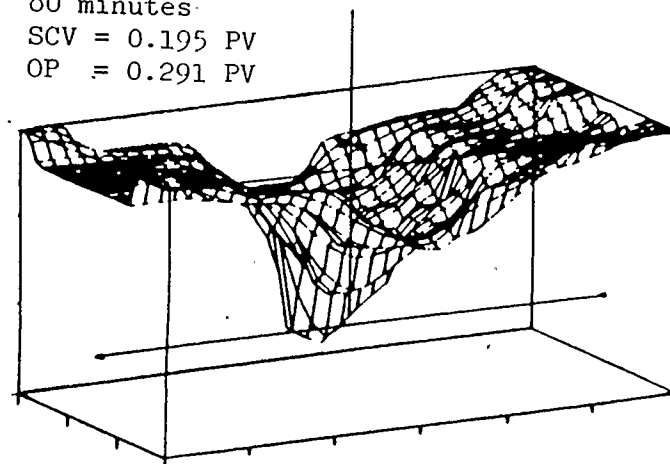
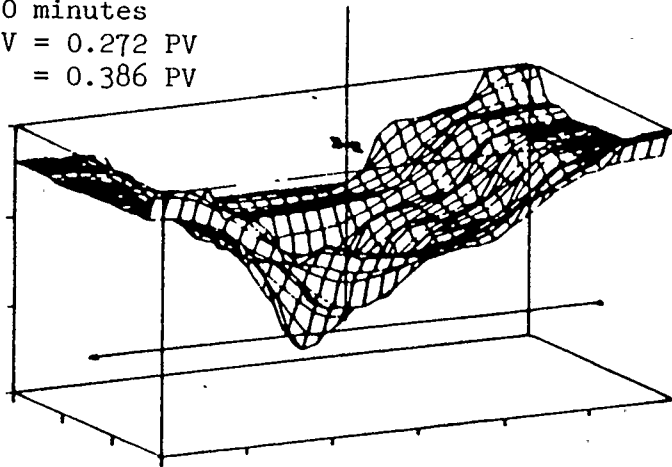
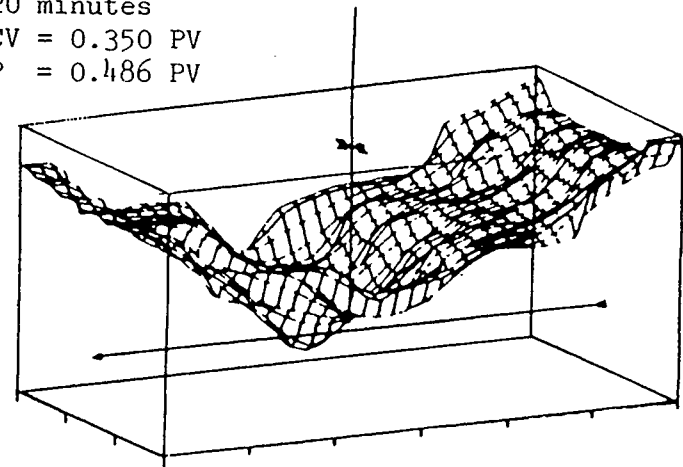


Figure 5.2.5a 3-dimensional steam chamber growth in Run #2, 20 to 80 minutes

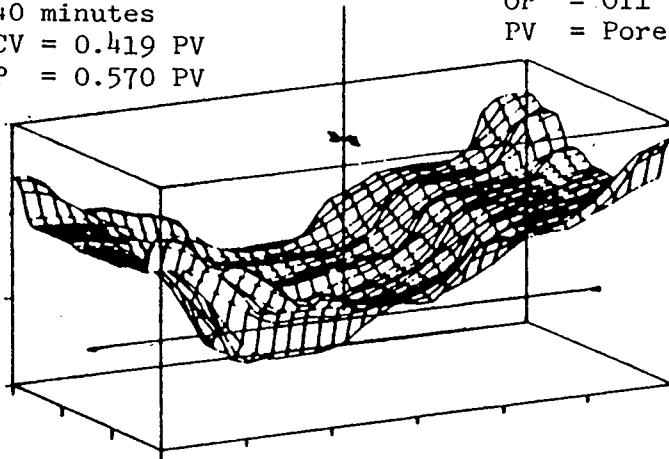
100 minutes
 SCV = 0.272 PV
 OP = 0.386 PV



120 minutes
 SCV = 0.350 PV
 OP = 0.486 PV



140 minutes
 SCV = 0.419 PV
 OP = 0.570 PV



Note:
 SCV = Steam Chamber Volume
 OP = Oil Produced
 PV = Pore Volume

160 minutes
 SCV = 0.482 PV
 OP = 0.640 PV

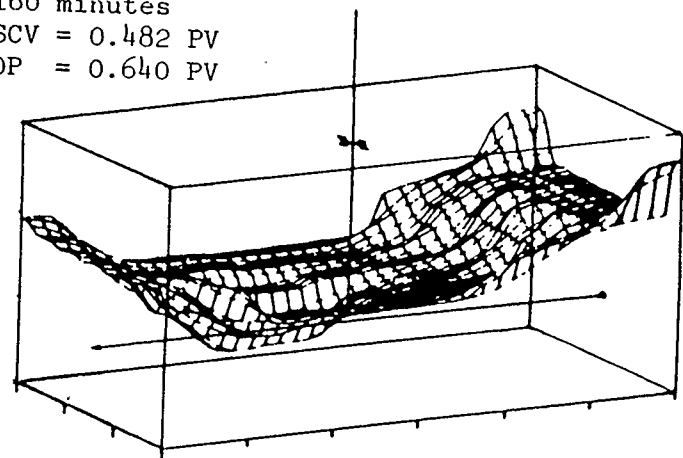
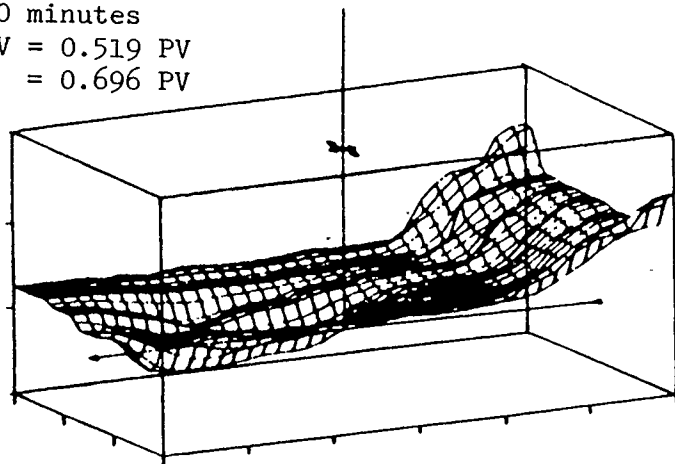
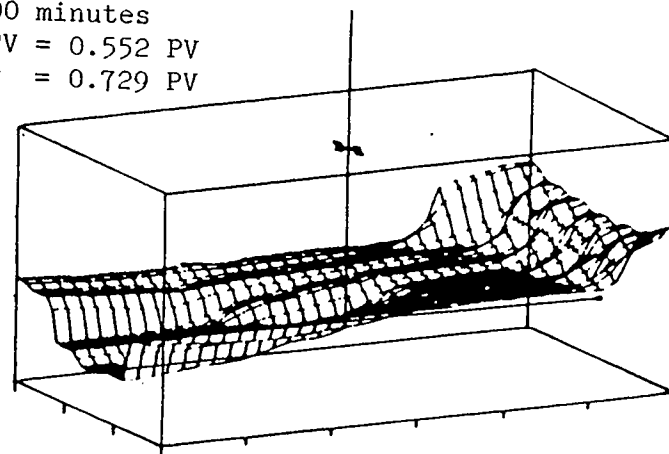


Figure 5.2.5b 3-dimensional steam chamber growth in Run #2, 100 to 160 minutes

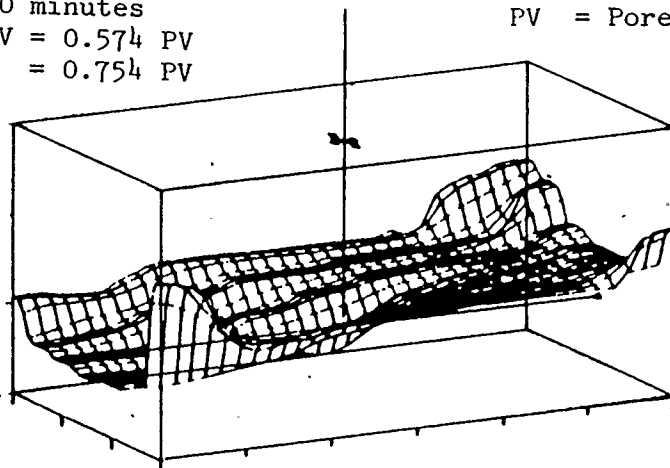
180 minutes
 SCV = 0.519 PV
 OP = 0.696 PV



200 minutes
 SCV = 0.552 PV
 OP = 0.729 PV



220 minutes
 SCV = 0.574 PV
 OP = 0.754 PV



Note:
 SCV = Steam Chamber Volume
 OP = Oil Produced
 PV = Pore Volume

240 minutes
 SCV = 0.589 PV
 OP = 0.784 PV

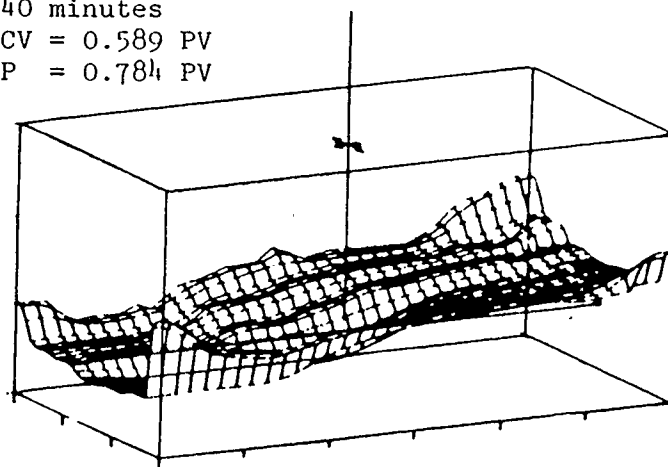


Figure 5.2.5c 3-dimensional steam chamber growth in Run #2, 180 to 240 minutes

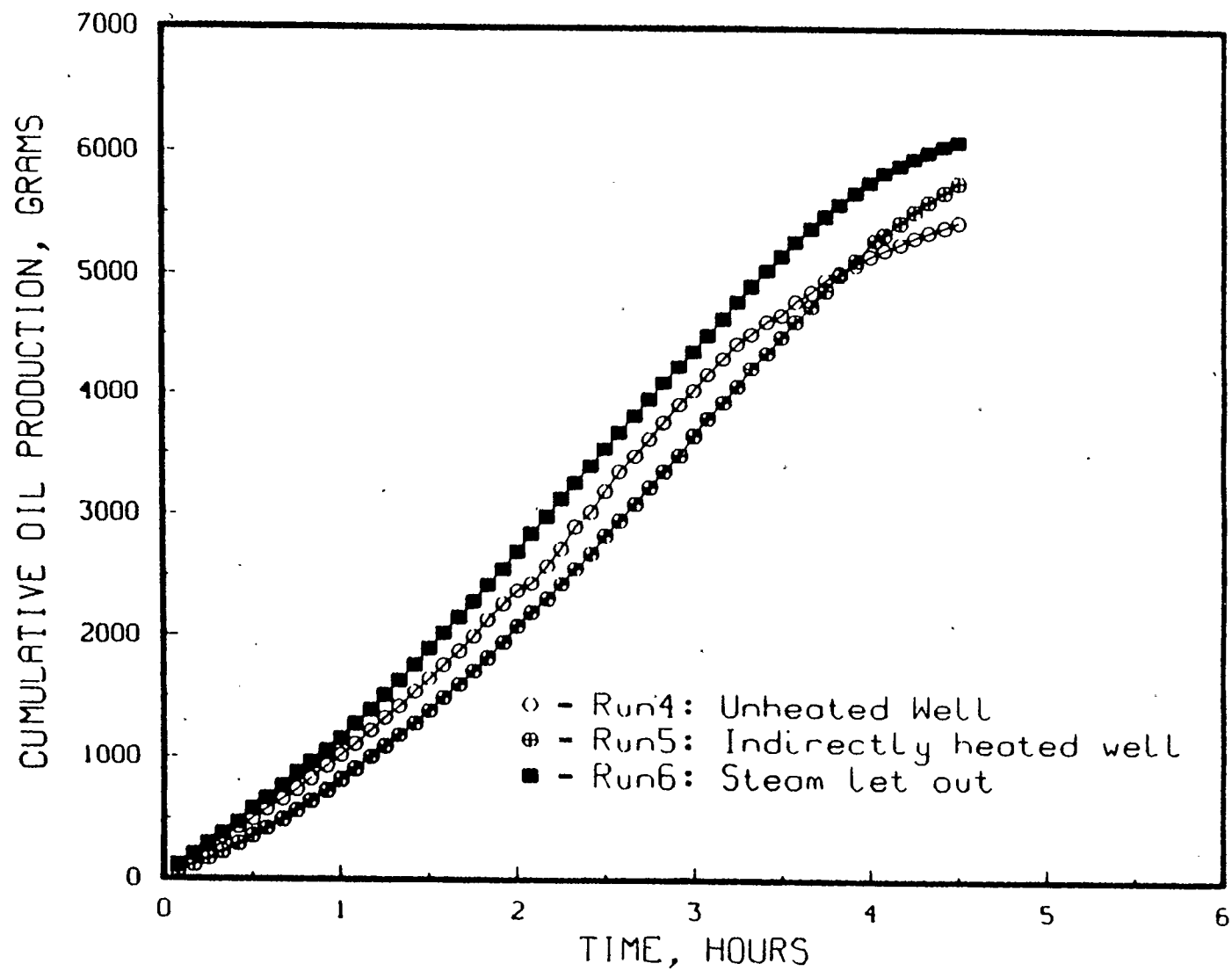
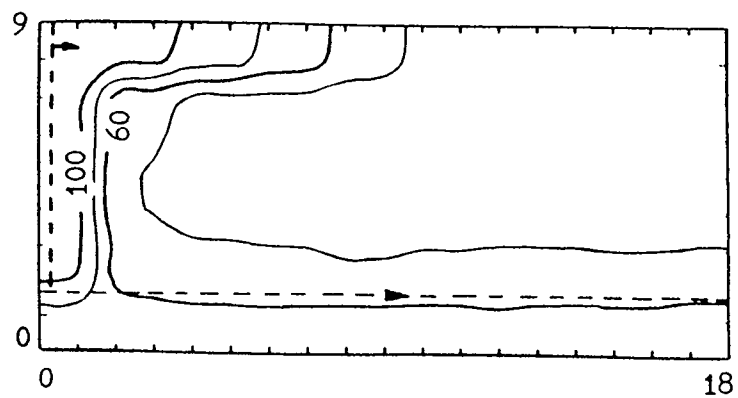


Figure 5.2.6 Comparison of cumulative oil production for Runs #4, #5 and #6

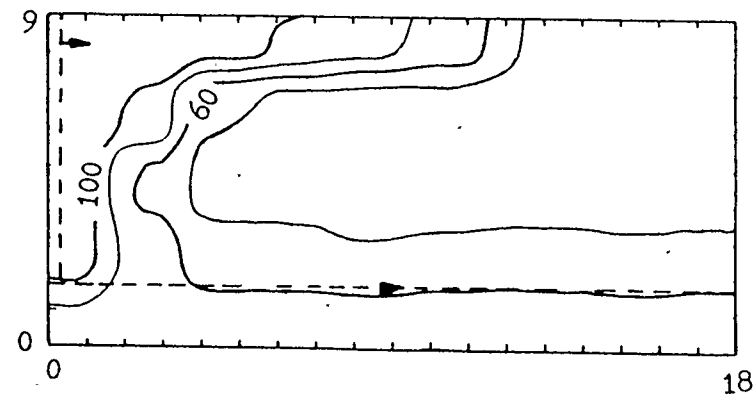
(Integrated Software Systems Corp.). Figures 5.2.5a to 5.2.5c shows the steam chamber movement in three dimensions.

The effect of heating the horizontal well was further investigated by performing the experiments in Run #4, #5 and #6. In these experiments only the hot end of the horizontal well was investigated. Run #4, #5 and #6 were performed with the well being unheated, indirectly heated and the steam being let out freely respectively.

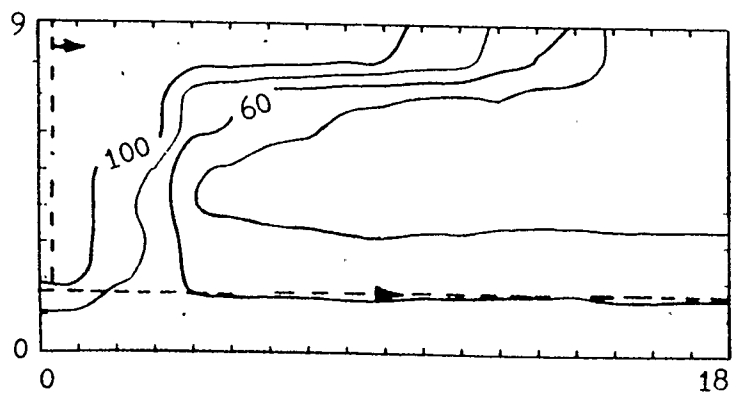
The production performance of the three experimental runs is shown in Figure 5.2.6. The figure shows conclusively that letting the steam out freely gave the best performance. However, it can also be observed that the performance of Run #4 (unheated) was better for most part of the experiment than that of Run #5 (indirectly heated). This observation suggested two possibilities. It should be mentioned again that the production valve for both the experiments was throttled such that only a minimal amount of steam was let out. It was possible that the production valve during Run #4 was throttled a little more open than during Run #5. However, the advantage of indirect heating was obvious toward the end of the recovery. Although Run #4 was classified as being unheated, the horizontal well was actually heated by the minimal amount of steam being let out. As mentioned earlier, there would be actually very little advantage of indirect heating at the hot end of the well if steam was let out of the production well. Figures 5.2.7a to 5.2.7c and 5.2.8a to 5.2.8c show the movement of the steam interface along the horizontal well for Run #4 (unheated production well) and Run #6 (steam let out freely of the production well)



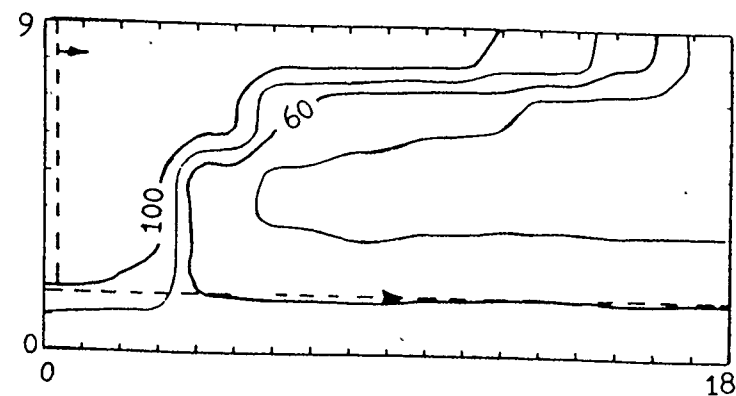
20 minutes



40 minutes



60 minutes



80 minutes

Figure 5.2.7a Movement of steam/oil interface in Run #4, 20 to 80 minutes

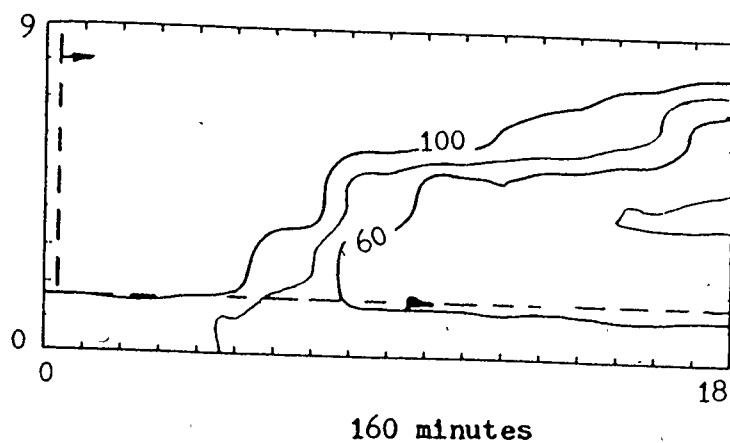
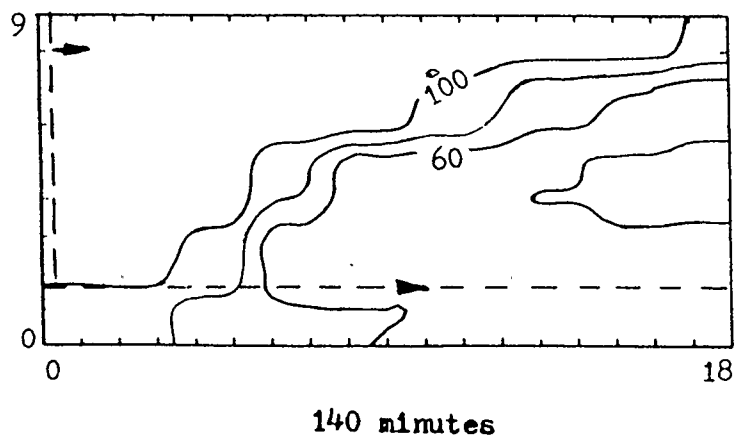
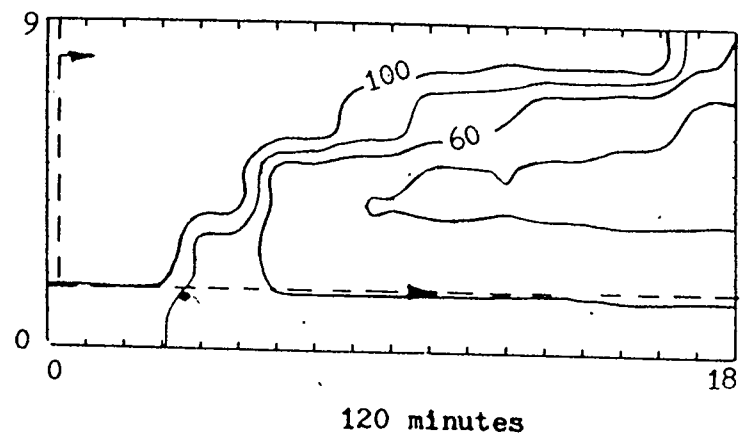
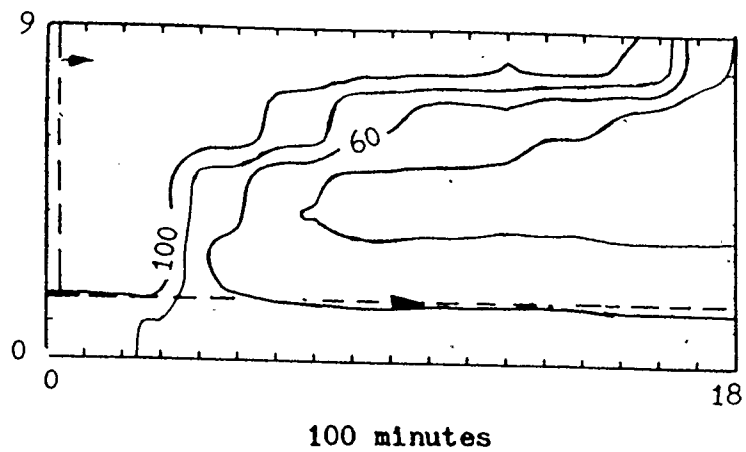
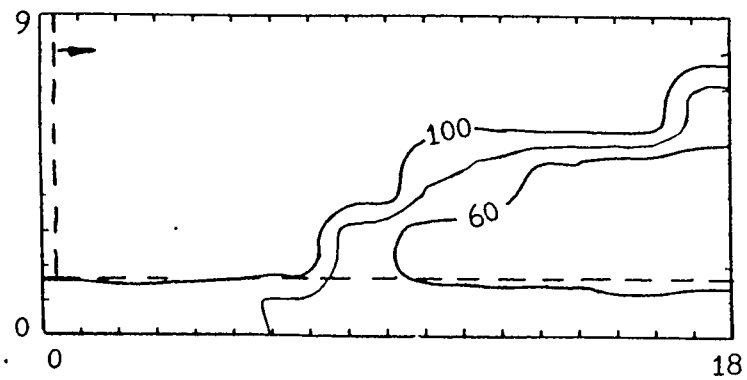
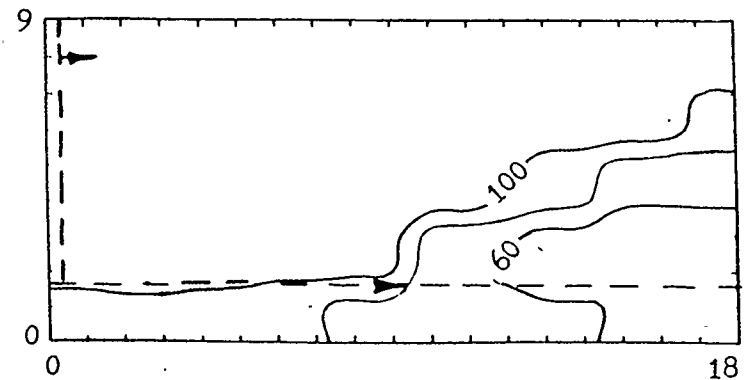


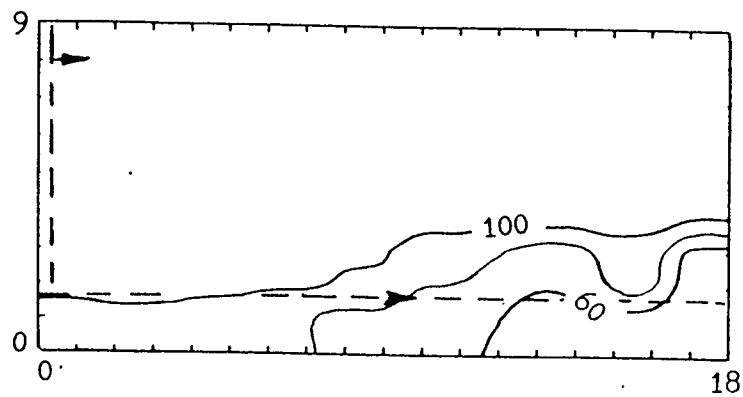
Figure 5.2.7b Movement of steam/oil interface in Run #4, 100 to 160 minutes



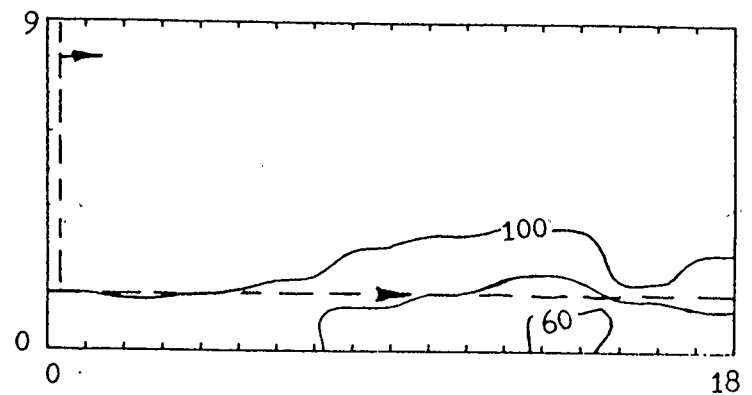
180 minutes



200 minutes



220 minutes



240 minutes

Figure 5.2.7c Movement of steam/oil interface in Run #4, 180 to 240 minutes

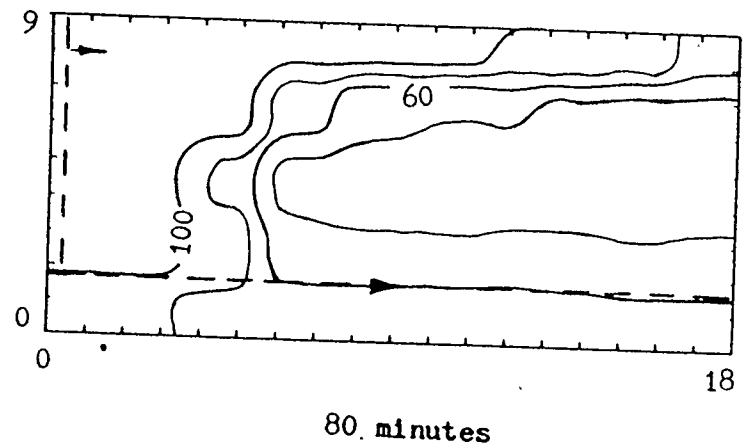
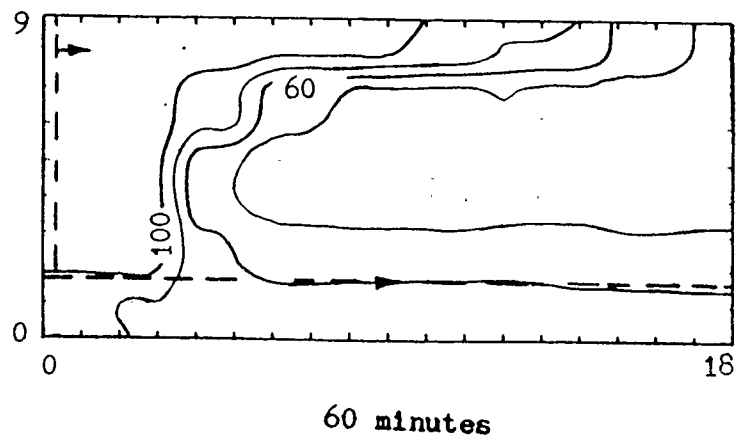
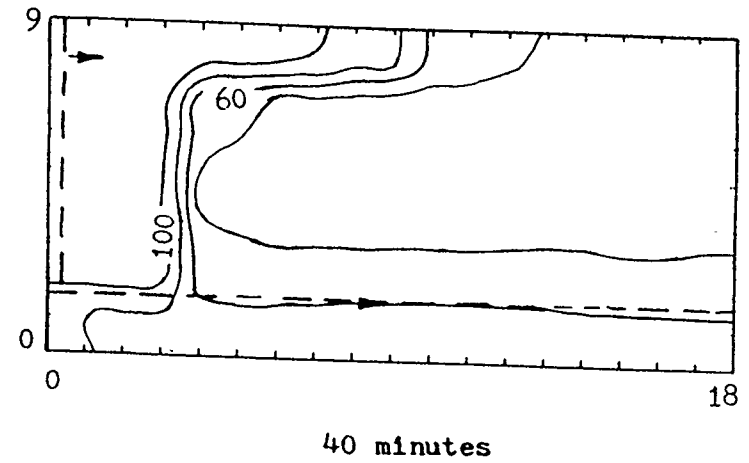
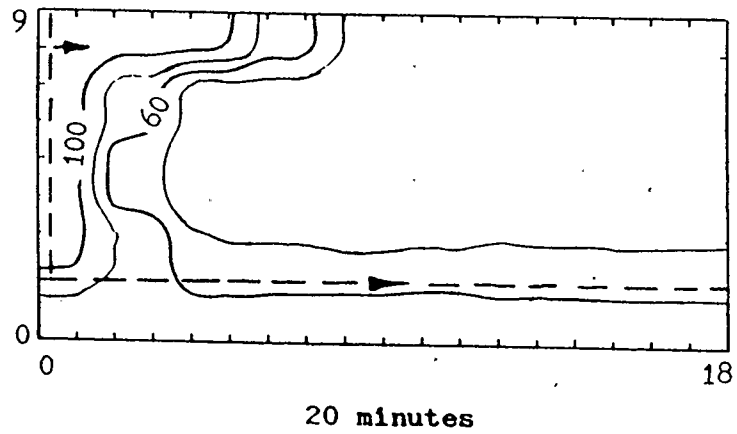


Figure 5.2.8a Movement of steam/oil interface in Run #6, 20 to 80 minutes

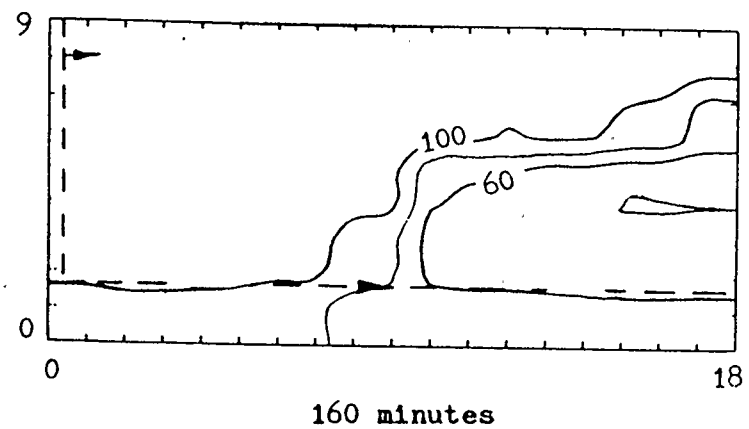
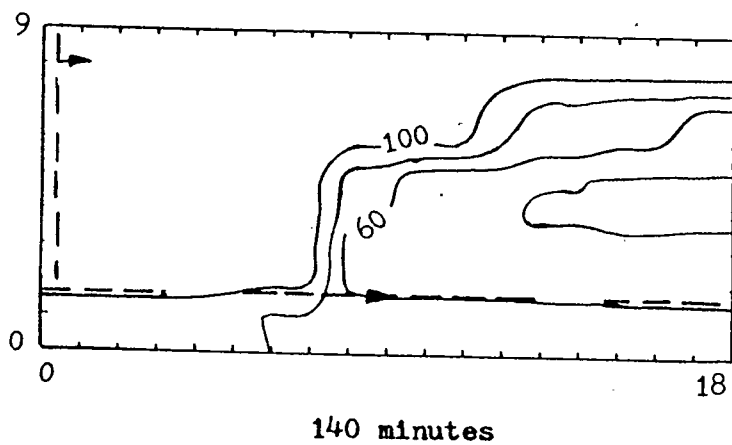
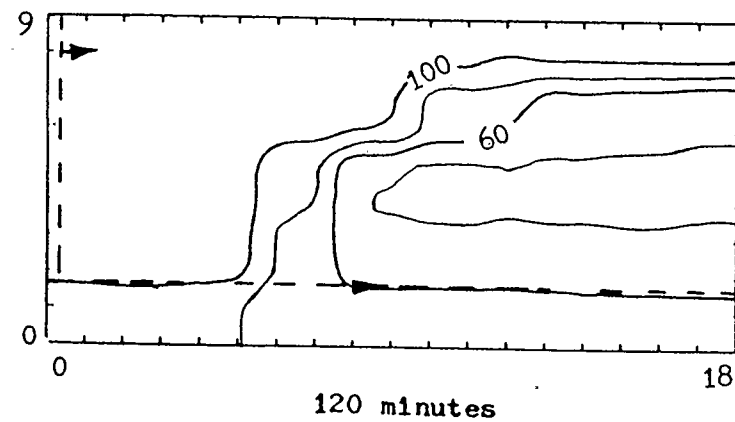
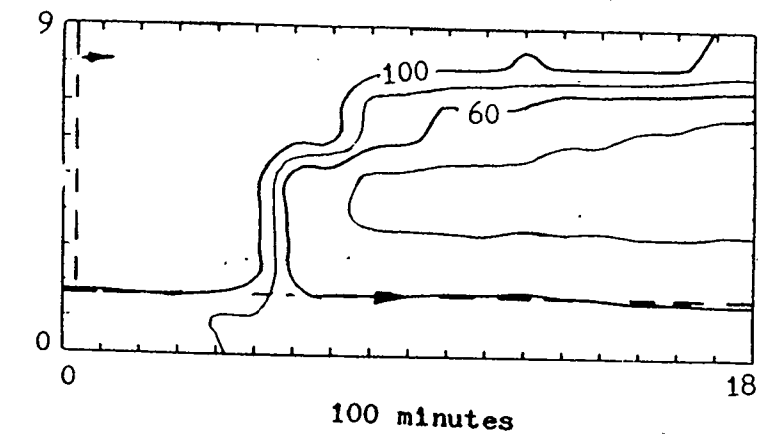


Figure 5.2.8b Movement of steam/oil interface in Run #6, 100 to 160 minutes

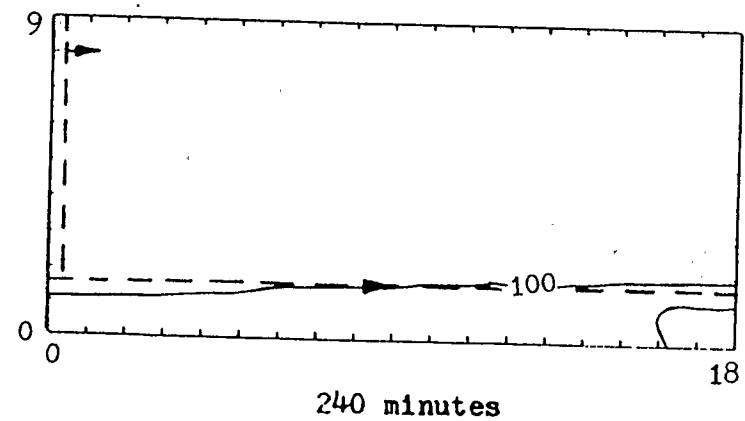
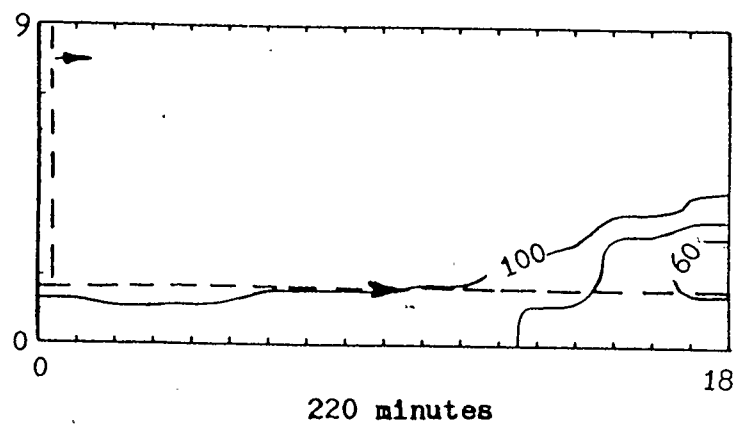
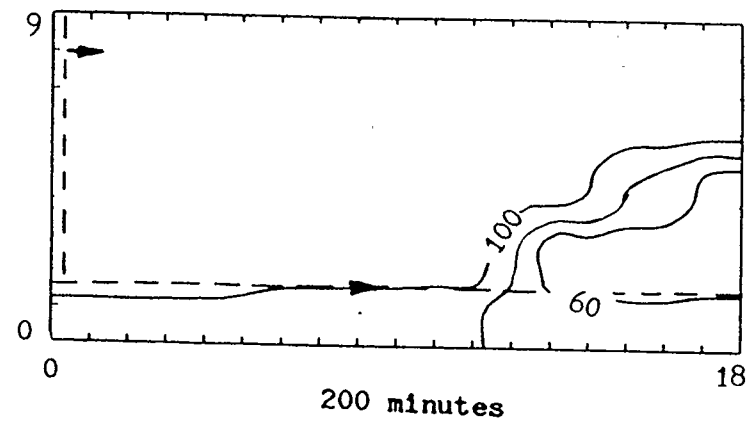
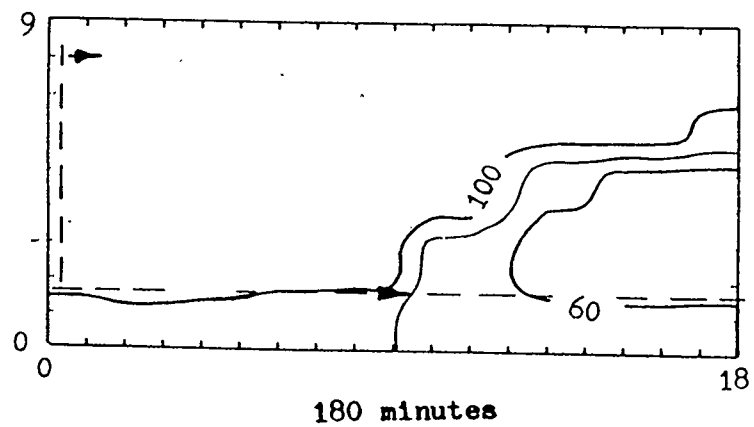


Figure 5.2.8c Movement of steam/oil interface in Run #6, 180 to 240 minutes

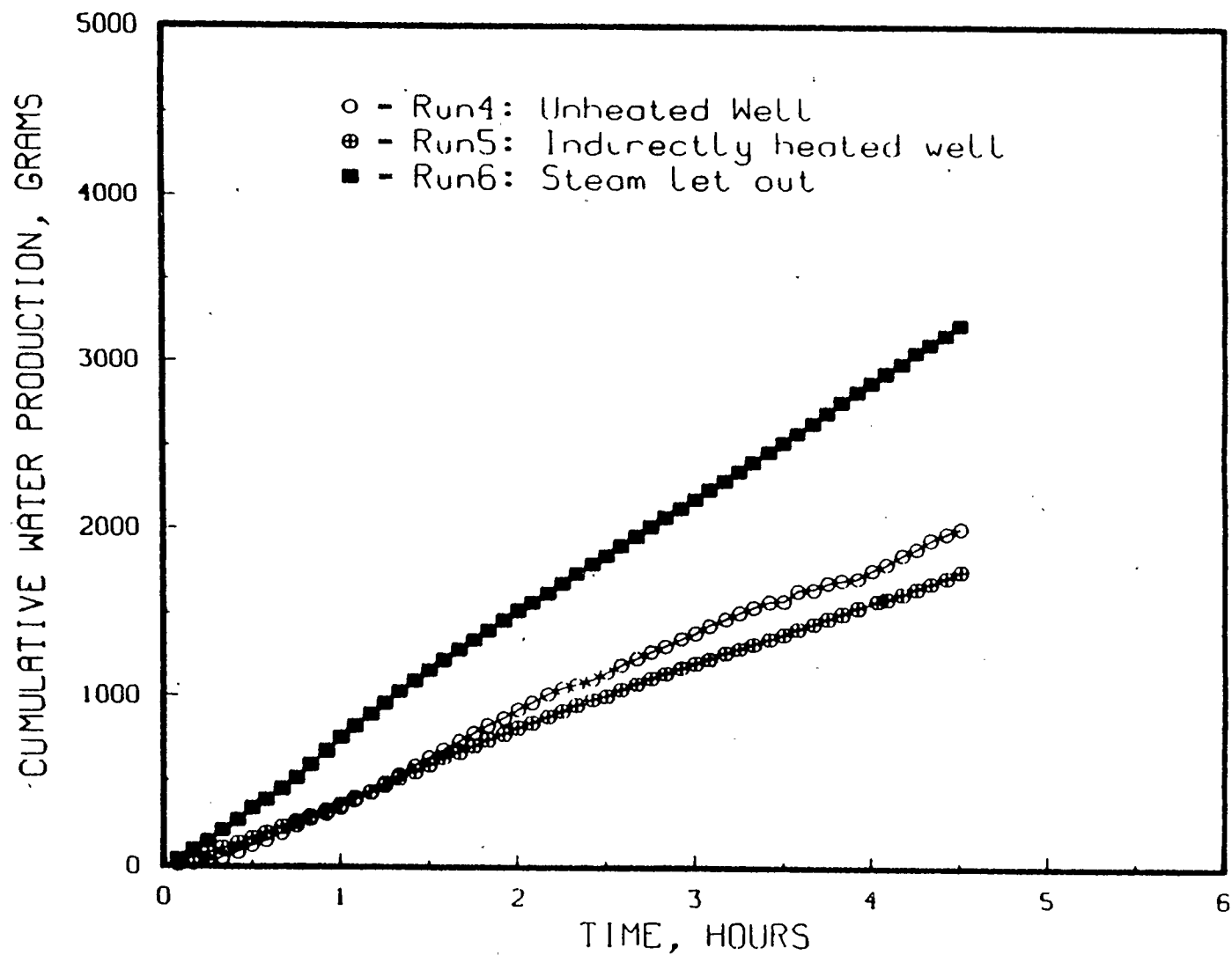


Figure 5.2.9 Comparison of cumulative water production for Runs #4, #5 and #6

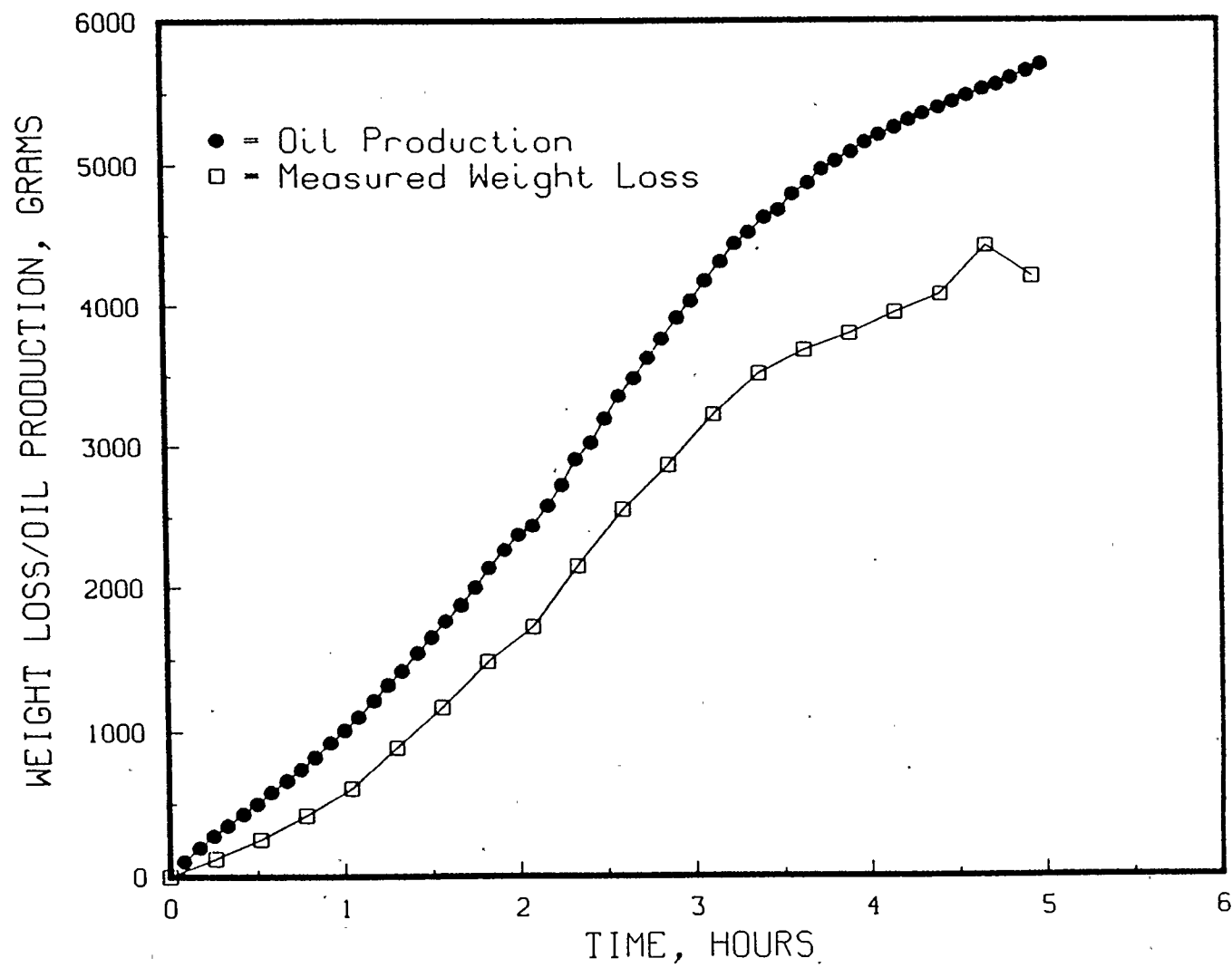


Figure 5.2.10 Measured weight loss and oil production in Run #4

respectively during the experiments. It is clear from these Figures that letting the steam out of the production well enhanced the growth of the steam interface along the well. This was due to the higher production well temperature effect described earlier.

Another interesting phenomenon can also be observed from Figure 5.2.9 which shows the cumulative water production obtained from sample analysis performed on fluids produced during the experiments. The water production represented a lower value than the actual steam input needed for the process since a small portion of the steam injected condensed and remained in the depleted reservoir. This effect is shown in Figure 5.2.10 for Run #4. The cumulative weight loss of the laboratory model measured by the load cell and the cumulative oil production obtained from the sample analysis were plotted with respect to experimental time in the Figure. It is observed that the cumulative measured weight loss was always smaller than the cumulative oil production. The difference in these values at any time gives the amount of steam condensate retained in the reservoir at the respective time. Assuming that the amount of steam condensate remained in the depleted reservoir for Run #4 and #6 was approximately of the same amount, Figures 5.2.6 and 5.2.9 can be used to estimate the incremental benefit for the process of letting the steam out compared to the case when a minimal amount of steam was let out. From the figures, at the end of the experiment at 4.5 hours, an additional 1300 grams of steam was needed to produce an extra 700 grams of oil. The oil/steam ratio obtained for this effort was 0.54. The question is whether it is economic to let steam out freely. Although less heat loss is

anticipated for the process in actual reservoirs, the laboratory experiments should give more reasonable results than those found with earlier models since the reservoir used was three-dimensional and insulated during the experiments. In Run #4 about 2000 grams of steam was needed to recover approximately 5500 grams of oil. The oil/steam ratio obtained was 2.25. Clearly, the effort of letting the steam out freely from the horizontal well from this point of view is not energy-efficient. However it is possible that there is an economic benefit involving some steam venting.

Another interesting observation can be seen from the two Figures. It is noticeable that the steam condensate produced from indirectly heating the horizontal well (Run #5) was significantly lower than the other two experiments. This does not mean that the process was better because the steam used for indirectly heating the well did not mix with the produced fluids. One would expect the energy requirement for Run #5 be greater than Run #4.

5.3 The effect of eliminating the use of the cold end of the horizontal well

The results of Run #1 and that of Run #7 are used to study this effect. It was noted that the steam chamber along the cold end of the horizontal well in Run #1 did not grow as fast as in the hot end. The purpose of Run #7 was to observe the advantage of the cold end of the horizontal if there was any. The production performance for the two experiments is shown in Figure 5.3.1. There was absolutely no advantage with the cold end of the well. For some reason, the

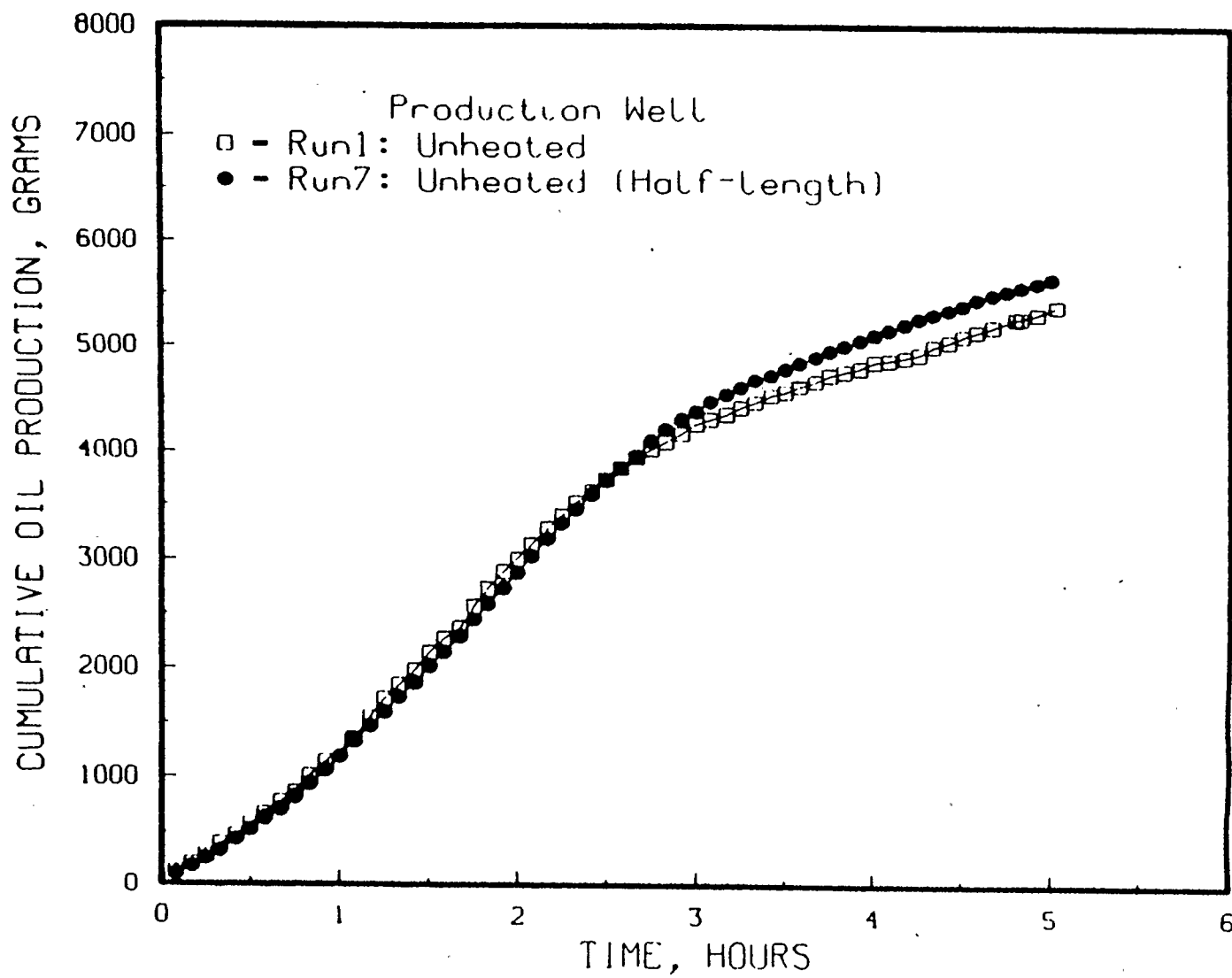


Figure 5.3.1 Effect of eliminating the use of the cold end of the horizontal well

production of Run #7 was even better than Run #1 which has a full length well. It is therefore unwise and not recommended that the cold end of the well be left cold for such well configuration. There is a major disadvantage associated with the cold end. The flow resistance of the produced fluids along that section of the well is too high so the fluids become backed up. This effect is discussed in section 6.3¹.

The cold end can be heated by introducing steam at the end of the horizontal well. This will heat the entire length of the horizontal well. Indirect heating can also be used but it is not as effective as introducing steam at the end of the horizontal well because of the convective nature of heat transfer in the latter case. It should also be pointed out that introducing steam at the end of the horizontal well is not an easy task. The injection pressure of steam for the horizontal well should be properly controlled. If the pressure is too high it will provide a backpressure which will cap the oil production at the middle of the reservoir. If the steam pressure is too low, there will be insufficient driving force for the fluids to flow within the "cold end" of the pipe which will result in the cooling of the well. The steam pressure can be controlled by trial and error, that is by changing the pressure and noting the immediate corresponding change in production rate. It is recommended that this process be further investigated.

¹A conclusion from the work described in this thesis is that the flow resistance along the well is of critical importance in scaled experiments such as these. This was not realized initially. It is discussed later.

5.4 Comparison of production performance between vertical and horizontal well steam injection

The cumulative oil production performance when using a vertical steam injector as opposed to using a horizontal one with a vertical fracture can be evaluated by comparing the production performance of Run #4 (vertical well steam injection) with the theoretical result using the TANDRAIN equation given by equation (3.1.24) (horizontal well steam injection) as shown in Figure 5.4.1. It is observed that the cumulative oil produced by the vertical steam injector was approximately 30 to 40 percent that of the horizontal steam injector's during the first two hours of the experiment. The result was not surprising since the vertical steam injector well was expected to perform less effectively. However, the effectiveness of the vertical steam injector is expected to increase with the number of injectors used. In principle, the performance of an "infinite" number of vertical steam injectors placed along the horizontal production well should equal that of a horizontal steam injector with a vertical planar fracture along it. This was observed in Run #12². Two vertical steam injectors were placed at each end of the reservoir model (Figure 4.7.4). The improved performance is shown in Figure 5.4.2. The cumulative oil production was between 55 to 65 percent that of the horizontal well injector's during the first two hours of the

²The performance of using 2 vertical steam injectors was first found to be lower than using one injector in Runs #8 to #11. This inconsistency was later discovered to be attributed to excessive flow resistance in the 3/8" production well used. Run #12 was performed with two vertical injectors with a 1" production well and the results obtained was as expected. This will be discussed in detail later.

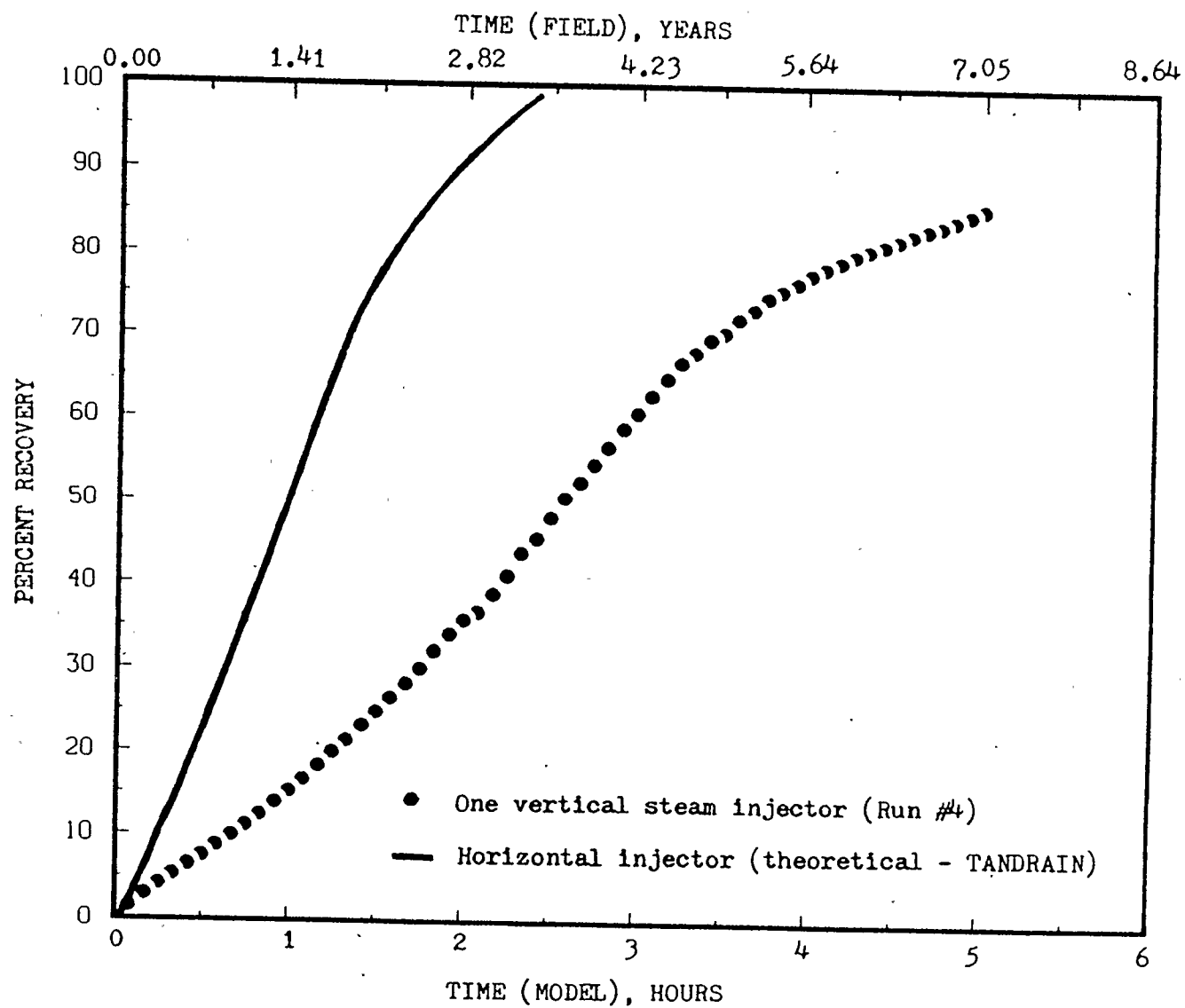


Figure 5.4.1 Performance using a single vertical steam injector (Run #4)

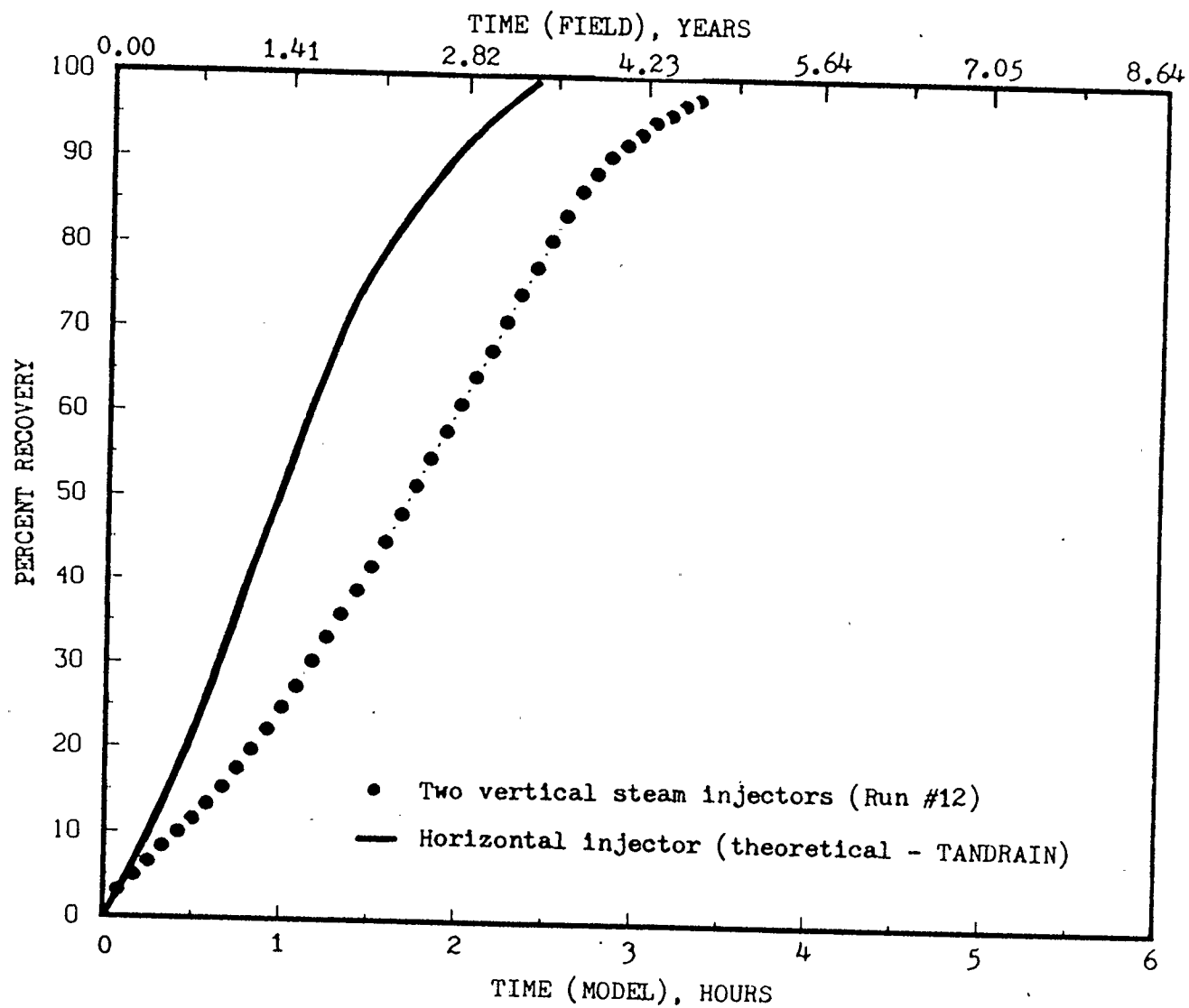


Figure 5.4.2 Performance using two vertical steam injectors (Run #12)

experiment. This is an impressive improvement since the injectors were positioned quite far apart (17.5 inches, approximately 3.5 times the horizontal distance to the no-flow boundary of the steam chamber). It is recommended further studies be performed to determine the optimum spacing of the vertical injectors.

5.5 Performance using two injectors

Run #8 was performed using two steam injectors each placed at one end of the reservoir model. The horizontal well was unheated. The steam pressure for both injectors was maintained at 7.5 psig. Figures 5.5.1 a, 5.5.1b and 5.5.1c shows the growth of the steam chambers along the central plane at both ends of the reservoir model. In these Figures, the production outlet was to the right of the reservoir model, It can be observed that the steam chamber at the end of the reservoir, that is at the far left of the reservoir model as shown in the figures, was not growing as expected. The production performance at the end of this experiment was approximately three-quarters of experiment Run #4, as shown in Figure 5.5.2 in which only one injector is located at the end of the reservoir model. The result was surprising because one would expect better performance in Run #8 with two injectors used instead of only one injector in Run #4. The reason that the steam chamber at the end of the reservoir model could not grow as expected was because there was insufficient driving force for the oil produced at this end to flow along the horizontal well. Since both steam chambers were maintained at the same pressure, the only driving force available for the flow of the oil produced along the well was the

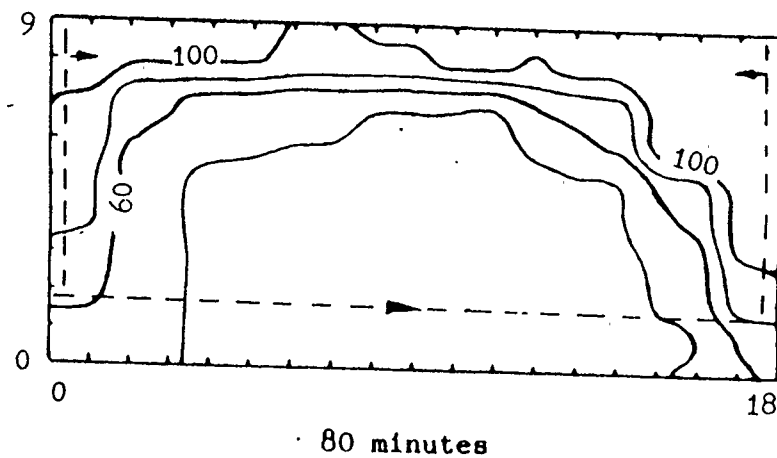
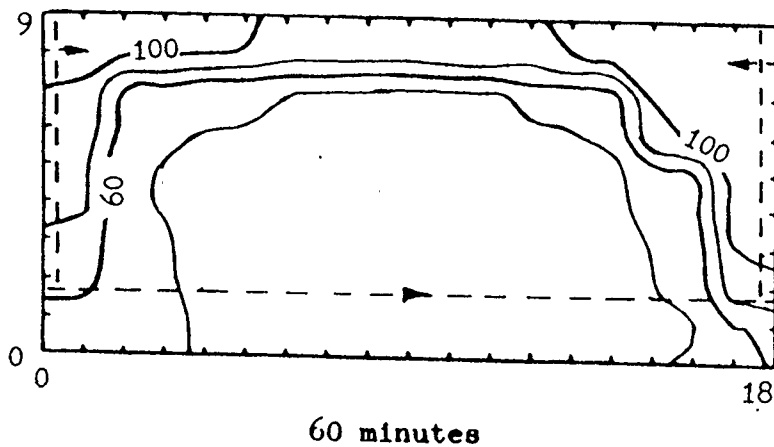
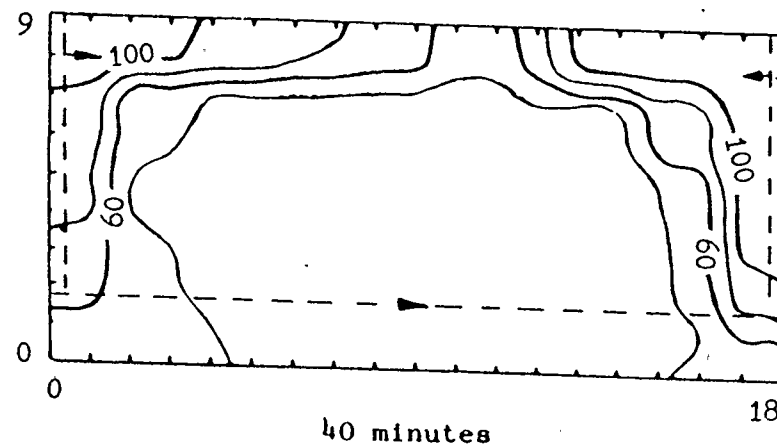
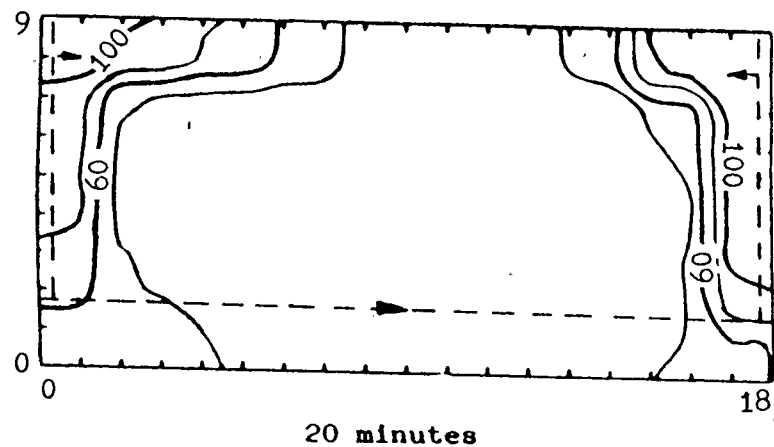


Figure 5.5.1a Movement of steam/oil interface in Run #8, 20 to 80 minutes

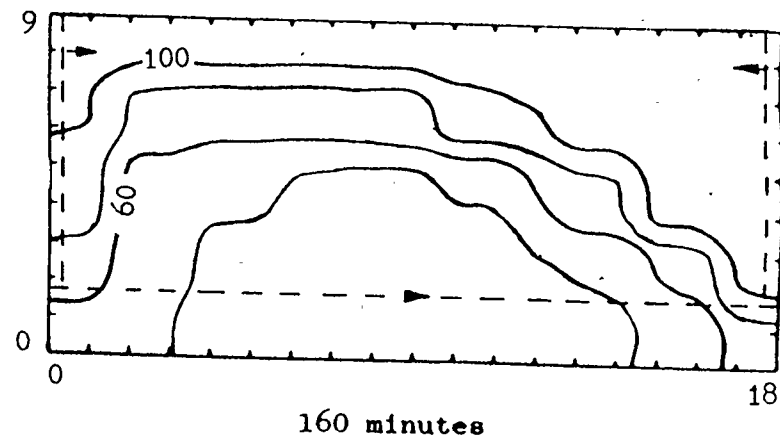
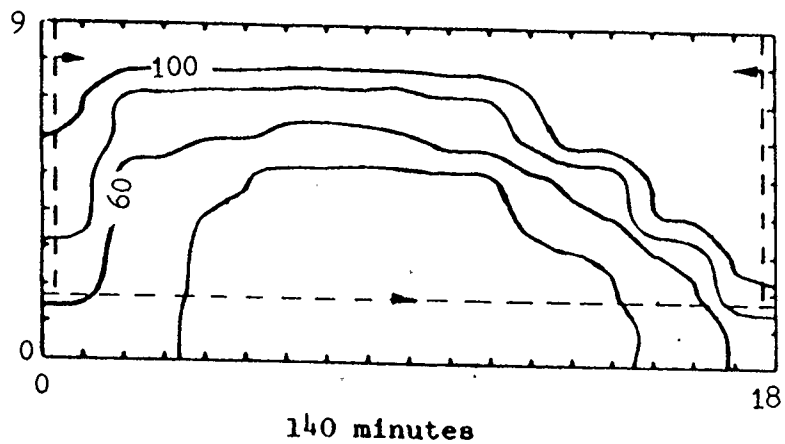
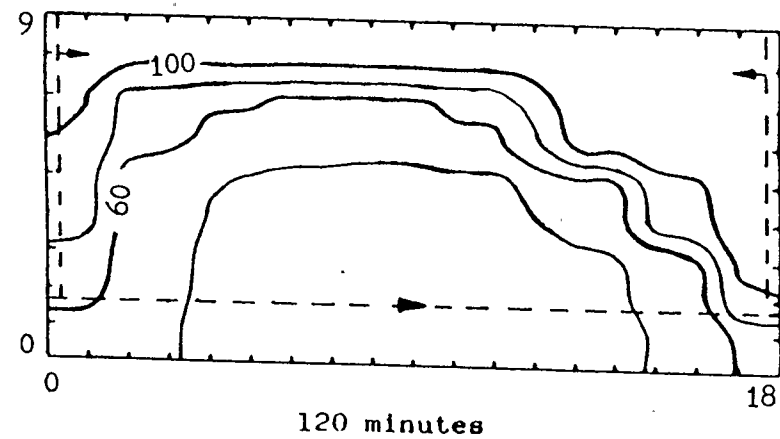
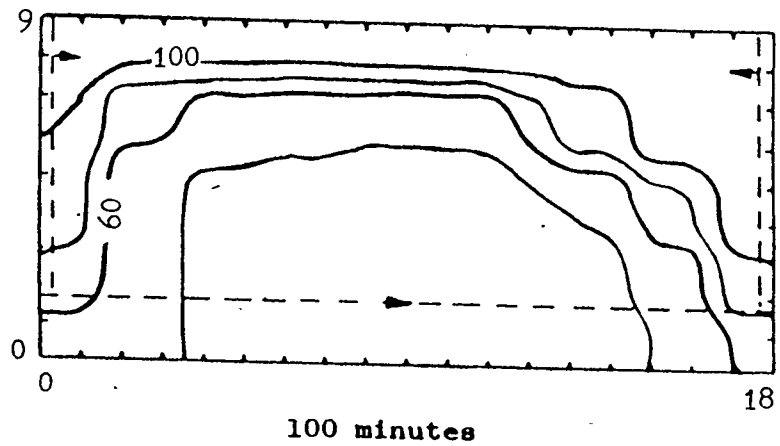
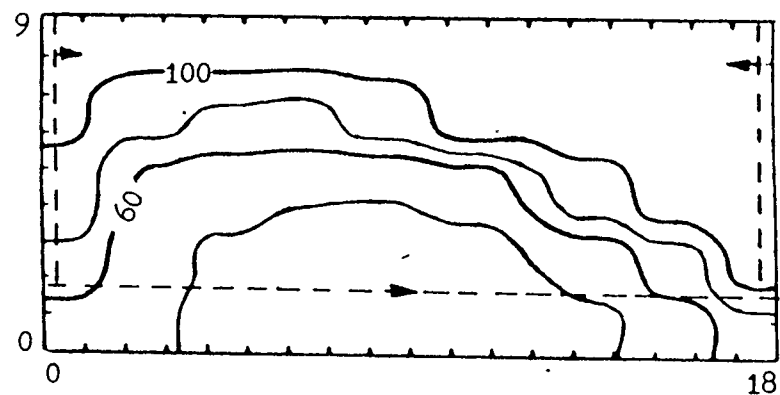
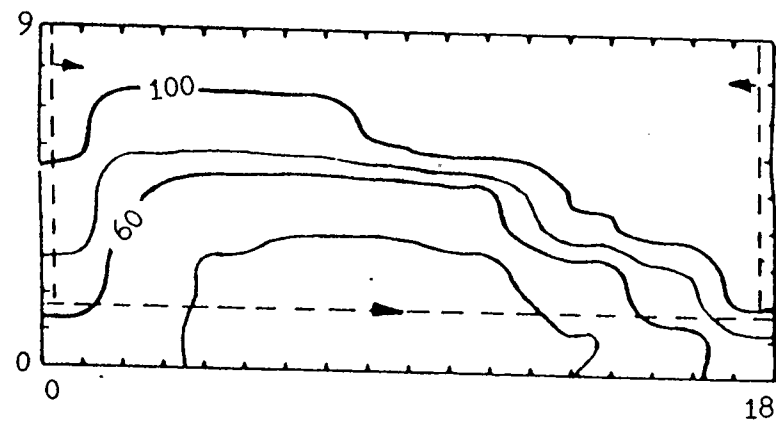


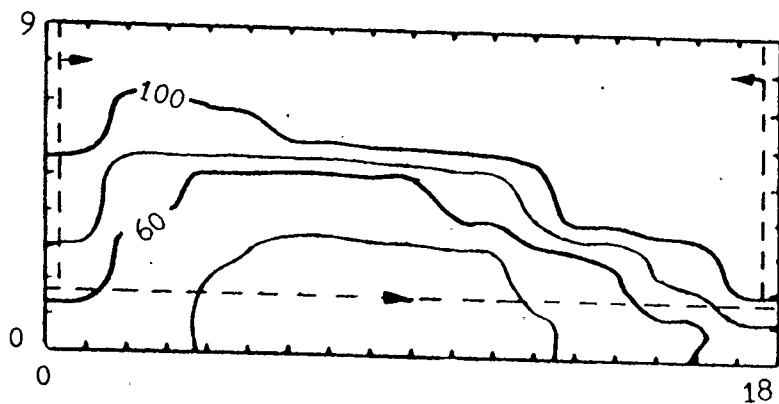
Figure 5.5.1b Movement of steam/oil interface in Run #8, 100 to 160 minutes



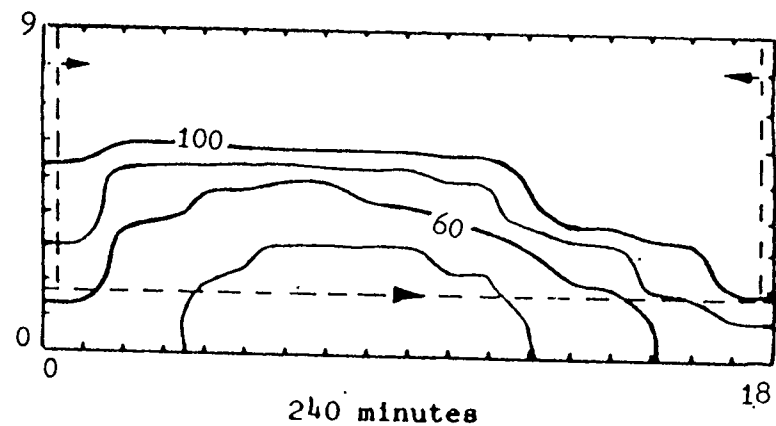
180 minutes



200 minutes



220 minutes



240 minutes

Figure 5.5.1c Movement of steam/oil interface in Run #8, 180 to 240 minutes

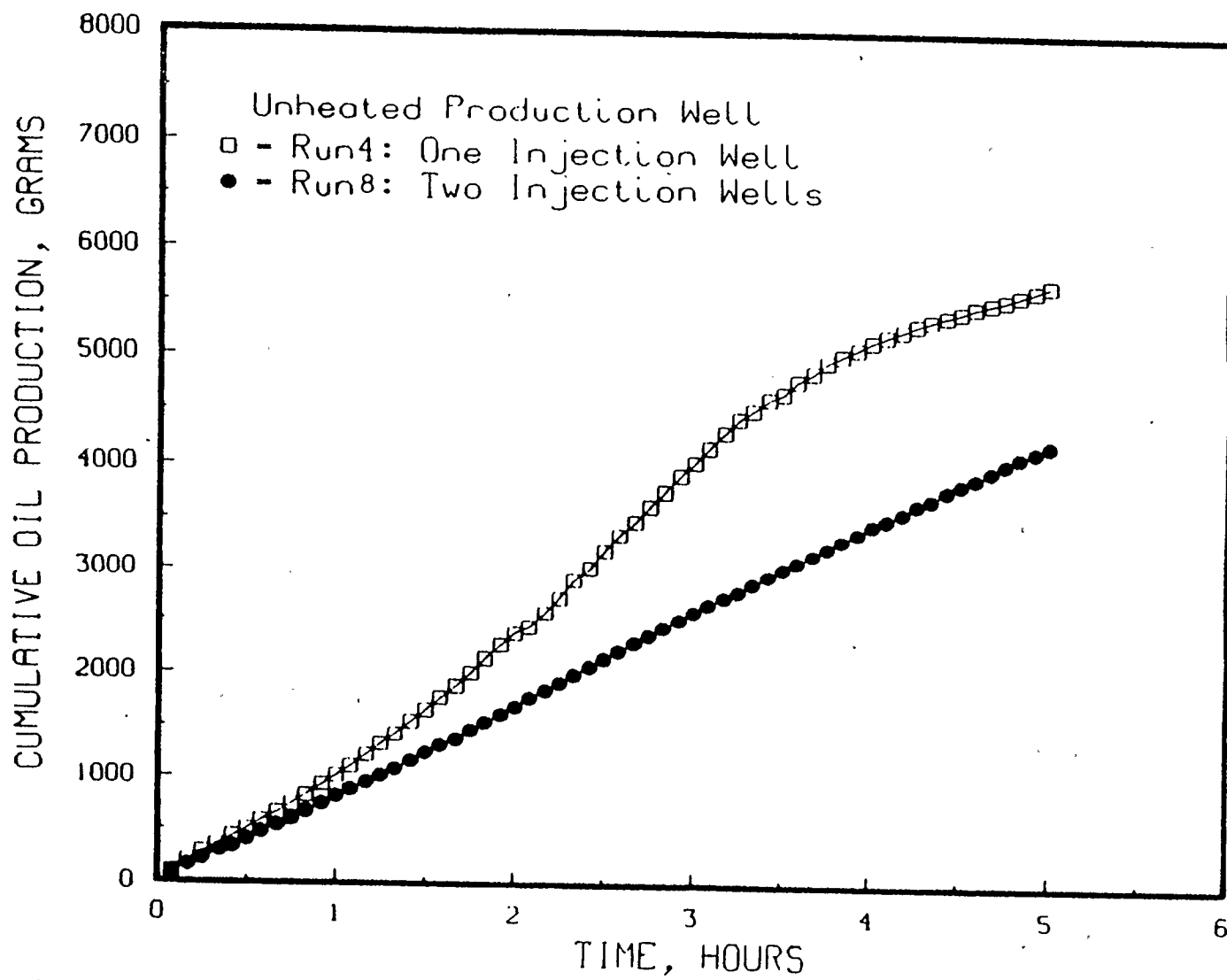
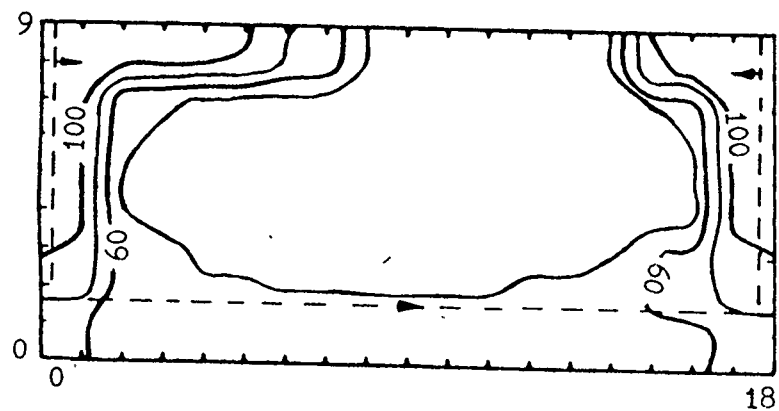


Figure 5.5.2 Comparison of cumulative oil production for Run #4 and Run #8

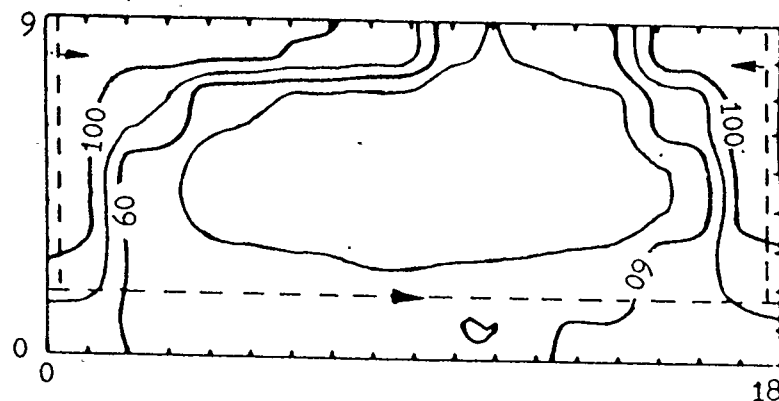
gravity head. The gravity head was insufficient to drive all oil produced at this end. These effects resulted in a backlog of heated oil produced at this end of the reservoir which can be observed from the figures.

In order to resolve the above-mentioned problem, a slight differential pressure along the horizontal well was thought to be sufficient. Run #9 was performed as in Run #8 but a differential pressure of 1 psig was imposed. The steam injector at the end of the reservoir was maintained at 8 psig while the well at the front of the model was maintained at 7 psig. Figures 5.5.3a to 5.5.3c shows the growth of the steam chambers along the central plane for different time levels. At times 20 and 40 minutes, the steam chamber at the end of the model was growing as expected. All the oil produced from the steam chamber was able to flow along the horizontal well. From time 60 minutes onwards, the growth of the steam chamber at the end of the reservoir was being retarded. As soon as the two steam chambers communicated, the differential pressure between the ends of the horizontal well disappeared and the only driving force left was the gravity head. Heated oil produced at the end of the model backlogged and similar behavior of the steam chamber was observed as in the previous experiment.

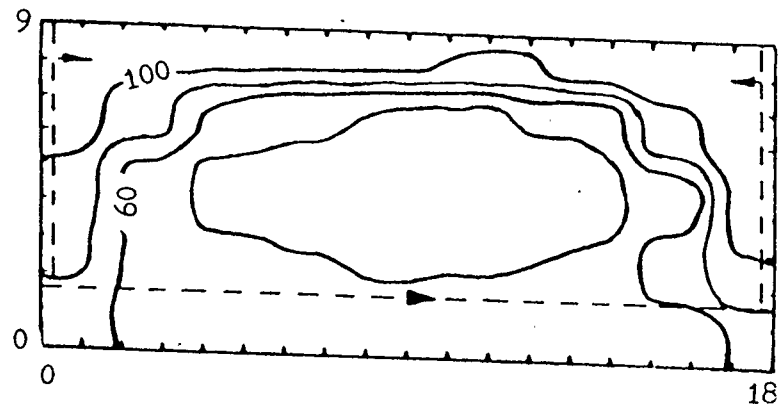
The results of both of these experiments did seem discouraging as they had serious negative implications on the drainage of oil along the horizontal well with a constant pressure chamber above it. Another experiment was performed to verify the observations from the previous two experiments. Run #10 was performed as in Run #9 but with the



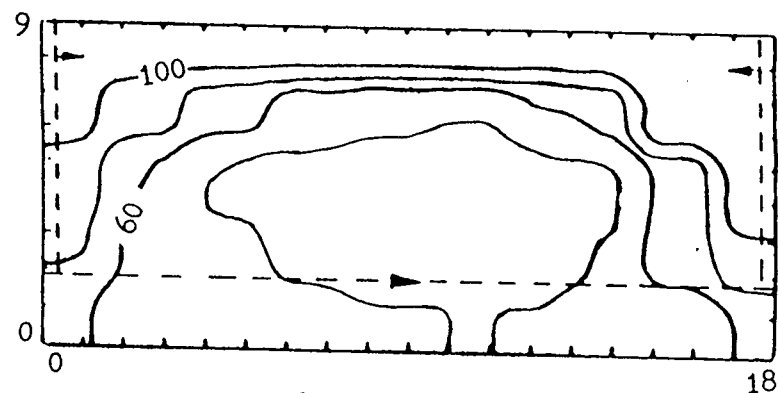
20 minutes



40 minutes



60 minutes



80 minutes

Figure 5.5.3a Movement of steam/oil interface in Run #9, 20 to 80 minutes

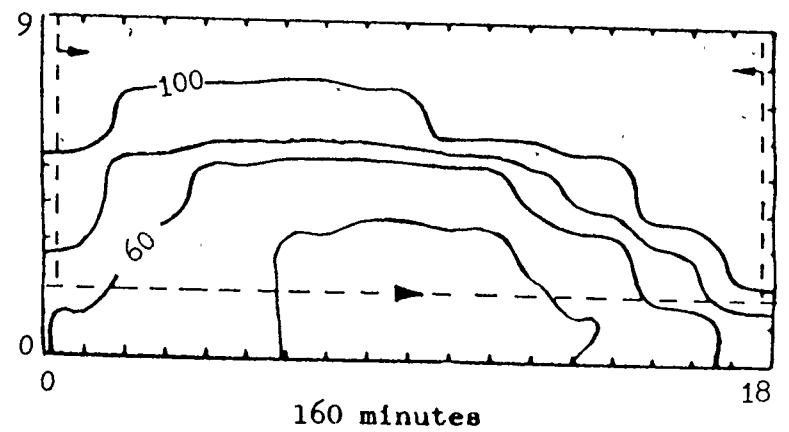
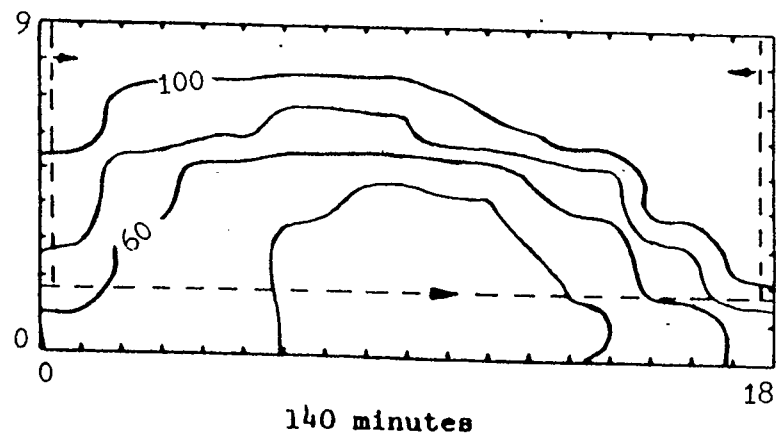
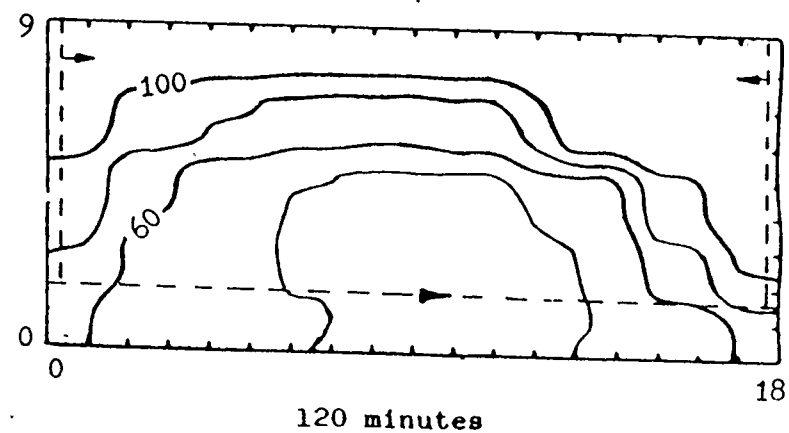
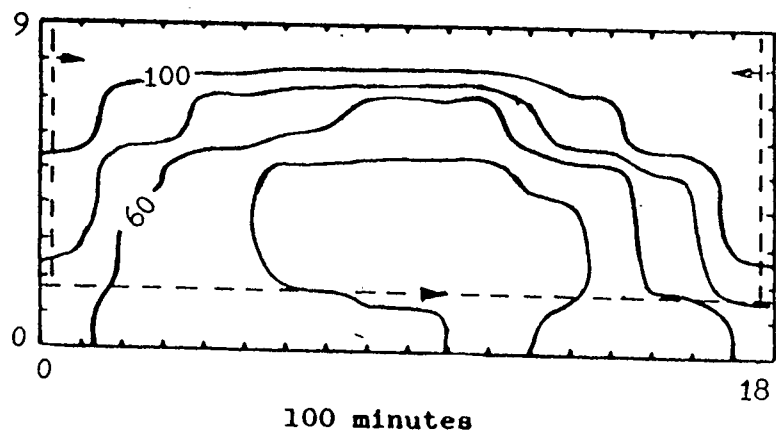


Figure 5.5.3b Movement of steam/oil interface in Run #9, 100 to 160 minutes

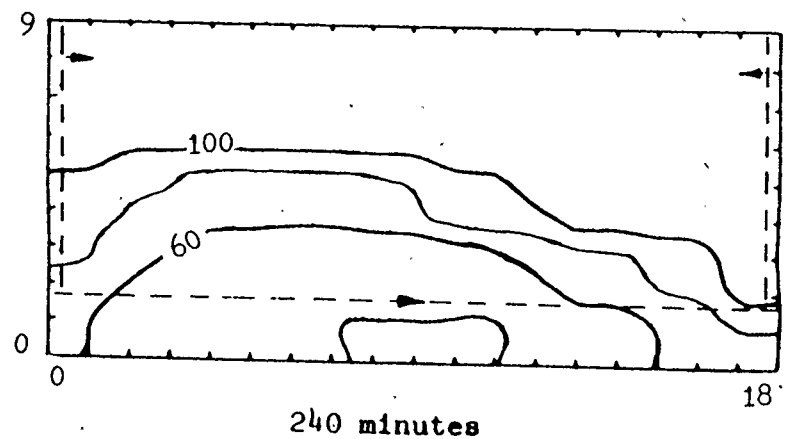
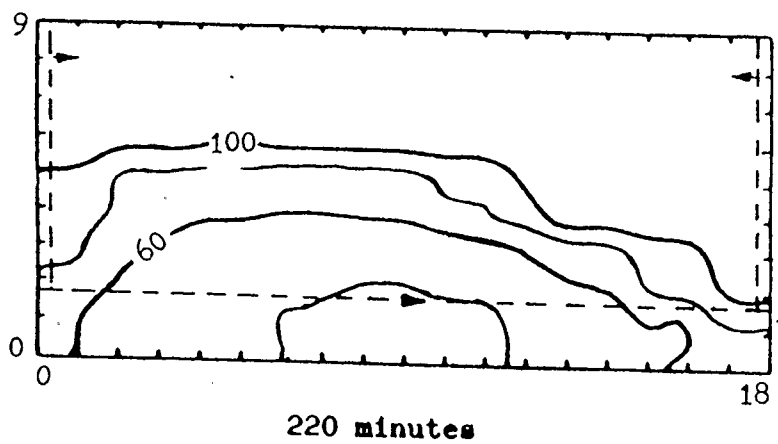
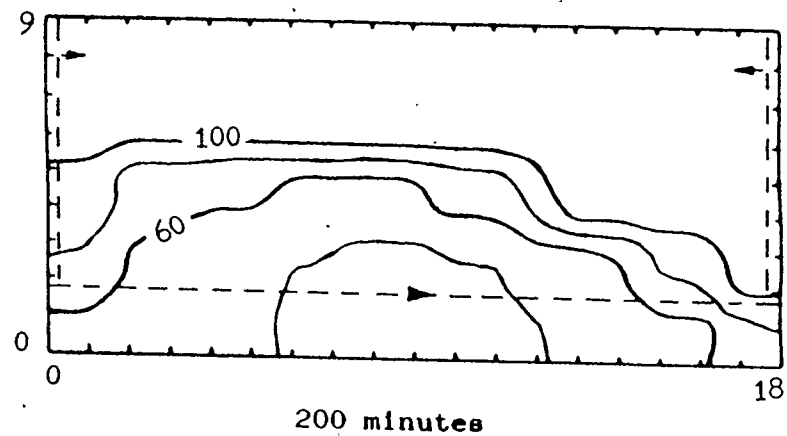
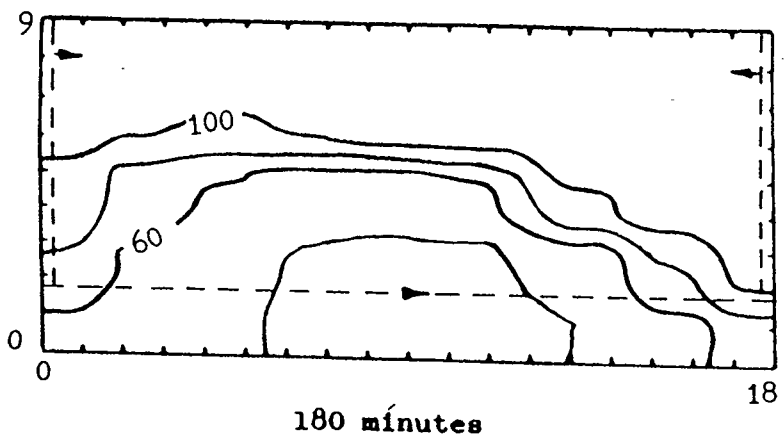


Figure 5.5.3c Movement of steam/oil interface in Run #9, 180 to 240 minutes

steam being let out of the production valve freely. Again, results obtained were quite similar to those of Run #9. The problem was therefore confirmed. The problem must be the result of too much flow resistance along the horizontal well. One obvious solution to the problem is to reduce the viscosity of the fluids flowing along the well. As mentioned earlier from the results of Run #6, the most effective method of heating the horizontal well was by introducing steam. Run #11 was thus performed with the exact same conditions as in Run #10 but with steam introduced at the end of the horizontal well. Figures 5.5.4a to 5.5.4c shows the growth of the steam chamber along the central plane of the reservoir model. Similar behavior was observed as in the previous experiment but the growth of the steam chamber at the end of the model was significantly faster. This observation suggested that the gravity head alone could be sufficient to drive the heated oil along the horizontal well if a bigger well was used or if the viscosity of the fluids within the well could be further reduced. This will be discussed further in the next chapter. It must be noted that it is imperative that the horizontal well be kept warm at all times. Increasing the size of the well will be useless if the well happened to cool off during the process, since bitumen is very viscous at low temperatures. The pressure drop along the pipe would be too large even if the pipe size was increased. The well can be kept warm by either indirect heating or by introducing steam at the end of the horizontal well. Indirectly heating is the recommended process because introducing steam is associated with problems mentioned earlier in section 5.3.

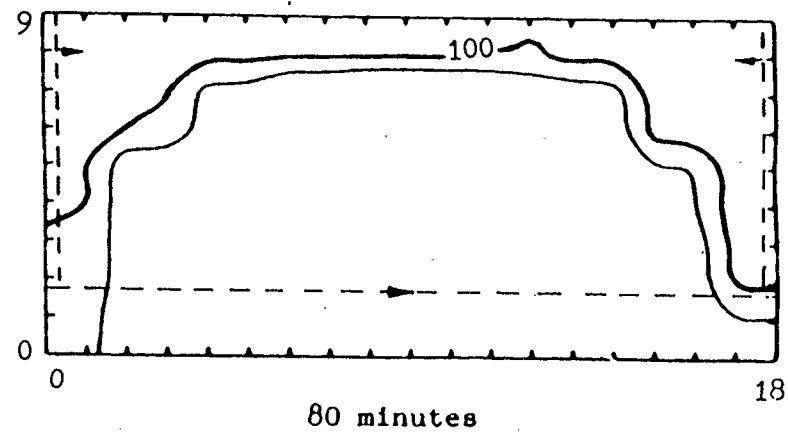
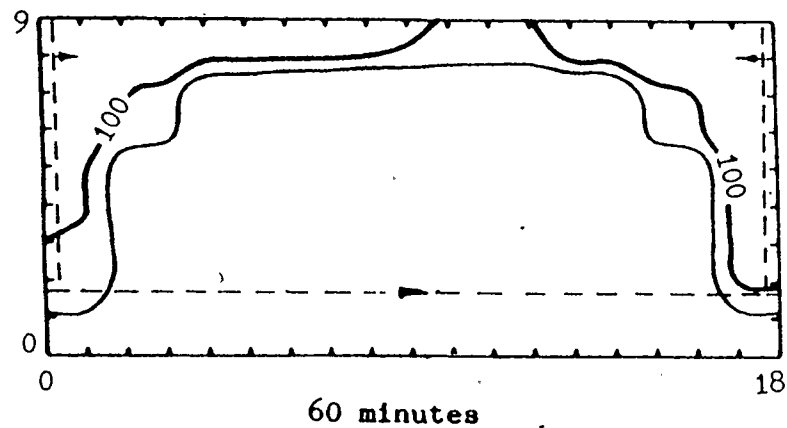
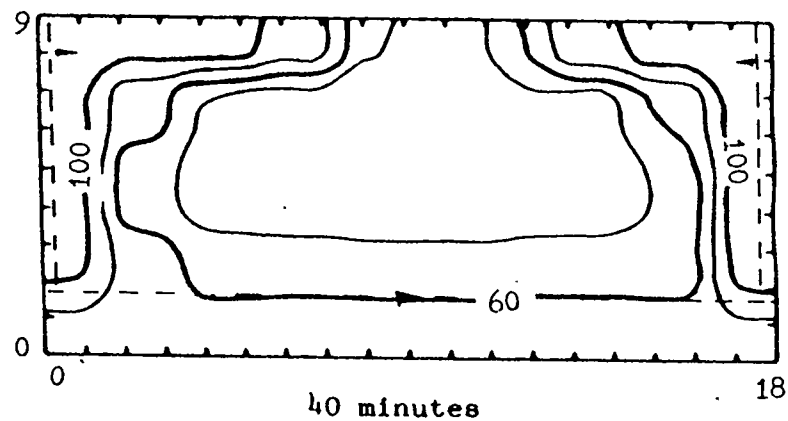
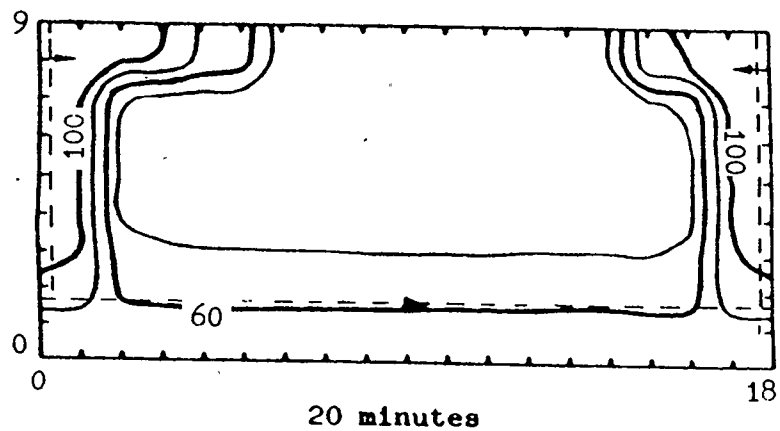


Figure 5.5.4a Movement of steam/oil interface in Run #11, 20 to 80 minutes

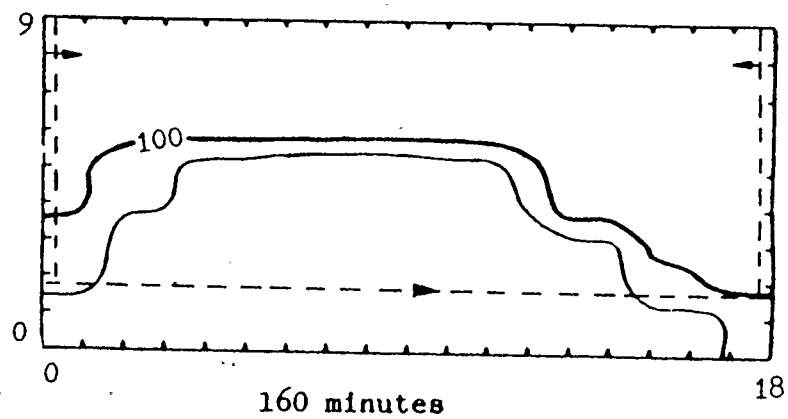
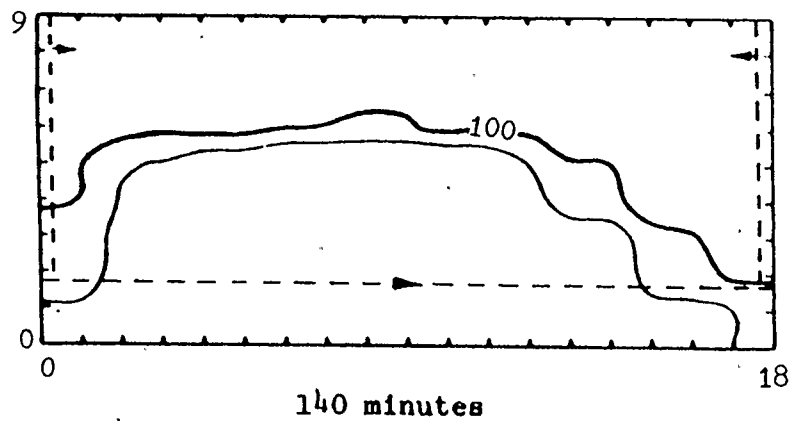
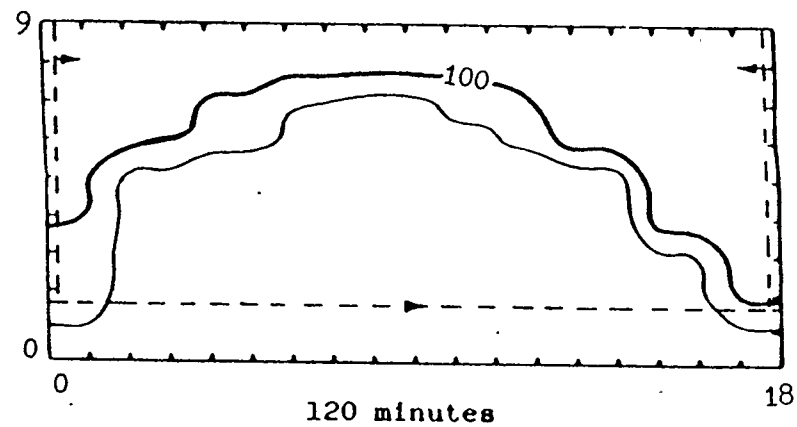
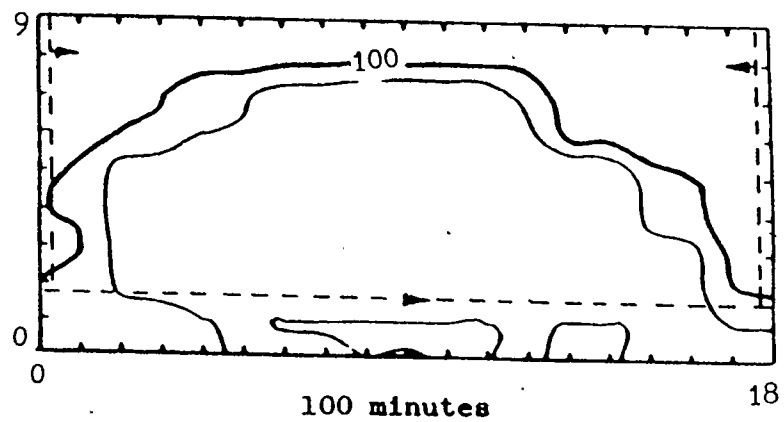


Figure 5.5.4b Movement of steam/oil interface in Run #11, 100 to 160 minutes

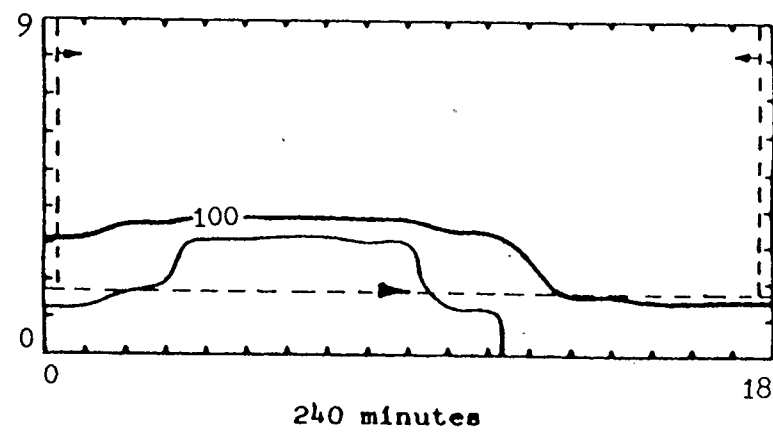
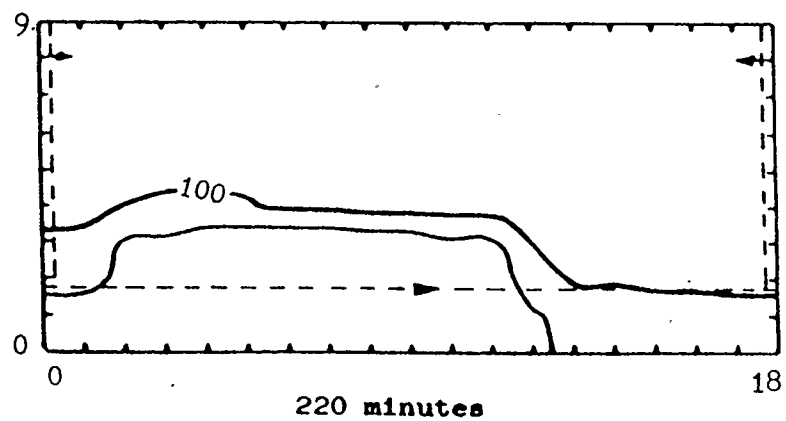
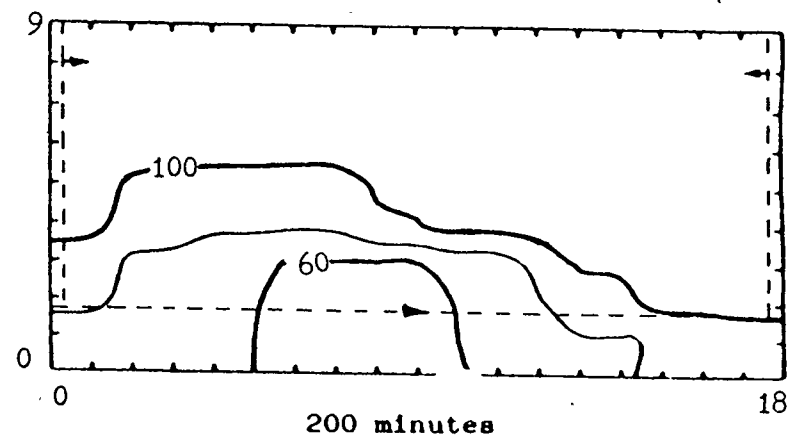
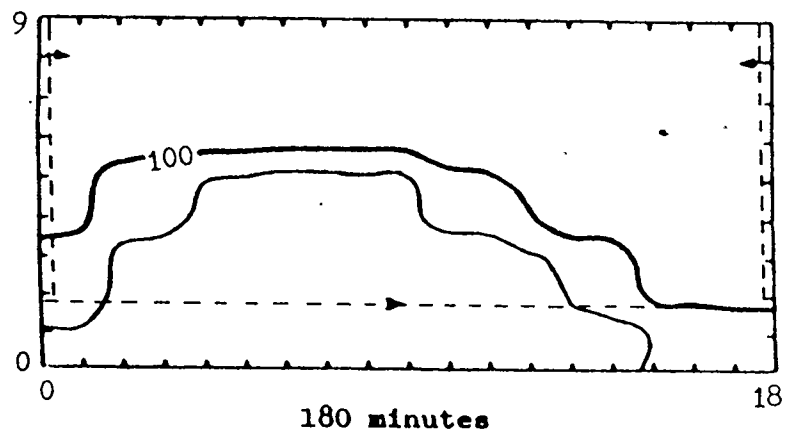


Figure 5.5.4c Movement of steam/oil interface in Run #11, 180 to 240 minutes

Run #12 was performed with using two vertical steam injectors each placed at one end of the reservoir model with a 1" horizontal production well instead of the 3/8" well used in all other experiments. The results of this experiment will be discussed in the next chapter.

CHAPTER 6

FURTHER DISCUSSION OF FLOW RESTRICTION ALONG THE HORIZONTAL PRODUCTION WELL

The experiments in Runs #8, #9, #10 and #11 discussed earlier in Chapter 5 gave rise to concerns that there might be a problem in the drainage of produced fluids within the horizontal well along a regime of constant pressure. The experiments clearly showed that the capacity of the horizontal well was insufficient to handle the rate of production of fluids from the steam chamber at the end of the reservoir model. The reason given earlier was that there was insufficient driving force to drain the produced fluids since the steam chambers at both ends were maintained at the same pressure. The only driving force available for the produced fluids was the gravity head resulting from the inclination of the bottom of the steam chamber above the horizontal well. On the other hand, the driving force might be sufficient if the resistance to flow along the horizontal well could be reduced. Since the permeability of the porous medium used in the experiments was a lot higher than in the field, the increased flow rate might be too much to handle for the horizontal well used in the experiment. The size of the horizontal well used was then questioned.

6.1 Sizing the horizontal well

For proper scaling of field conditions to laboratory conditions, Butler (1985a) proposed that the B_3 factor and the dimensionless time, T' , must be equal for both field and laboratory

conditions. Any combination of these dimensionless numbers are acceptable. The B_3 factor and the dimensionless time are given in equation (6.1.1) and (6.1.2) and a combination of the two dimensionless numbers is given in equation (6.1.3).

$$B_3 = \sqrt{\frac{KgH}{\phi \Delta S_o \alpha m \nu_s}} \quad (6.1.1)$$

$$T' = \frac{t}{H} \sqrt{\frac{Kg\alpha}{\phi \Delta S_o m \nu_s H}} \quad (6.1.2)$$

$$\frac{T'}{B_3} = \frac{t\alpha}{mH^2} \quad (6.1.3)$$

Equation (6.1.2) indicates that it is possible to compensate for a low permeability K by employing a matrix with high thermal diffusivity α (Butler, 1986b). Low mobility of the oil can be compensated by allowing a deeper heat penetration below the steam/oil interface. This is not realistic because the reservoir must be infinite in extent. To overcome this problem, not only should T' given in equation (6.1.2) be the same for the model and the field but also that the dimensionless number given by equation (6.1.1) should be made equal. When B_3 is the same for the model and the field, then the heat penetration into the interface will be equivalent for the model and the

field.

For dimensional similarity between the laboratory reservoir model and the fields, equation (6.1.4) can be written.

$$\left(\frac{t\alpha}{mH^2} \right)_{\text{model}} = \left(\frac{t\alpha}{mH^2} \right)_{\text{field}} \quad (6.1.4)$$

Since $(\alpha/m)_{\text{model}} \approx (\alpha/m)_{\text{field}}$ equations (6.1.5) and (6.1.6) can be written.

$$\left(\frac{t}{H^2} \right)_{\text{model}} = \left(\frac{t}{H^2} \right)_{\text{field}} \quad (6.1.5)$$

$$\therefore \frac{t_{\text{model}}}{t_{\text{field}}} = \frac{H_{\text{model}}^2}{H_{\text{field}}^2} \quad (6.1.6)$$

For a three-dimensional system, the ratio of the volumes is given by equation (6.1.7).

$$\frac{Q_{\text{model}}}{Q_{\text{field}}} = \frac{H_{\text{model}}^3}{H_{\text{field}}^3} \quad (6.1.7)$$

The rate of drainage can thus be written as in equation

(6.1.8).

$$\frac{q_{\text{model}}}{q_{\text{field}}} = \frac{Q_{\text{model}}/t_{\text{model}}}{Q_{\text{field}}/t_{\text{field}}} \quad (6.1.8)$$

Using equations (6.1.6) and (6.1.7), equation (6.1.8) can be written as in equation (6.1.9).

$$\frac{q_{\text{model}}}{q_{\text{field}}} = \frac{H_{\text{model}}^3}{H_{\text{field}}^3} \cdot \frac{H_{\text{field}}^2}{H_{\text{model}}^2} = \frac{H_{\text{model}}}{H_{\text{field}}} \quad (6.1.9)$$

Using the Hagen-Poiseuille equation for laminar flow in a pipe, equation (6.1.10) can be written.

$$\frac{q_{\text{model}}}{q_{\text{field}}} = \frac{\left(\frac{\pi R^4 \Delta P}{\mu L} \right)_{\text{model}}}{\left(\frac{\pi R^4 \Delta P}{\mu L} \right)_{\text{field}}} \quad (6.1.10)$$

If there is to be equivalent fluid static head above the horizontal well in the field and in the model then,

$$\left(\frac{\Delta P}{\Delta \rho g H} \right)_{\text{model}} = \left(\frac{\Delta P}{\Delta \rho g H} \right)_{\text{field}} \quad (6.1.11)$$

$$\text{or} \quad \frac{\Delta P_{\text{model}}}{\Delta P_{\text{field}}} = \frac{H_{\text{model}}}{H_{\text{field}}} = \frac{L_{\text{model}}}{L_{\text{field}}} \quad (6.1.12)$$

So, for both the field and the model to have the same pressure gradient ($\Delta P/L$) in their respective horizontal wells, using equations (6.1.9), (6.1.10), (6.1.11) and (6.1.12), equations (6.1.13) and (6.1.14) can be written.

$$\frac{q_{\text{model}}}{q_{\text{field}}} = \frac{R_{\text{model}}^4}{R_{\text{field}}^4} \cdot \frac{\mu_{\text{field}}}{\mu_{\text{model}}} \quad (6.1.13)$$

$$\frac{R_{\text{model}}}{R_{\text{field}}} = \left[\frac{H_{\text{model}}}{H_{\text{field}}} \cdot \frac{\mu_{\text{model}}}{\mu_{\text{field}}} \right]^{1/4} \quad (6.1.14)$$

The result is very interesting. The scaling factor for the horizontal well is not proportional to the ratio of the respective H values but to the one fourth power of the ratio.

If we consider a 7" well in the field, the diameter of the horizontal well in the model should be approximately 4" using equation (6.1.14). The well used in the experiments has a diameter of 0.34" with an inner tubing of 3/16". Hence, the well was sized too small according to the equation. This might have resulted in impeding the flow of produced fluids along the well in Run #9 to Run #12. Since the only driving force causing the fluids to flow along the well was its

gravity head the result of under-sizing the well can be quite detrimental. However, it does not mean that the diameter of the horizontal well in the model must be 4" because the size of the well in the field might be over-sized. Using a 4" well in the 9" depth model might therefore be unnecessary. Thus, Run #12 was performed with a 1" production well with two injectors placed at each end of the reservoir model. It should also be noted that the 7" well could also be undersized. The results of Run #12 showed that the 1" well was sufficient in size. This will be further discussed in the next section.

The results of experiments Runs #8 to #11 gave rise to the question on how to properly size the horizontal well. If the size of the 7" well in the field is insufficient to handle the flow, then the steam chamber at the end of the horizontal well will be limited in growth thus resulting in lower production than predicted for the case of a pair of horizontal well placed at the bottom of the reservoir with a vertical fracture along the wells. It is interesting to study the pressure drop along the horizontal well. The gravity head that is necessary for the flow of oil and the oil flow rate along the production well can also be studied. The following section will discuss this subject.

6.2 Pressure drop along the horizontal production well

If we have a pair of horizontal wells (one injector and one producer) at the bottom of the reservoir, there are three mechanisms involved in the recovery of the bitumen. Figure 6.2.1 illustrates the

three mechanisms. The first mechanism, A, is gravity drainage. It can be described by Butler's TANDRAIN theory. The drainage equation without depletion effects can be written as:

$$\frac{\partial q}{\partial x} = 2 \sqrt{\frac{1.5 \phi \Delta S_o K g \alpha (H-y)}{m \nu_s}} \quad (6.2.1)$$

The second mechanism, B, can be described as follow. Consider two wells as shown in Figure 6.2.2. One well acts as the injector while the other acts as the producer. Imagine the advancing steam forms a "line drive" (Muskat, 1937) in between the two wells displacing and driving the oil into the producer well as shown in (b) in Figure 6.2.1. Steady state Darcy equation can be written for the injector as:

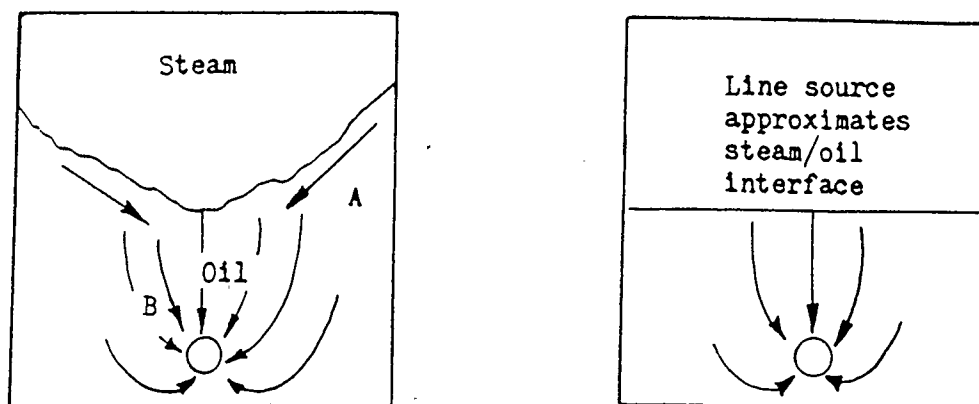
$$q = - \frac{2\pi r_i K L}{\mu} \left(\frac{dP}{dr_i} \right) \quad (6.2.2)$$

Integrating equation (6.2.2), equation (6.2.3) is written.

$$-(P - P_{wi}) = \frac{q\mu}{2\pi K L} \ln(r/r_{wi}) \quad (6.2.3)$$

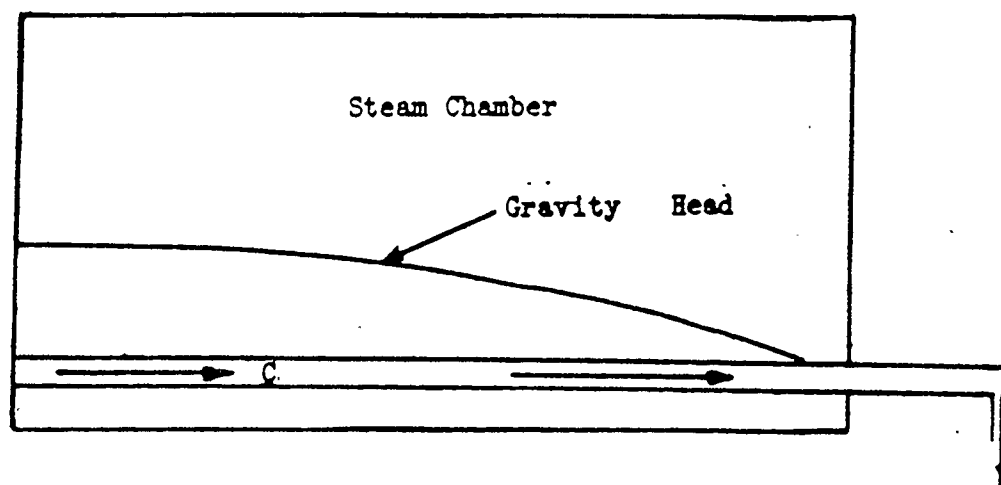
Similary, the Darcy equation for the producer can be written as:

$$(P - P_{wp}) = \frac{q\mu}{2\pi K L} \ln(r_p/r_{wp}) \quad (6.2.4)$$



a) Mechanisms A and B

b) Line source approximation



c) Mechanism C

Figure 6.2.1 Mechanisms of drainage of oil in the SAGD process

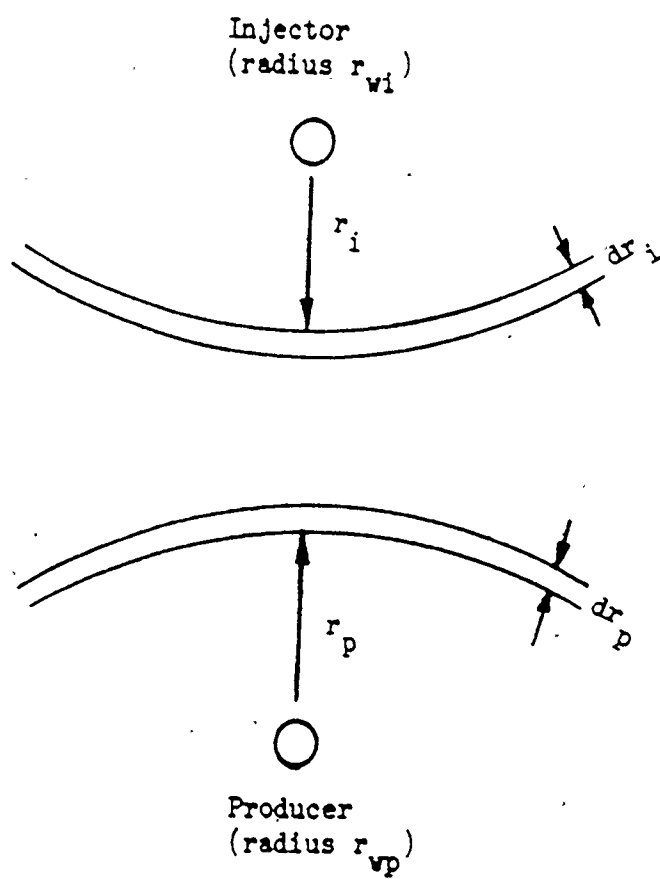


Figure 6.2.2 Steady state Darcy flow between injector and producer

Subtracting equation (6.2.3) from equation (6.2.4) yields equation (6.2.5).

$$P = \frac{P_{wp} + P_{wi}}{2} + \frac{q\mu}{4\pi KL} \ln(r_p/r_i) \quad (6.2.5)$$

The potential P represents the potential of any point between the two wells. $(P_{wp} + P_{wi})/2$ represents the potential at the midpoint between the producer and the injector. It can be approximated to be equal to the pressure of the steam chamber plus the gravity head. Equation (6.2.5) can then be written to represent the pressure at the (Muskat's line source assumption) production well as in equation (6.2.6). This is the line source assumption illustrated in Figure 6.2.1.

$$P_{wp} = P_{sc} + \rho gy + \frac{q\mu}{4\pi KL} \ln(r_{wp}/2y) \quad (6.2.6)$$

This well-known equation was developed by Muskat (1937). Equation (6.2.6) is rewritten in a modified form:

$$\frac{\partial q}{\partial x} = \frac{4\pi K}{\mu \ln(2y/r_{wp})} (P_{sc} + \rho gy - P_{wp}) \quad (6.2.7)$$

Equation (6.2.7) represents steady state radial flow of oil for the second mechanism.

The third mechanism of flow, C , shown in Figure 6.2.1 is the flow along the production well and can be described by Hagen-Poiseuille

law (Bird et al, 1960) for flow through an annulus. For an inner tubing radius of κr_{wp} the equations for the flow is given in equations (6.2.8) and (6.2.9).

$$q = \frac{\pi r_{wp}^4 C}{8\mu} \left[\frac{\partial P_{wp}}{\partial x} \right] \quad (6.2.8)$$

$$\text{where} \quad C = (1 - \kappa^4) - (1 - \kappa^2)^2 / \ln (1/\kappa) \quad (6.2.9)$$

The three equations of (6.2.1), (6.2.7) and (6.2.8) can be solved simultaneously for the flow rate, q , the pressure along the production well, P_{wp} , and the gravity head, y , as the function of the independent variable x . Basically, the three unknowns, q , P_{wp} , and y , can be solved with a set of boundary conditions. The appropriate boundary conditions are:

1) At the end of the horizontal well,

$$q = 0$$

2) At the front of the horizontal well,

$$P_{wp} = P_{sc}$$

$$y = r_{wp}$$

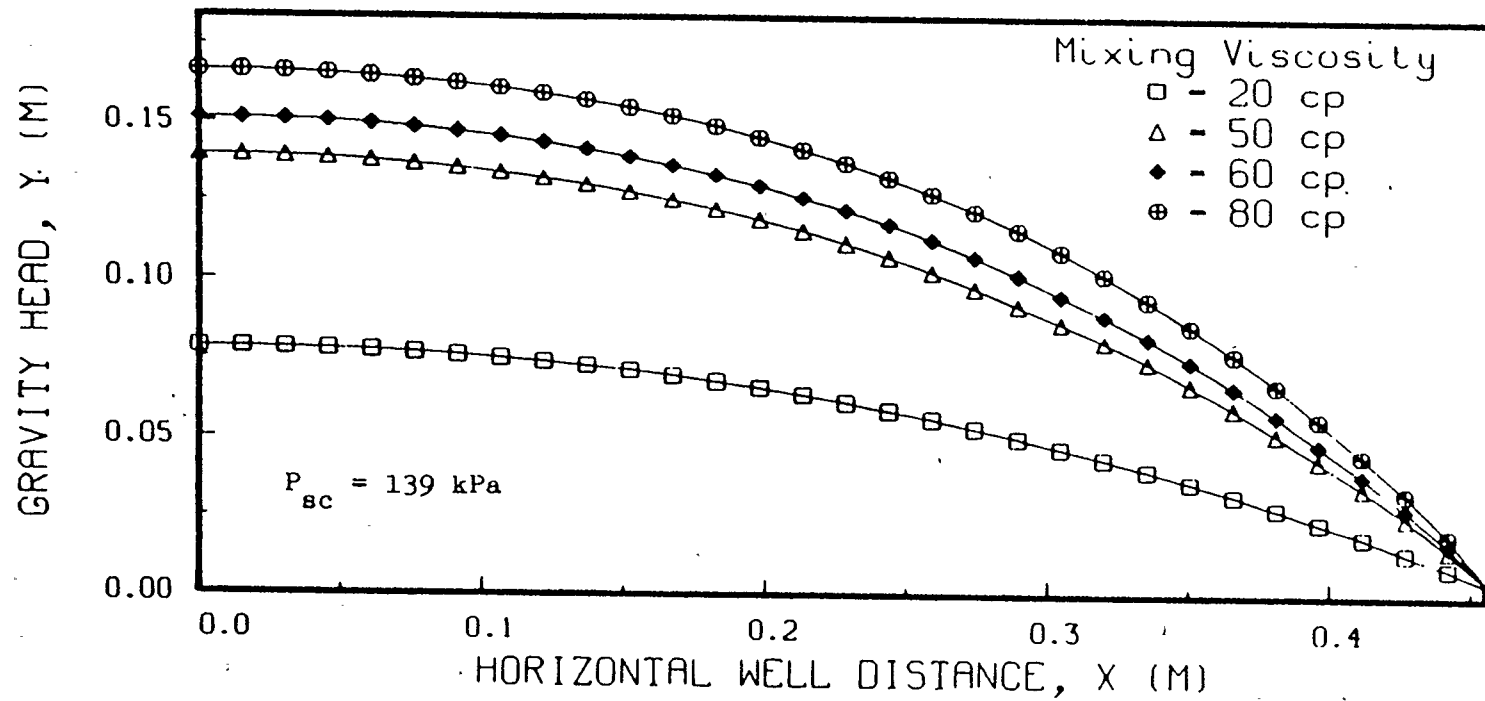
Using the above boundary conditions the three equations were discretized using a forward and backward differencing scheme and solved simultaneously for the three dependent variables in a computer programme (Appendix B). The following discussion will involve the results of simulation studies performed with the computer programme.

6.3 Results of the computer simulation

6.3.1 Laboratory conditions

The parameters for the reservoir model (Table 4.3) were first used for computer simulations. Thirty one grid points were used along the horizontal well for these simulations. It is interesting to study the effects of viscosity of fluids within the production well (called the mixing viscosity) and the well size on the performance of the production well.

The effect of viscosity was first studied for the 3/8" production well. For all these studies the inner tubing size used was 3/16". A wall thickness of 35/1000" was also taken in account in all the simulations performed for the laboratory model. Figure 6.3.1 shows the effect on the gravity head. It can be observed that there was a dramatic effect for a slight change in viscosity. The mixing viscosity used was from 20 to 80 centipoise which was not a realistic range at which the reservoir model operated. According to the results, for a production well temperature of about 88 °C which translates to a mixing viscosity of approximately 150 centipoise, there would still be significant amount of production for the experiments. Figure 6.3.2 shows the oil flow rate along the production well. The reason the simulation study was not carried out for a mixing viscosity of 150 centipoise was because the equations fail if the gravity head at any grid point was greater than the height of the reservoir model due to the argument of a logarithmic term becoming negative. According to Figure 6.3.1 the gravity head at the end of the horizontal well would



* Please refer to Table 4.3 for parameters used in the simulation

Figure 6.3.1 The effect of mixing viscosity on gravity head using a 3/8" production well in the model

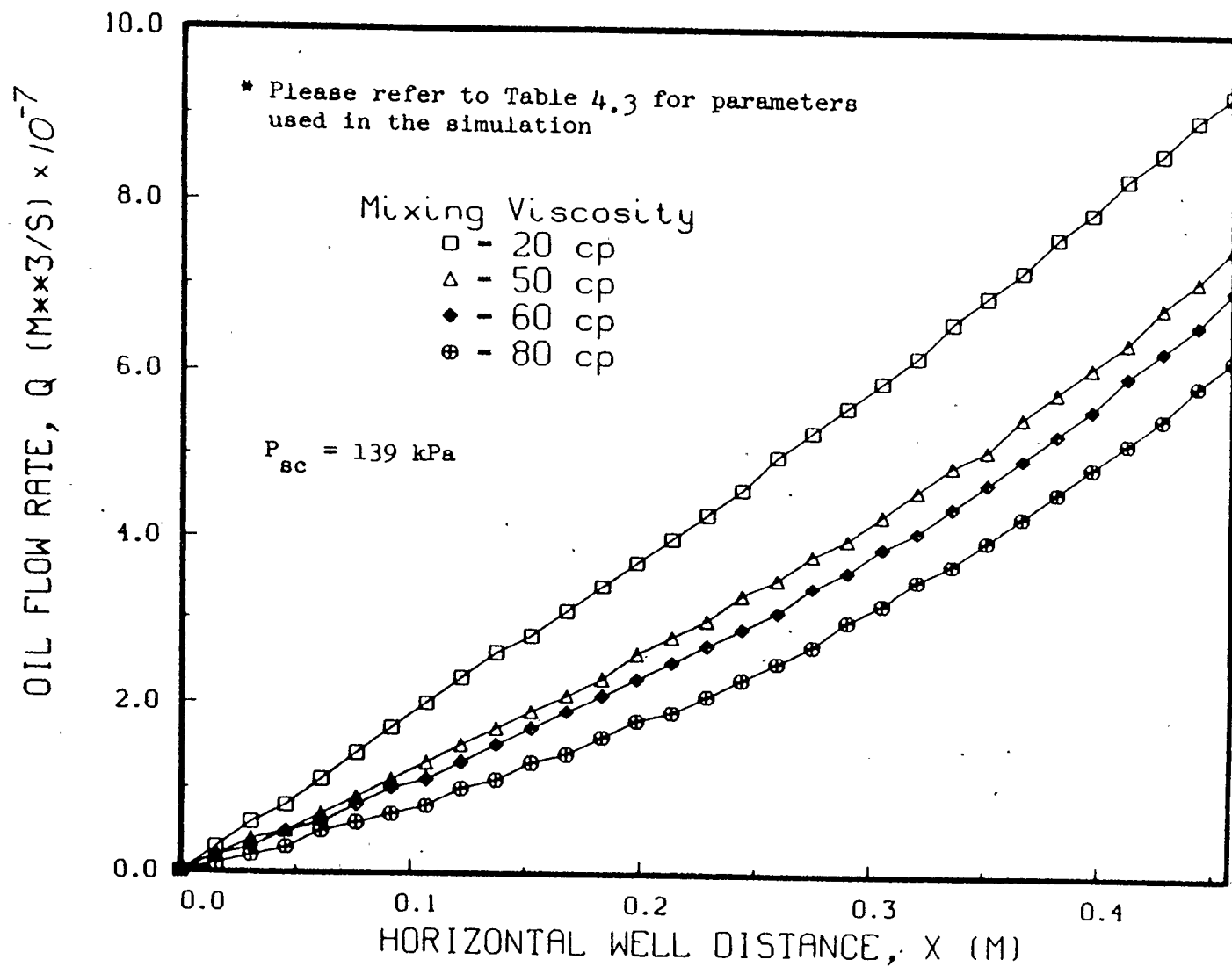


Figure 6.3.2 The effect of mixing viscosity on oil flow rate along a 3/8" production well in the model

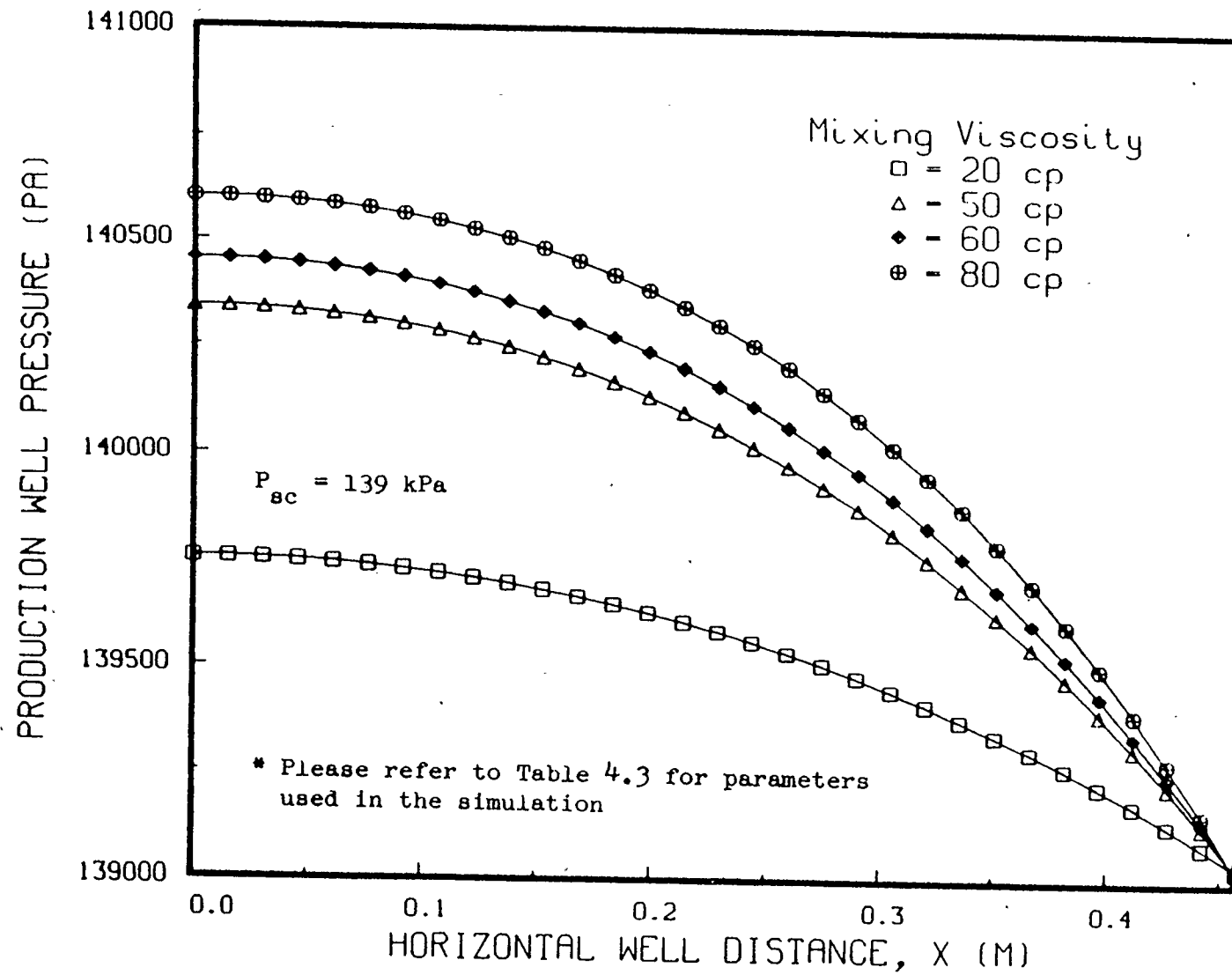
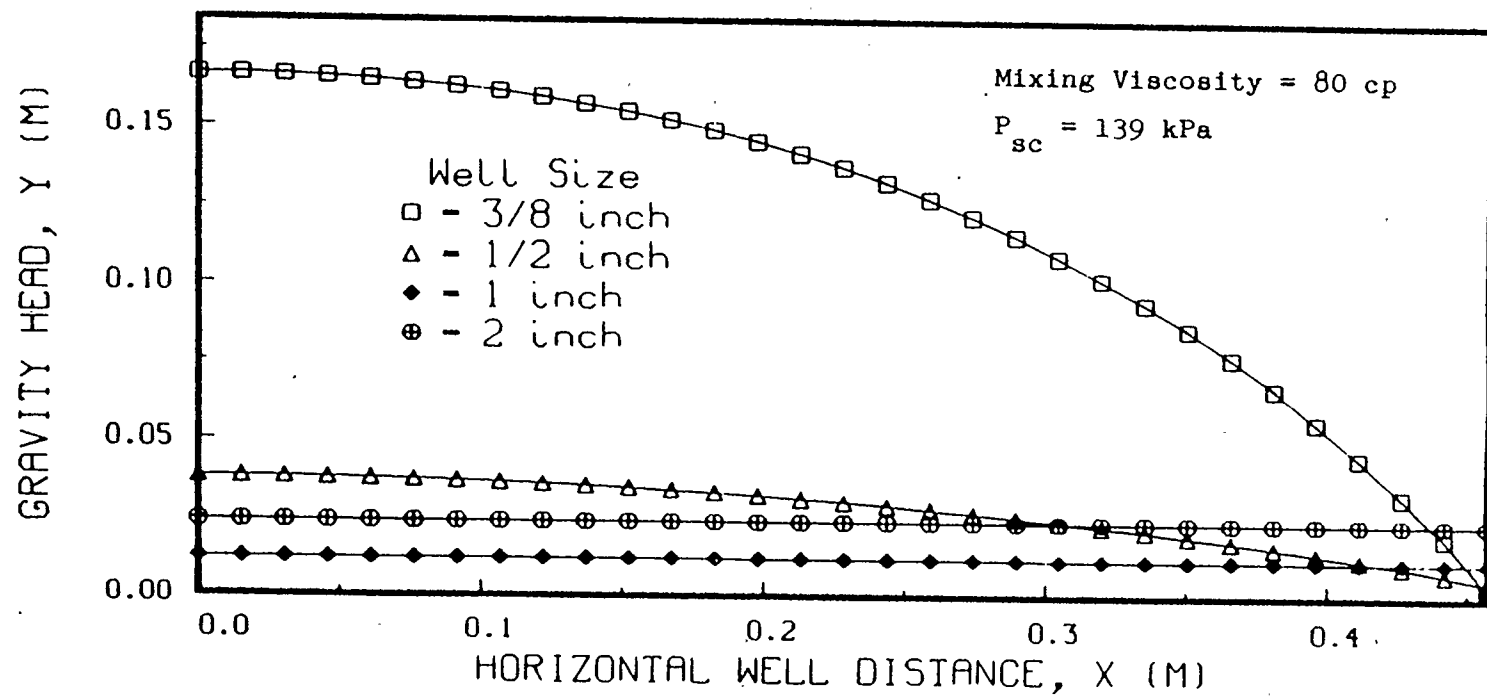


Figure 6.3.3 The effect of mixing viscosity on production well pressure using a 3/8" production well in the model.

approach the height of the reservoir. This was observed in experiment Run #8. Figure 6.3.3 shows the calculated effect of viscosity on the wellbore pressure. As expected the pressure drop for the least mixing viscosity gave the least pressure drop and the highest mixing viscosity produced the most pressure drop.

The effect of the well size was next studied. The mixing viscosity used was 80 centipoise. Figures 6.3.4, 6.3.5 and 6.3.6 shows the effect on gravity head, oil flow rate along the production well and production well pressure respectively. For the case studied the effect of using a 1/2" well instead of a 3/8" well was quite dramatic. It is therefore crucial that the size of the horizontal well be large enough. For the cases of 1" and 2" well sizes there was hardly any pressure drop as shown in Figure 6.3.6. The maximum oil flow rates along the well for these well sizes as shown in Figure 6.3.5 were approximately the calculated values using the TANDRAIN equation (equation (3.1.23)). The results were expected to be so because the gravity head for the two cases were insignificant and so the maximum oil production rate along the well should approximate that of equation (3.1.23).

The next study was to use a well size of 1" with various mixing viscosity values that are within the experimental range. The reason for this study was to investigate the flow resistance of the 1" well that was used in one of the experiments. Figure 6.3.7 shows the the effect of various mixing viscosity values on the gravity head. The highest mixing viscosity of 2000 centipoise corresponds to a temperature of approximately 50 °C while the lowest viscosity value of 50 centipoise corresponds to 109 °C. The range of the mixing



* Please refer to Table 4.3 for parameters used in the simulation

Figure 6.3.4 The effect of well size on gravity head in the model

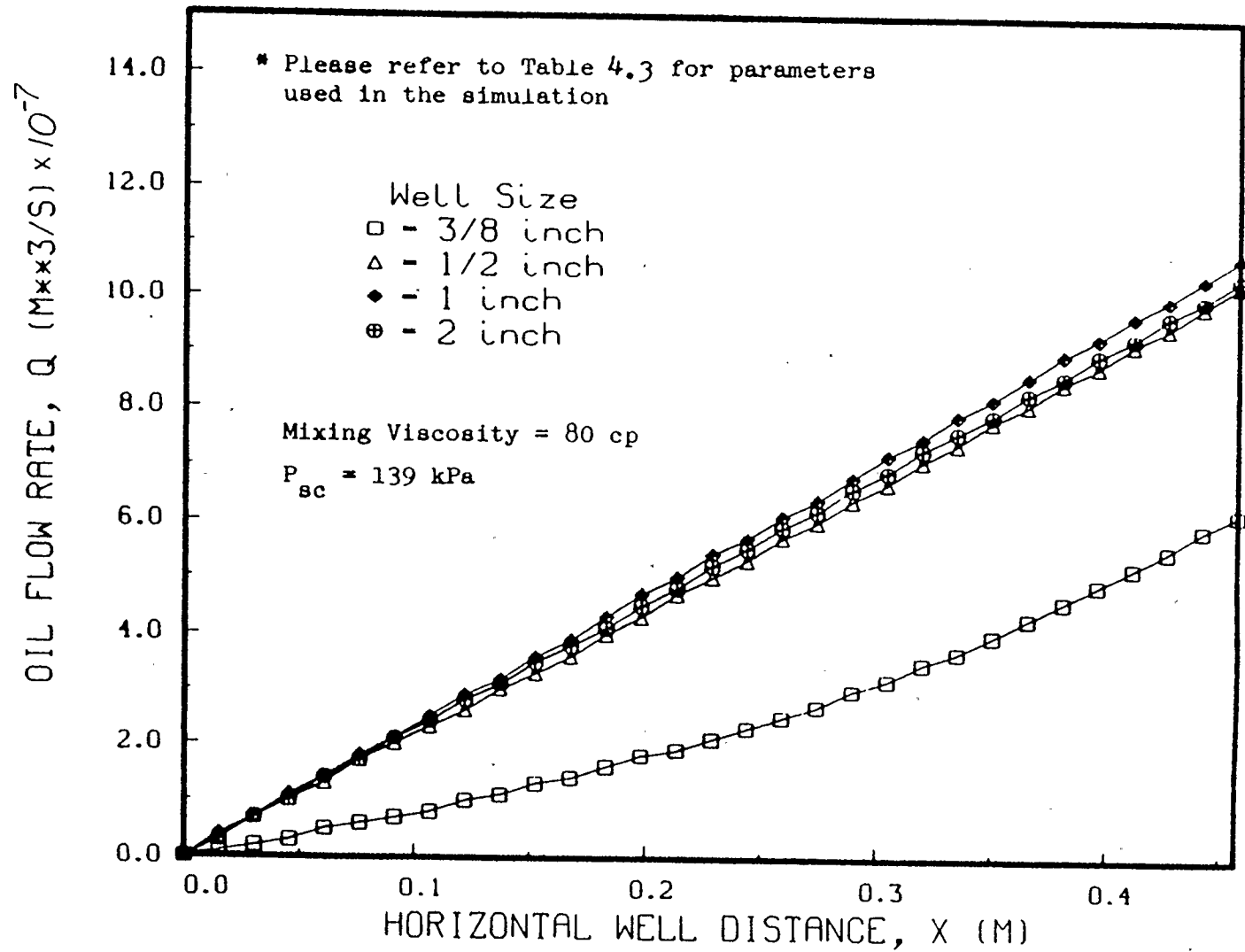


Figure 6.3.5 The effect of well size on oil flow rate along the production well in the model

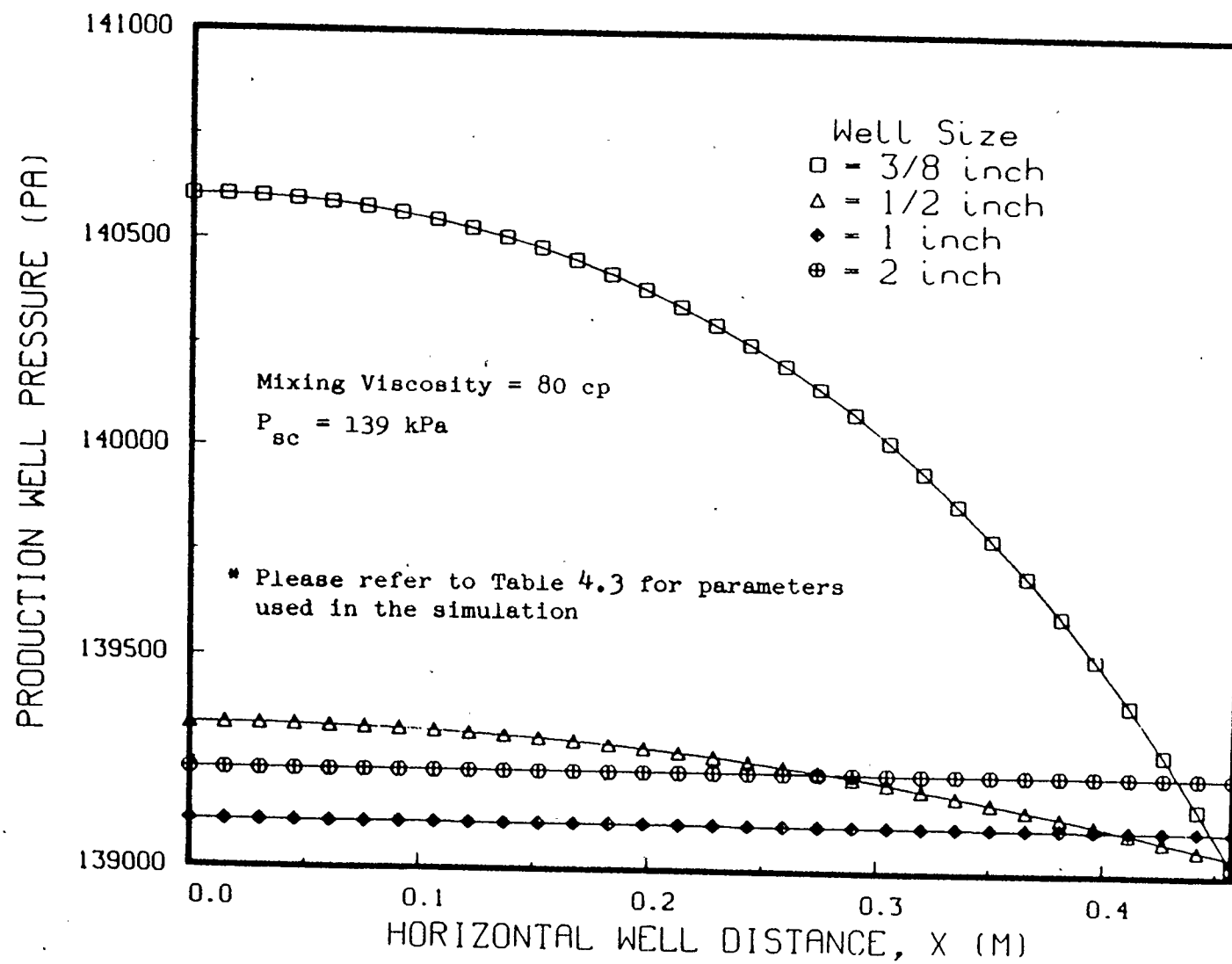
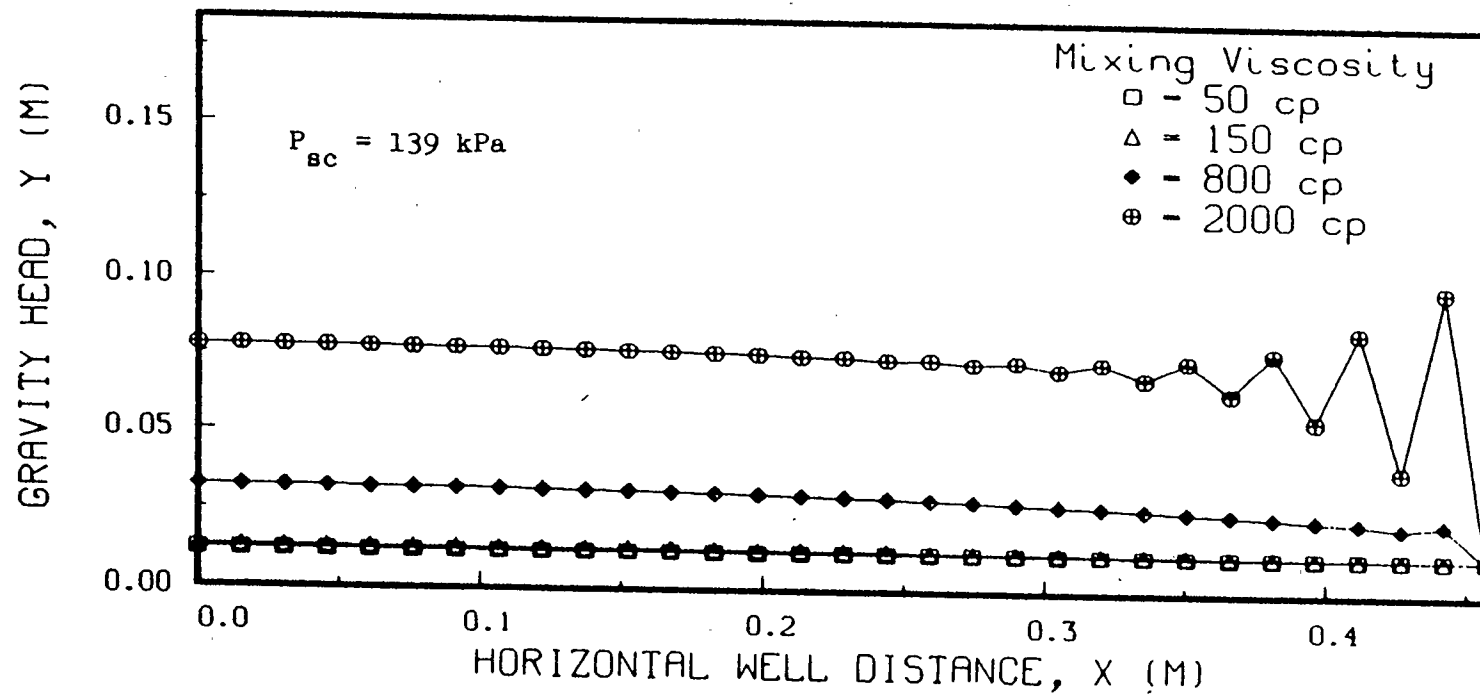


Figure 6.3.6 The effect of well size on production well pressure in the model



* Please refer to Table 4.3 for parameters used in the simulation

Figure 6.3.7 The effect of mixing viscosity on gravity head using a 1" production well in the model

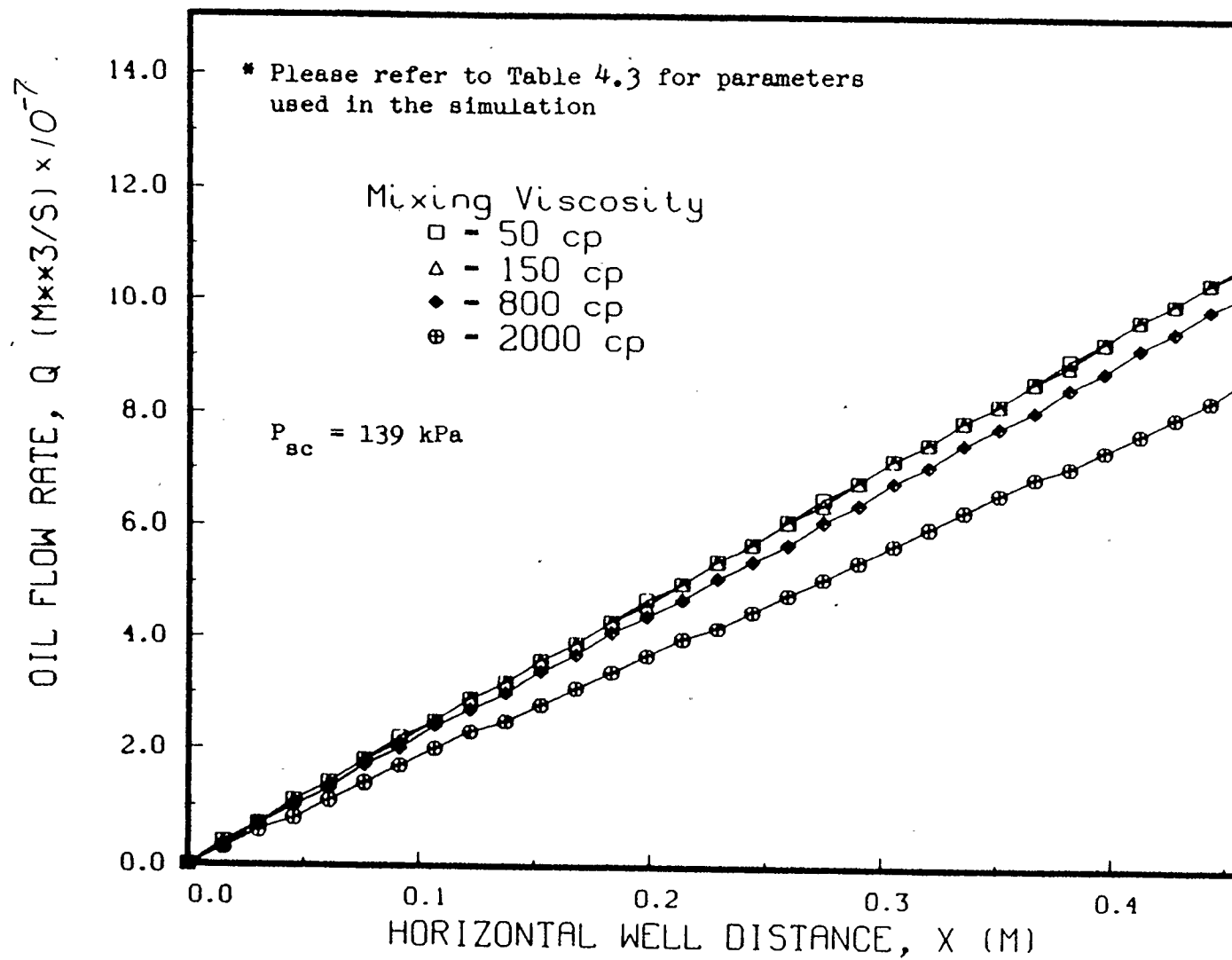


Figure 6.3.8 The effect of mixing viscosity on oil flow rate along a 1" production well in the model

viscosities studied was selected at practical values.. The results shows that for a production well temperature of 109 °C the maximum gravity head at the end of the production was quite insignificant. The gravity heads for the production well temperature of 88 °C (150 centipoise) and 60 °C (800 centipoise) were also relatively insignificant. For a well temperature of 50 °C (2000 centipoise) the gravity head became quite significant. In other words, the oil produced at the end of the steam chamber will back up if the well temperature is too low. It is therefore imperative to maintain the well temperature at a reasonably high temperature. Correspondingly, the expected oil flow rate is shown on Figure 6.3.8. Again, the maximum oil flow rate for the cases of insignificant gravity heads approximate the calculated oil production rate using equation (3.1.23). From the results of these studies, the recommended experiments using a 1" horizontal production well should have no problem with the drainage of oil. It can also be observed there was a region of instability for the case of 2000 centipoise. This was due to the finite differencing scheme used. Instability can be expected when there is a steep change in gradient. The results of Run #12 verified that flow restriction along the 1" production well is minimal as predicted by the simulation studies. As mentioned earlier Run #12 was performed with the same conditions as Run #8 (please refer to Table 4.5) but with a 1" production well instead of the 3/8". Both wells were operated at 7.5 psig and no differential pressure was set between the two wells throughout the experiment. The growth of the steam chamber along the central plane of the reservoir is shown in Figures 6.3.9a and 6.3.9b.

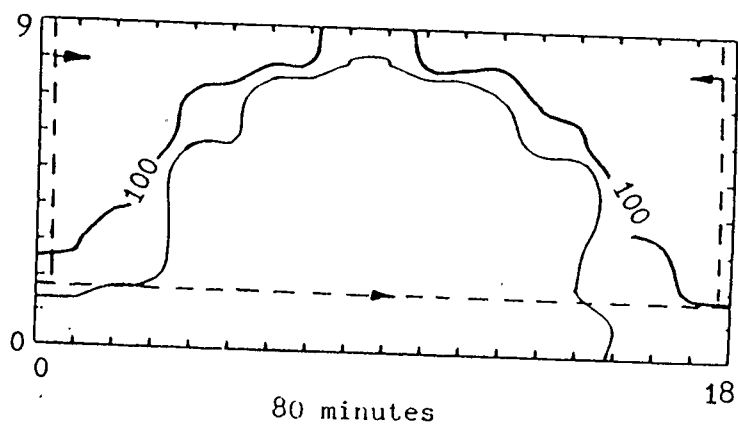
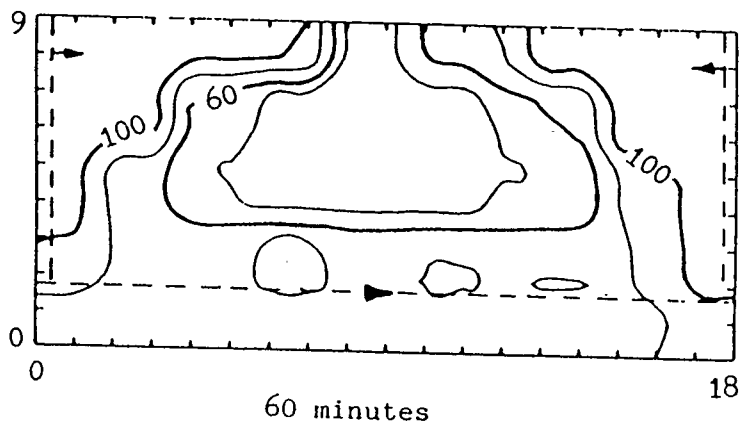
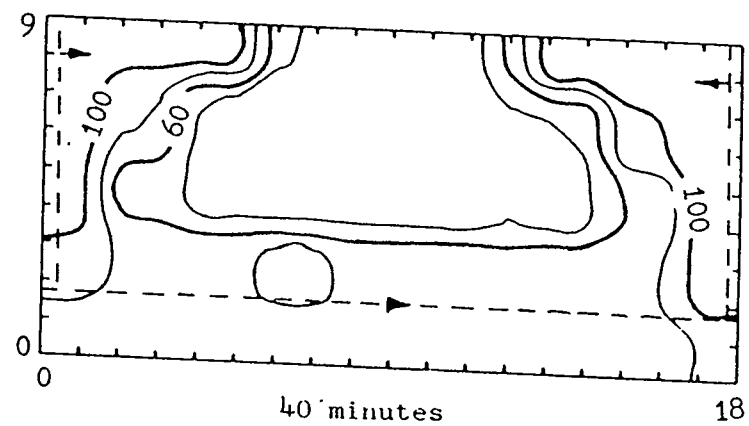
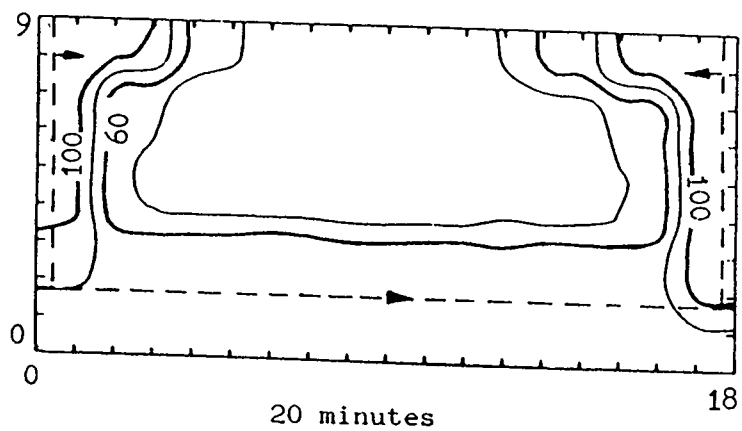


Figure 6.3.9a Movement of steam/oil interface in Run #12, 20 to 80 minutes

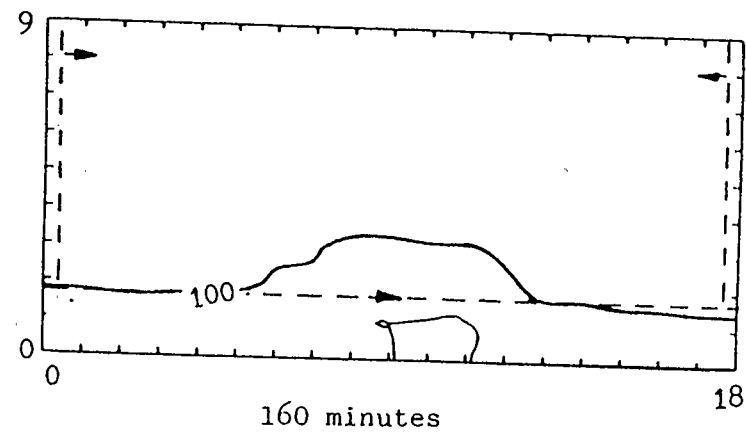
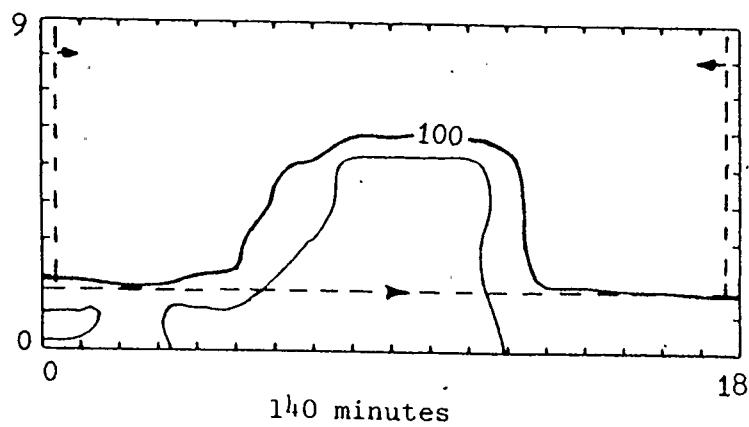
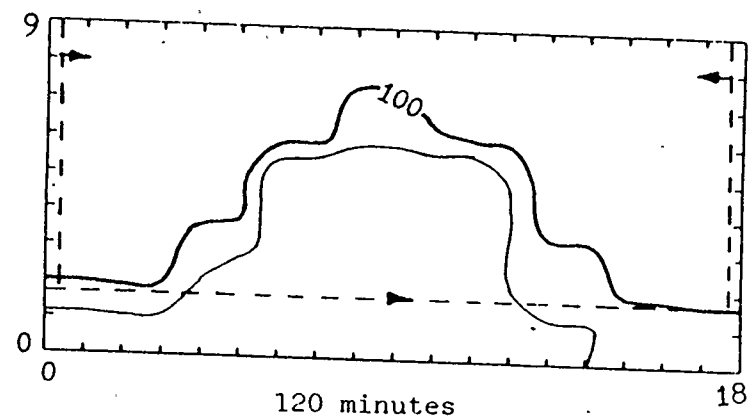
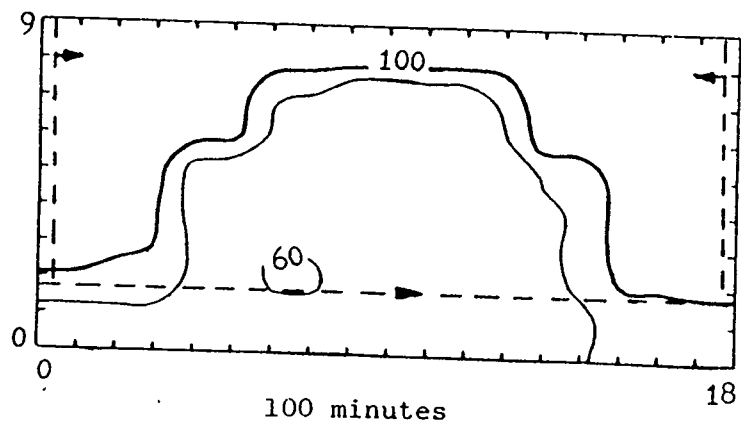


Figure 6.3.9b Movement of steam/oil interface in Run #12, 100 to 160 minutes

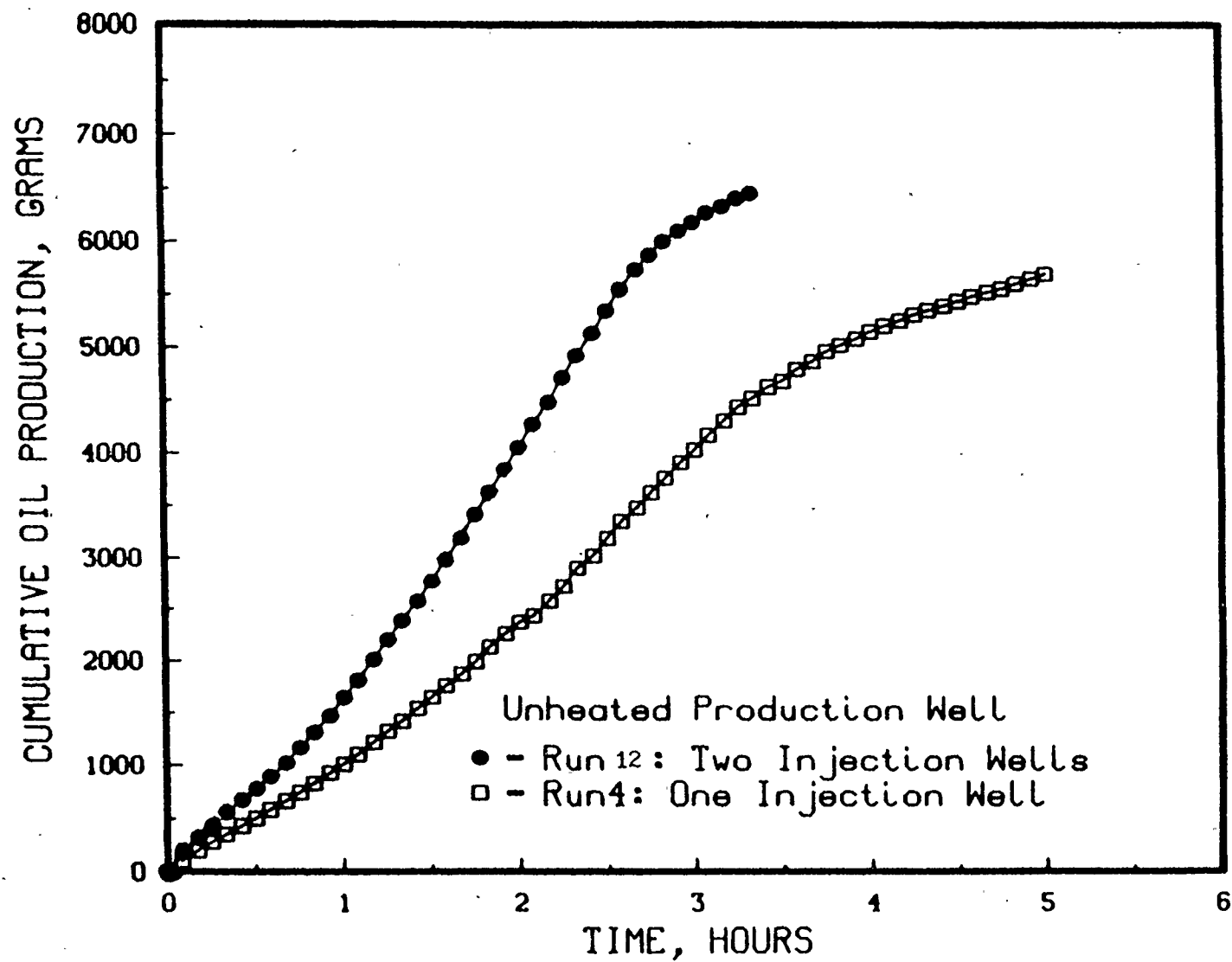


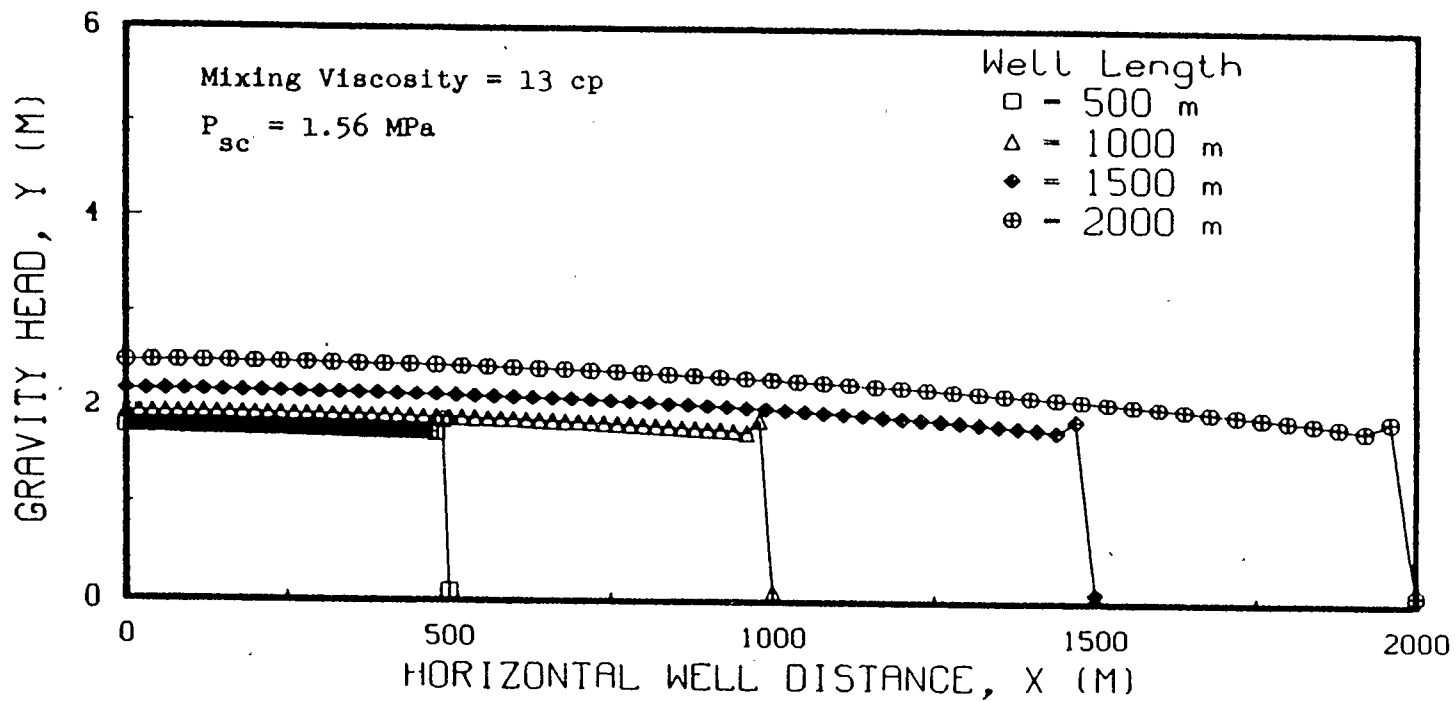
Figure 6.3.10 Comparison of cumulative oil production for Run #4 and Run #12

It can be observed that the steam chambers at both injectors grew as expected throughout the experiment. Produced fluids at the end (left hand side in the Figures) of the reservoir model did not back up as in Runs #8 to #11. Figure 6.3.10 compares the oil production performance between Run #12 with Run #4 in which one injector was placed at the end of the reservoir. It can be observed that Run #12 produced almost twice the amount of oil Run #4 produced during the experiment. The experiment thus proved that there would be no problem in the drainage of produced fluids within the horizontal production well along a regime of constant pressure if the well is sized correctly.

6.3.2 Field conditions

A series of calculations were made using the computer programme to evaluate the wellbore effects for field conditions. The effect of the length of the horizontal well on the gravity head formation and the oil production rate would be of importance. The programme was run using reservoir parameters taken from Table 4.3 for the fields. Fifty one grid points were used along the horizontal well. A practical mixing viscosity of 13 centipoise which corresponds to a well temperature of 154 °C was used. A well size of 7" with an inner tubing of 2 1/4" were used. The wall thickness of the well was not taken into account.

The effect of the well length on the gravity head is shown in Figure 6.3.11. Four well lengths were used. The well with a length of 2000 m gave the the maximum growth in the gravity head. The result obtained was expected. However, the effect of reducing the well length



* Please refer to Table 4.3 for parameters used in the simulation

Figure 6.3.11 The effect of well length on gravity head using a 7" production well in the field

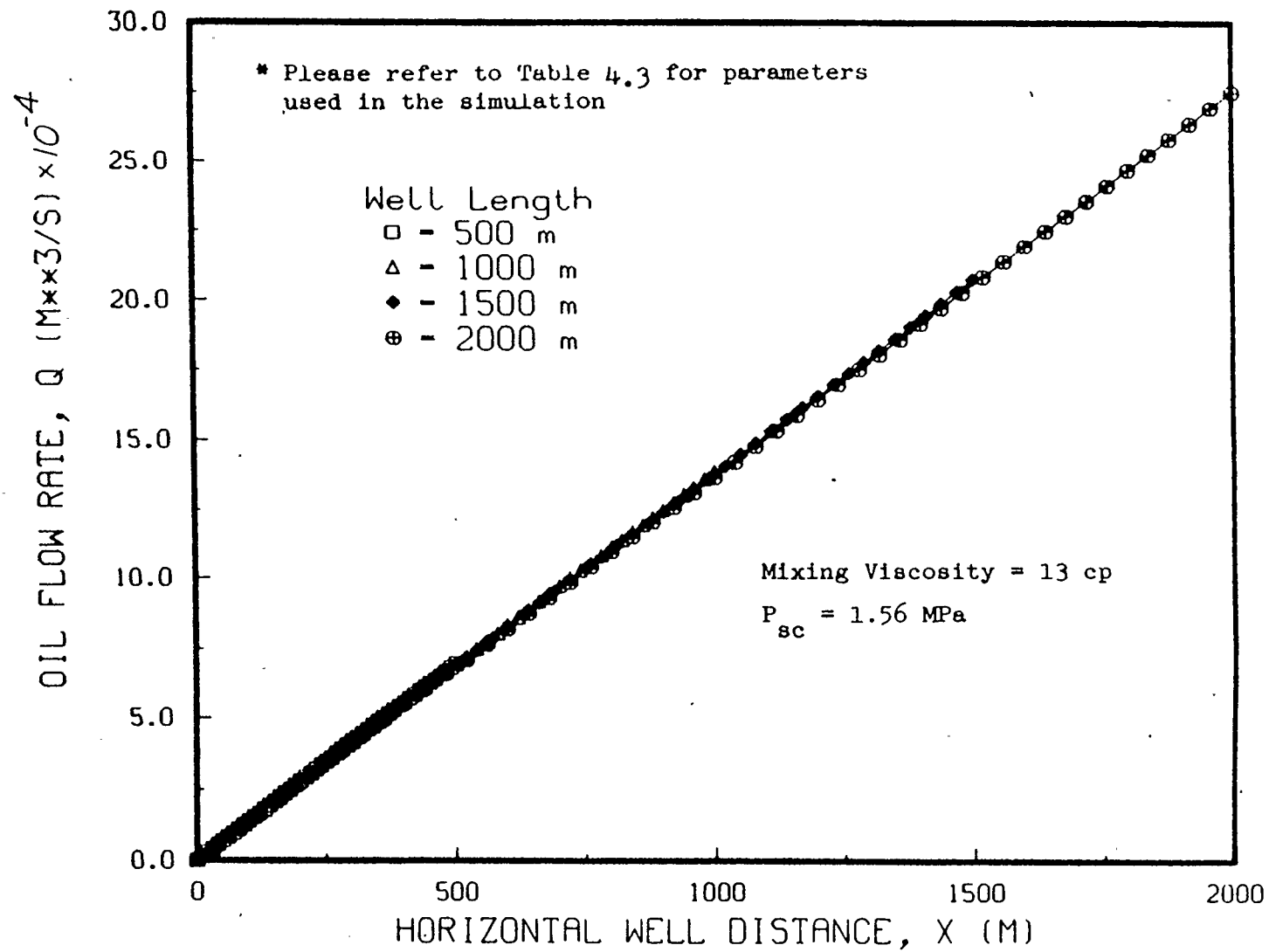


Figure 6.3.12 The effect of well length on oil flow rate along a 7" production well in the field

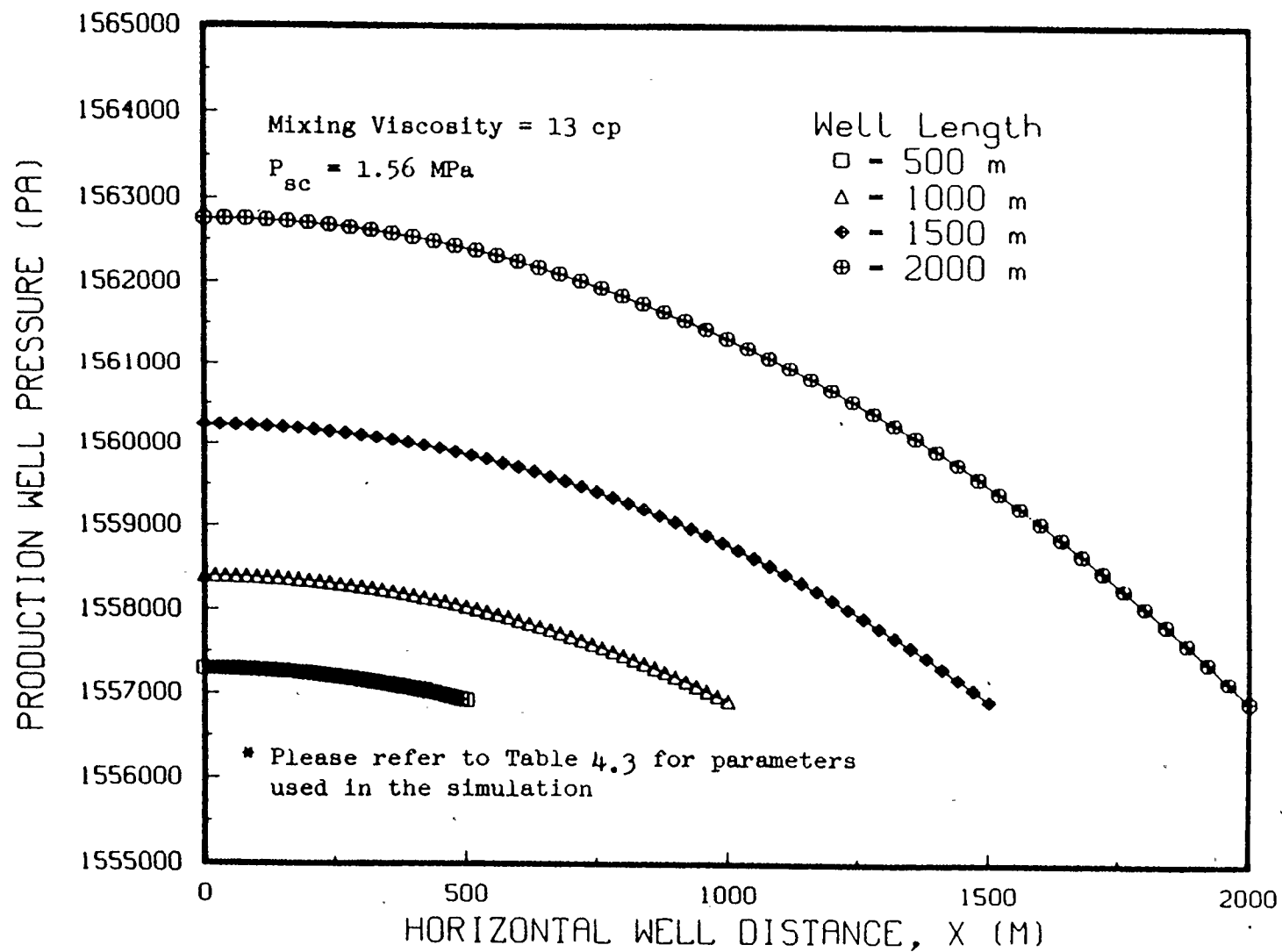
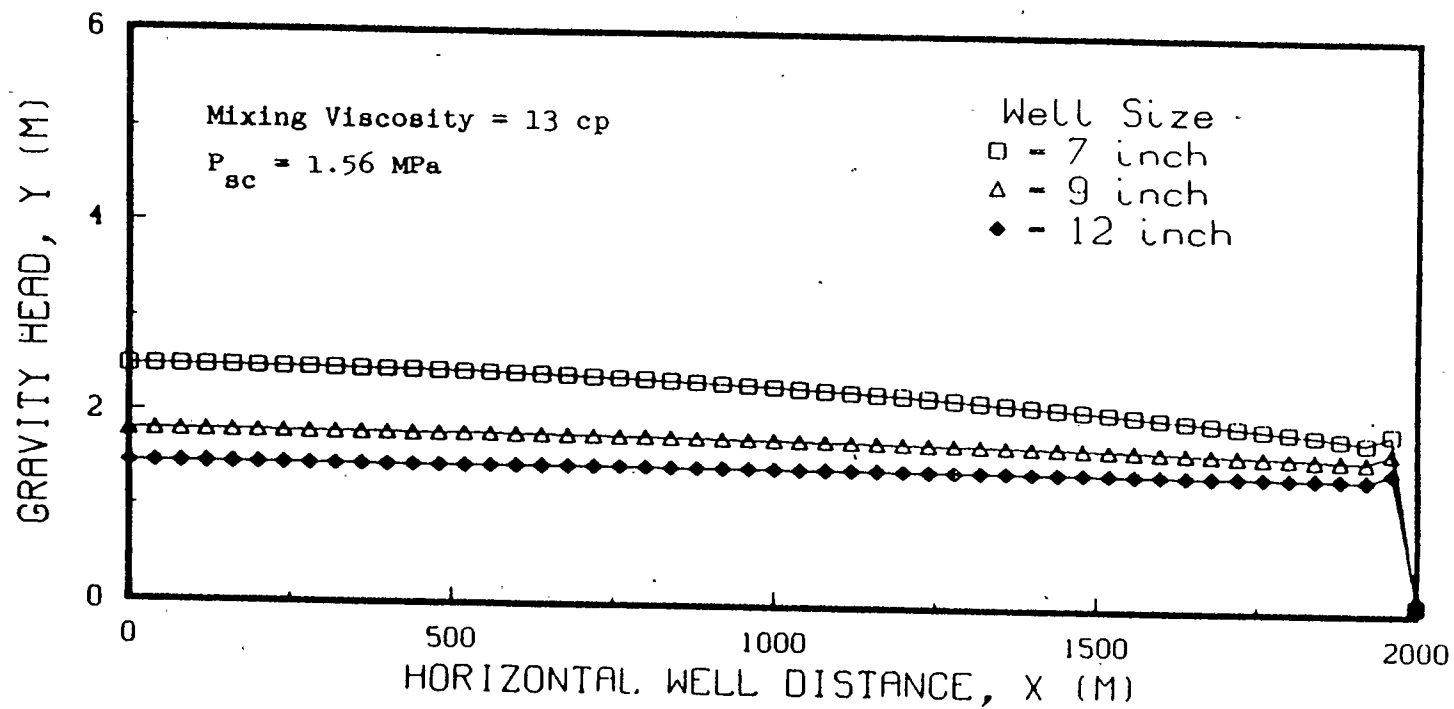


Figure 6.3.13 The effect of well length on production well pressure using a 7" production well in the field

by a factor of 4 (500 m) did not significantly reduce the gravity head. The corresponding oil flow rate along the well and the production well pressure along the well are shown in Figures 6.3.12 and 6.3.13. The results obtained were expected.

The next study was to observe the effect of increasing the well size for a well length of 2000 m. Three well sizes of 7", 9" and 12" were used. The mixing viscosity used was 13 centipoise which corresponds to a temperature of 154 °C for the Cold Lake bitumen. The effect on the gravity head is shown in Figure 6.3.14. There was quite a dramatic effect in increasing the well size from 7" to 9". The effect was equivalent to reducing the well length to 500 m for a 7" well. The result was expected as the pressure drop along the well is proportional the first power of the well length but inversely proportional to the fourth power of the well radius according to Hagen-Poiseuille equation. However, increasing the well size from 9" to 12" does not effect the change in the gravity head too significantly. This shows that there is little advantage in increasing the well size to 12". Although significant improvement was observed in decreasing the gravity head by increasing the well size, there was actually quite insignificant improvement in oil production rate as can be observed in Figure 6.3.15. The improvement was too insignificant to justify an increase in well size from the standard 7" well used in the field. It is thus not recommended that the well size of 7" in the field be increased.

The final topic of interest was to observe the effect of the number of grid points used for discretizing the horizontal production



* Please refer to Table 4.3 for parameters used in the simulation

Figure 6.3.14 The effect of well size on gravity head in the field

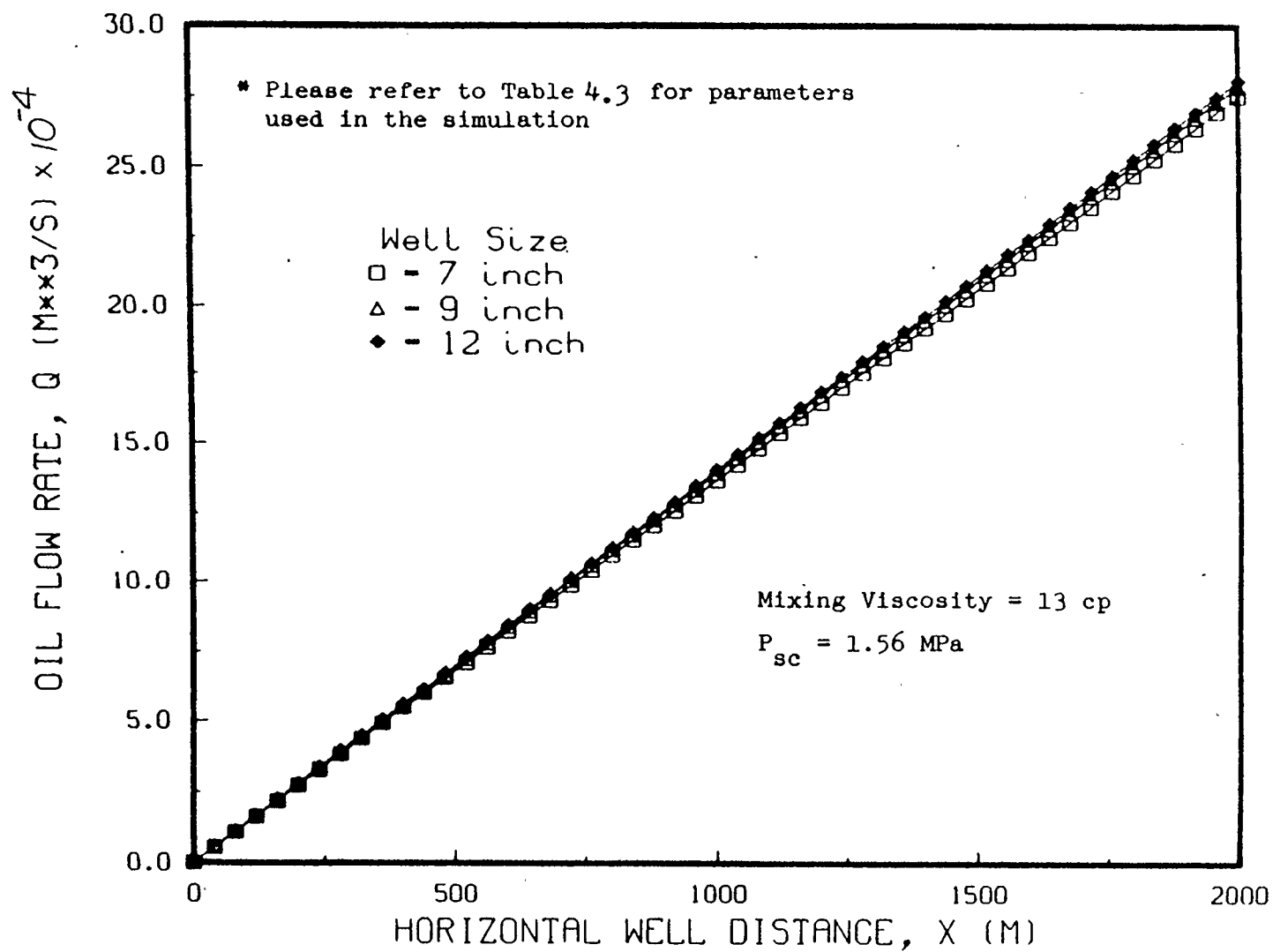


Figure 6.3.15 The effect of well size on oil flow rate along the production well in the field

well. This should provide a rough check on the reliability of the finite difference scheme used in the computer programme. The same criteria was used with a 7" production well of 2000 metres. The programme was run with 31, 51, 71 and 101 grid points along the well. It was found that there was improvement in the results obtained using more grid points but the improvement was relatively insignificant. The results showed that as the number of grid points was increased the production rates calculated approached the production rate calculated by equation (3.1.23). The calculated production rates were slightly greater than the theoretical rate calculated with no backup fluids. Since the calculated rates decreased and approached the theoretical rate as the number of grid points was increased, the creditability of the computer programme was verified.

CHAPTER 7

CONCLUSIONS AND RECOMMENDATIONS

A three-dimensional reservoir model apparatus was successfully developed for studying the use of vertical steam injectors with horizontal well production in the SAGD process.

The effect of indirectly heating the horizontal production well was found to be effective at the cold end of the well. It promoted significant additional ultimate oil recovery as well as recovery rate. Indirect heating was recommended for keeping the production well hot because it did not have the problem of "capping" the drainage of oil from the steam chamber as found in introducing steam at the end of the horizontal well. Introducing steam at the end of the horizontal well was also found to be an effective way of keeping the wellbore hot. But, it was found that drainage of oil from the steam chamber can be impeded if the process was not used properly. It recommended that more experiments be performed to study this process. If the steam injection pressure at the end of the production well can be properly controlled to alleviate the capping problem the method will be effective in keeping the well warm. The purpose of keeping the well warm is to decrease the viscosity of the bitumen in the well. An alternative to this is to introduce solvents at the end of the production well. This alternative is attractive because of two advantages. First, the method is effective in decreasing the viscosity of the bitumen in the well. Secondly, solvents are used to dilute the produced bitumen at the surface before it can be transported to the refinery for processing in

the first place. So, by using this method it is no longer necessary to keep the well warm thereby saving energy costs. However it is anticipated that the injection pressure of the solvents must be properly controlled so that the capping problem does not arise as in the case of introducing steam at the end of the production well. It is recommended that this process be investigated. Letting the steam out of the production well freely was found to be another effective way of keeping the production well hot. However its advantage can be overshadowed by the uneconomic waste of steam. It is thus recommended that only a minimal amount of steam be let out should this process be used.

The cumulative oil production performance using a single vertical steam injector was found to be between 30 to 40 percent that of a horizontal steam injector's. It was expected that as the number of vertical injectors is increased the performance will approach that of the horizontal injector's. This was verified by the results of Run #12 in which two injectors was used. The performance of using the two injectors resulted in an increase of 55 to 65 percent that of the horizontal injector's. This was a significant and impressive increment. It is thus recommended that further studies be performed to determine an optimum vertical well spacing.

The performance of using more than one injector was first studied experimentally using two injectors spaced along the horizontal production well. It was found that there was a problem of drainage of produced fluids along the horizontal well between the injectors due to insufficient driving force. The 3/8" production well was found to be

too small for effective drainage of the produced fluids. The flow resistance was too high along the horizontal production well. A sizing criterion was then developed for properly sizing production wells in laboratory scale models from field conditions based on the dimensionless time, T' and the B_3 factor. The sizing criterion further confirmed that the production well used in the experiments was too small. An experiment using a 1" horizontal production well with two vertical steam injectors was performed to elucidate the problem of the drainage of produced fluids along the production well. The experiment showed that the flow of the produced fluids was not restricted within the 1" well. It was thus found that the flow resistance along the production well is of critical importance in laboratory experiments.

The mechanisms of drainage of the produced fluids in the SAGD process was studied and a theory was formulated. Based on the theory a computer programme was developed to predict the pressure profile of the production well, the oil flow rate along the well and the resulting gravity head of the heated oil backed up by the impediment of flow along the well. It was found that the drainage of oil along the well was very sensitive to the viscosity of the fluids within the well (or the wellbore temperature), the wellbore size and the well length. The 3/8" production well used in the experiments was found to be too small for draining the produced fluids along a region of constant steam pressure. However the use of a 1" production well was found to be sufficient to alleviate the problem of drainage along the well in these simulation studies. This was verified by the experiment performed using a 1" production well instead of the 3/8" well. It was also found

that increasing the well size from 7" to 9" or 12" in the field does not improve the oil flow rate significantly. Thus the 7" well was found to be a practical size in the field.

REFERENCES

- American Society for Testing and Materials (ASTM), "Standard Test Method for Water and Sediment in Crude Oil by the Centrifuge Method (Laboratory Procedure)", Designation D4007-81 (1981).
- Bird, R. B., Stewart, W.E. and Lightfoot, E.N., Transport Phenomena, Ch. 2, John Wiley and sons, New York, U.S.A..
- Butler, R. M., "Rise of Interfacing Steam Chambers" J. Can. Pet. Tech., 70-75 (May-June 1987).
- Butler, R.M. et al., "Theoretical Studies On The Gravity Drainage of Heavy Oil During In-situ Steam Heating", J. Can. Pet. Tech., 59, 455-460 (August 1981a).
- Butler, R.M. and Stephens, D.J., "The Gravity Drainage of Steam-Heated Oil to Parallel Horizontal Wells", J. Can. Pet. Tech., 90-96 (April - June 1981b).
- Butler, R.M., "A New Approach To The Modelling Of Steam-Assisted Gravity Drainage", J. Can. Pet. Tech., 42-51 (May-June 1985a).
- Butler, R.M., "New Interpretation of the Meaning of the Exponent "m" in the Gravity Drainage Theory for Continuously Steam Wells" AOSTRA J. of Research, 2, 1, 67-71 (1985b).
- Butler, R. M., "Technical challenges in the in-situ recovery by bitumen", Text of talk presented at the Second District Meeting of the Canadian Institute of Mining in Hinton, Alberta (September 10-13 1985c).
- Butler, R.M., "Rise of interfering steam chambers", Presented at the 37th Ann. Tech. Mtg. of Petroleum Society of CIM, Calgary, Alberta (June 1986a).
- Butler, R.M., Thermal Recovery, Ch. 7, Lecture Notes for ENCH-647, The University of Calgary (September 1986b).
- Chung, K.H., "Steam-Assisted Gravity Drainage", PhD Thesis, University of Calgary, Alberta (Feb., 1988)
- Chung, K.H and Butler, R.M., "Geometrical effect of Steam Injection on the formation of Emulsions in the Steam-Assisted Gravity Drainage Process", 38th Ann, Tech. Mtg. of Petroleum Society of CIM, Calgary, Alberta (June 1987)
- Farouq Ali, S.M., "Current Status of Steam Injection As a Heavy Oil Recovery Method" J. Can. Pet. Tech., 54-68 (Jan-Mar 1974).

- Griffin, P.J. and Trofimenkoff, P.N., "Laboratory Studies of the Steam-Assisted Gravity Drainage Process", Presented at the Advances in Petroleum Recovery and Upgrading Technology Conference, 1984, Calgary, Alberta (June 14-15, 1984)
- Grigg, M., "Load Cell Amplifier Circuit", Department of Chemical and Petroleum Engineering, The University of Calgary, Calgary, Alberta, 1987
- Integrated Software Systems Corp., "Displa, Pocket Guide, Current with version 10.0", San Diego, Ca., 1986
- Joshi, S.D., "A Laboratory Study of Thermal Oil Recovery Using Horizontal Wells", Paper no. SPE/DOE 14916, Presented at the SPE/DOE Fifth Symposium on Enhanced Oil Recovery of the Soc. Pet. Eng. and Dept. of Energy, Tulsa (1986)
- Muskat, M., Flow of Homogeneous Fluids, International Human Resources Development Corporation, Boston, U.S.A., 1982, 175-8.
- Prats, M., Thermal Recovery, Monograph - Volume 7, SPE of AIME, Henry L Doherty Memorial Fund of AIME, 1982
- Sampson, R.J., "Surface II Graphical System", rev. 1, Computer Services Section, Kansas Geological, Lawrence, Kansas (1978)

Appendix A Computer programme for the data acquisition system

```
10 REM TEE S. ONG
20 REM M.SC. WORK, 1986-1988
30 REM THIS PROGRAM RUNS THE 3-D SAGD APPARATUS
40 REM DATA IS ACQUIRED FROM TAURUS ONE DATA ACQUISITION SYSTEM
50 REM OPEN SERIAL COMMUNICATION PORTS
60 OPEN "COM1:9600,E,7,1" AS #1 'OPEN COMMUNICATION WITH TAURUS
70 OPEN "COM2:" AS #2 'OPEN SWITCH CONTROLLING MOTOR IN FORWARD MOTION
80 PRINT "TURN MOTOR ON NOW!"
90 LINE INPUT "IS THE MOTOR TURNED ON? " ;XON$
100 IF XON$ = "NO" THEN 80
110 DIM T(50) 'MEASURED THERMOCOUPLE VALUE IN °C
120 LINE INPUT "DO YOU WANT A PRINTOUT? YES OR NO ";PR$
130 LINE INPUT "DO, YOU WANT TO STORE READINGS INTO FLOPPY DISK? YES OR
NO
";FA$
140 IF FA$ = "NO" THEN 190
150 LINE INPUT "PLEASE ENTER NAME OF DATA FILE ";FILE$
160 FILE$ = "B:" + FILE$ 'WRITE FILE IN B: DRIVE
170 PRINT "YOUR PRESENT DATA FILE NAME IS ";FILE$
180 OPEN "O",3,FILE$ 'SET BUFFER #3 FOR DRIVE B:
190 IF PR$ = "NO" THEN 260
200 LPRINT CHR$(27)"1"CHR$(10) 'SET PRINTER FORMAT
210 LPRINT "TEE S. ONG"
220 LPRINT "EXPERIMENT: ";FILE$
230 LPRINT "DATE :";DATE$
240 LPRINT "TIME :";TIME$
250 LPRINT CHR$(12)
260 REM INITIATE COMMUNICATION WITH TAURUS ONE
270 PRINT #1,"$A0,1,IN" 'INITIATE COMMUNICATION TO BUFFER #1
280 INPUT #1, A$,B$ 'TAURUS'S RESPONSE TO BUFFER #1
290 PRINT A$,B$ 'PRINT TAURUS'S RESPONSE ON SCREEN
300 PRINT #1, "$A0,1,UC CA (18,18)" 'SET HANDSHAKE MODE
310 INPUT #1, AA$,BB$,CC$ 'TAURUS'S RESPONSE
320 PRINT AA$,BB$,CC$ 'PRINT RESPONSE ON SCREEN
```

```

330 REM RECORD INITIAL READING OF LOAD CELL
340 PRINT #1, "$A0,1,RD AN(4,3)" 'TELL TAURUS TO TAKE LOAD CELL READING
350 INPUT #1, D$,E$,F$ 'TAURUS'S RESPONSE
360 PRINT D$,E$,F$ 'PRINT RESPONSE ON SCREEN
370 IF PR$ = "NO" THEN 390
380 LPRINT "INITIAL RAW READING OF LOAD CELL = ";:LPRINT F$
390 XLO = VAL(F$) 'DEFINE XLO TO BE INITIAL LOAD CELL READING
400 REM RECORD TIME OF START OF EXPERIMENT
410 TTO$ = TIME$ 'INITIALIZE EXPERIMENTAL TIME
420 XT1 = VAL(LEFT$(TTO$,2))*60!
430 XT1 = XT1 + VAL(MID$(TTO$,4,2))
440 XT1 = XT1 + VAL(RIGHT$(TTO$,2))/60!
450 N = 0
460 REM RECORD READING OF LOAD CELL
470 PRINT #1,"$A0,1,RD AN(4,3)" 'TELL TAURUS TO READ LOAD CELL
480 INPUT#1,A1$,B1$,C1$ 'TAURUS'S RESPONSE
490 PRINT A1$,B1$,C1$ 'PRINT RESPONSE ON SCREEN
500 XL = VAL(C1$) 'DEFINE XL TO BE SUBSEQUENT LOAD CELL READINGS
510 XLF = (XLO-XL)*2.232 'DEFINE XLF TO BE LOSS IN WEIGHT OF RESERVOIR
520 TT$ = TIME$ 'READ TIME OF DATA ACQUISITION
530 XT2 = VAL(LEFT$(TT$,3))*60!
540 XT2 = XT2 + VAL(MID$(TT$,4,2))
550 XT2 = XT2 + VAL(RIGHT$(TT$,2))/60!
560 XTR = XT2 - XT1 'DEFINE XTR AS EXPERIMENTAL TIME
570 REM RECORD ALL THERMOCOUPLE READINGS
580 FOR I = 0 TO 44
590 N$ = STR$(I)
600 PRINT #1,"$A0,1,RD TT(0"+N$)" 'TELL TAURUS TO READ THERMOCOUPLES
610 INPUT#1, A2$,B2$,C2$ 'TAURUS'S RESPONSE
620 'PRINT I,A2$,B2$,C2$ 'PRINT RESPONSE ON SCREEN WHEN NEEDED
630 T(I) = VAL(C2$)/10! 'VALUE OF THERMOCOUPLE READINGS IN °C
640 T(I) = INT(T(I)) 'CONVERT READINGS TO INTEGERS
650 NEXT I
660 REM TURN MOTOR ON
670 CLOSE #2

```



```
680 FOR I = 1 TO 16995 'SET TIME FOR FORWARD MOTION OF MOTOR TO GIVE
1" OF TRAVEL
690 NEXT I

700 REM TURN MOTOR OFF

710 OPEN "COM2:" AS #2

720 REM PRINT DATA ON COMPUTER SCREEN

730 PRINT "STEP NUMBER = ";N

740 PRINT "EXPT. TIME = ";:PRINT USING "###.##";XTR;:PRINT " MINS"

750 IF N = 0 THEN 760 ELSE 770

760 PRINT "LOSS IN WEIGHT = ";INT(XLF);:PRINT "GRAMS"

770 PRINT ""

780 FOR N1 = 0 TO 4

790 NT = N1 + 20

800 FOR N2 = N1 TO NT STEP 5

810 PRINT USING "#####";T(N2);

820 NEXT N2

830 PRINT USING "#####";T(NT+5);

840 PRINT USING "#####";T(NT+10);

850 PRINT USING "#####";T(NT+15);

860 PRINT USING "#####";T(NT+20)

870 IF N1 = 4 THEN 890

880 PRINT " "

890 NEXT N1

900 PRINT ""

910 IF FA$ = "NO" THEN 1000

920 REM PRINT DATA ON FLOPPY DISK

930 PRINT #3, N

940 PRINT #3, XTR

950 IF N = 0 THEN 960 ELSE 970

960 PRINT #3,INT(XLF)

970 FOR I = 0 TO 44

980 PRINT #3,T(I)

990 NEXT I

1000 IF PR$ = "NO" THEN 1250

1010 REM PRINT DATA ON PRINTER

1020 LPRINT "STEP NUMBER = ";N
```

```
1030 LPRINT "EXPT. TIME  = ";:LPRINT USING "###.##";XTR;:LPRINT" MINS"
1040 IF N = 0 THEN 1050 ELSE 1070
1050 LPRINT "LOSS IN WEIGHT = ";INT(XLF);:LPRINT " GRAMS";
1060 LPRINT " (";:LPRINT C1$;:LPRINT ")"
1070 LPRINT CHR$(10)
1080 FOR N1 = 0 TO 4
1090 NT = N1 + 20
1100 FOR N2 = N1 TO NT STEP 5
1110 LPRINT USING "#####";T(N2);
1120 NEXT N2
1130 LPRINT USING "#####";T(NT+5);
1140 LPRINT USING "#####";T(NT+10);
1150 LPRINT USING "#####";T(NT+15);
1160 LPRINT USING "#####";T(NT+20)
1170 IF N1 = 4 THEN 1190
1180 LPRINT " "
1190 NEXT N1
1200 LPRINT ""
1210 LPRINT ""

1220 IF N=2 OR N=6 THEN 1230 ELSE 1250
1230 LPRINT CHR$(12)
1240 REM NEXT STEP
1250 N = N + 1
1260 FOR I = 1 TO 250000! 'SET TIME FOR REVERSE MOTION OF MOTOR
1270 NEXT I
1280 IF N = 7 THEN 1300 ELSE 520
1290 REM RESET POSITION OF THERMOCOUPLES
1300 FOR I = 1 TO 100000!
1310 NEXT I
1320 GOTO 450
1330 END
```

Appendix B Computer programme for simulation of the steady state flow
along the horizontal well

```

c TEE S. ONG
c THE UNIVERSITY OF CALGARY
c M.SC. THESIS WORK
c TO SIMULATE THE PRESSURE DROP AND OIL FLOW RATE ALONG THE HORIZONTAL
c WELL. THE GRAVITY HEAD RESPONSIBLE FOR THE FLOW IS ALSO SIMULATED
c THE FORWARD AND BACKWARD FINITE DIFFERENCE METHOD IS USED

      %global ansi77,card
c Flow rate of oil q (m3/s); well pressure p (Pa); gravity head y (m);
c Distance along the well x (m);
c Rate of change of q w.r.t x, dq (m3/s/m)

      real q(0:200,0:200),p(0:200,0:200),y(0:200,0:200),x(0:200)
      real kk,mu,m,dq(0:200)
      character*32 fname1,fname2
      write (*,*) "Enter input data file name: "
      read (*,"(a32)") fname1
      open (7, file=fname1, form="formatted", mode="in")
      write (*,*) "Enter output file name: "
      read (*,"(a32)") fname2
      open (8, file=fname2, form="formatted", mode="out")

c READ RESERVOIR PARAMETERS FROM DATA FILE
c Read number of grid points

      read (7,*) n
c Read length of production well (m)

      read (7,*) xl
c Read value of permeability (m2)

      read (7,*) kk
c Read value of thermal diffusivity (m2/s)

      read (7,*) alp
c Read value of the product of porosity and change in residual oil
c saturation

      read (7,*) fidso
c Read the dimensionless factor m

```

```

      read (7,*) m
c Read value of kinematic viscosity of oil at steam temperature ( $\text{m}^2/\text{s}$ )
      read (7,*) vs
c Read the value of mixing viscosity of fluid in well (Pa.s)
      read (7,*) mu
c Read the value of radius of the horizontal well (m)
      read (7,*) rw1
c Read the value of radius of the inner tubing (m)
      read (7,*) rw2
c Read the value of the pressure of the steam chamber (Pa)
      read (7,*) psc
c Read the value of the reservoir height (m)
      read (7,*) h
c Read the value of the density of the oil ( $\text{kg}/\text{m}^3$ )
      read (7,*) ro
      write (*,*) " Data file used = ", fname1
c OTHER CONSTANTS
c Gravitational constant ( $\text{m}/\text{s}^2$ )
      g=9.807
c The value of  $\pi$ 
      pi=3.142
c The ratio of inner tubing radius to production well radius
      rr=rw2/rw1
c The value of c defined in equation (6.2.9)
      cc=(1.0-rr**4)-(1.0-rr**2)**2/alog(1.0/rr)
c CALCULATE DISTANCE OF GRID POINTS
      hh=x1/(n-1)
      x(1)=0
      do 2 i=2,n
      x(i)=hh+x(i-1)
      2 continue

```

```

c START ITERATION
    k=1
c SET BOUNDARY CONDITIONS
    write(*,*) "enter an initial guess of q(n): "
    read(*,*)q(k,n)
5 y(k,n)=rw1
    dq1 = 2.0*(1.5*fids0*kk*g*alp*(h-y(k,n))/(m*vs))**0.5
    p(k,n)=psc+ro*g*y(k,n)-dq1*mu*alog(2.*y(k,n)/rw1)/(4.*pi*kk)
    write(6,50) k,n,q(k,n),p(k,n),y(k,n)
    do 10 i = n,2,-1
        dq(i)= 2.0*(1.5*fids0*kk*g*alp*(h-y(k,i))/(m*vs))**0.5
        q(k,i-1)=q(k,i)-dq(i)*(x(i)-x(i-1))
        p(k,i-1)=p(k,i)+8.*mu*(x(i)-x(i-1))*q(k,i-1)/(pi*rw1**4*cc)
c SET UP COEFFICIENTS FOR SOLVING THE VALUE OF Y(I-1)
        aa=ro*g*4.0*pi*kk/mu/dq(i)
        bb=4.0*pi*kk*(psc-p(k,i-1))/mu/dq(i)+alog(rw1/2.0)
        y(k,i-1)=p(k,i-1)/ro/g
        call newton(aa,bb,y(k,i-1))
7 write(6,50) k,i-1,q(k,i-1),p(k,i-1),y(k,i-1)
50 format(1x,i3,2x,i3,2x,f15.10,2x,f10.1,2x,f15.10)
10 continue
    if(k.eq.1) then
        q(k-1,n)=0.8*q(k,n)
        q(k-1,1)=0.
    endif
    if(abs(q(k,1)).gt.1e-10) then
        q(k+1,n)=q(k,n)-q(k,1)*(q(k,n)-q(k-1,n))/(q(k,1)-q(k-1,1))
        k=k+1
        goto 5
    endif
c PRINT RESULTS
    write(8,100) k
    write(8,105) kk
    write(8,110) x1
    write(8,115) rw1

```

```

write(8,120) alp
write(8,130) m
write(8,140) h
write(8,160) vs
write(8,170) psc
write(8,180) mu
write(8,*)" x (m)      q (m**3/s)      pwf (Pa)      y (m)"
do 20 i=1,n
write(8,200) x(i),q(k,i),p(k,i),y(k,i)
20 continue
100 format(1x,"Number of iterations = ",i3)
105 format(1x,"Permeability of porous medium = ", e10.3," m**2")
110 format(1x,"Length of horizontal well = ",f10.4," m")
115 format(1x,"Radius of horizontal well = ",f6.4," m")
120 format(1x,"Thermal diffusivity = ",e10.3," m**2/s")
130 format(1x,"m-factor = ",f5.2)
140 format(1x,"Height of formation = ",f10.4," m")
160 format(1x,"Kinematic viscosity = ",e10.3," m**2/s")
170 format(1x,"Steam chamber pressure = ",f10.1," Pa")
180 format(1x,"Mixing Viscosity in well = ",e10.3," Pa.s")
200 format(1x,f10.4,2x,f12.8,2x,f12.1,2x,f10.7)

stop
end

c =====
c Subroutine for solving root y(k,i):
c =====

subroutine newton(aa,bb,x)
imax=20000
ii=1
100 continue
5 zz=x*(alog(x)-aa*x-bb)/(1.0-aa*x)
xx=x
x=x-zz
if (x.lt.0.0) then
x=abs(x)

```

```
endif
if (abs(x/xx-1.0).gt.1.0e-5) then
ii=ii+1
if (ii.gt.imax) then
print*, "No root - imax exceeded"
stop
end if
goto 100
end if
return
end
```